ENVIRONMENTAL DIFFERENCES IN TROPICAL SOIL TEMPERATURES IN KENYA

by

William Davis Mace

A thesis submitted to the faculty of
The University of Utah
in partial fulfillment of the requirements for the degree of

Master of Science

in

Geology

Department of Geology and Geophysics

The University of Utah

December 2012

The University of Utah Graduate School

STATEMENT OF THESIS APPROVAL

The thesis of **William Davis Mace**

has been approved by the following supervisory committee members:

Thure E. Cerling	, Chair	**6/1/12** Date Approved
Francis H. Brown	, Member	**6/1/12** Date Approved
David S. Chapman	, Member	**6/1/12** Date Approved

and by **Douglas K. Solomon** , Chair of

the Department of **Geology and Geophysics**

and by Charles A. Wight, Dean of The Graduate School.

ABSTRACT

Environmental temperature differences within tropical soils are a function of the total solar radiation received at the surface, and also depend on woody vegetation cover. Environmental soil temperature is recorded by carbon isotope substitutions during the formation of calcite, which is preserved in paleosols. Therefore, analysis of preserved carbonates can be used as a proxy indicator of paleotemperatures. Preliminary data from hominid sites in the Turkana Basin show that soil temperatures have been in excess of 30°C for much of the past 4-6 million years in that region. In this study two years of continual subsurface soil monitoring were conducted at 28 sites within and around Kenyan National Parks and we present annual and seasonal averages of soil temperatures at a depth of 25 cm within different microclimates, which should approximate the absolute formation temperature of soil carbonates in present day tropical soils. In addition, we use an iterative method to solve the heat diffusion equation to estimate the soil surface temperature. In the tropics, where the solar angle is high throughout the year, observed environmental temperature differences over small spatial distances are as high as 30°C in the most extreme contrasts between grassland and forested microclimates. Average soil temperatures at 25 cm depth are highest in the Turkana basin where annual and seasonal averages are in excess of 30°C. These results are consistent with the paleotemperature measurements, indicating that temperatures are as hot today as they have been over the past several million years.

TABLE OF CONTENTS

LIST OF TABLES

LIST OF FIGURES

CHAPTER 1

INTRODUCTION

Earth's dynamic climate system naturally experiences gradual changes over time. However, during the last century, since the dawn of the modern industrial age, Earth's climate has been changing at a much more accelerated rate. It is widely accepted that human activities have been amplifying changes in global temperature through burning large amounts of fossil fuels. The product of the combustion of fossil fuels, carbon dioxide, is a greenhouse gas that alters atmospheric transparency making it more opaque to long wave radiation emitted from the Earth's surface into space. The result is the inability of the surface to radiate the heat necessary to maintain a balanced surface energy budget which leads to an increase in the globally averaged surface air temperature and therefore, continued climate change [*IPCC*, 2007].

In addition to atmospheric emissions of green house gases, humans have also been altering the way that the Earth's surface absorbs energy from the sun through changes in land use practices [*Chapin*, 2002]. Altering the landscape through cities, deforestation, and livestock grazing, change how the Earth absorbs and reflects solar radiation. The amount of radiation reflected back into space by the surface is known as the albedo. Naturally the Earth has an average albedo of about 0.3 [*Wallace and Hobbs*, 2006]. The difference in albedo between a forest canopy and grassland is significant;

0.08 and 0.30, respectively, which has a major influence on the amount of energy available within an ecosystem [*Chapin*, 2002; *Robert et al.*, 2008; *Vitousek*, 1994]. Together these changes, the greenhouse effect and land use practices, translate to an increase in the global temperature and ultimately to global climate change. During the last century, globally averaged surface temperature has risen by approximately 0.75 °C. Computer model simulations predict that in the coming decades, globally averaged surface temperatures will increase between 1–6°C [*IPCC*, 2007]. The magnitude of observable change will vary greatly across different regions of the planet and furthermore, the magnitude of changes will be different for each of the many ecosystems within a given landscape.

Ecosystems are governed by the local climate, soil parent material, topography, potential biota, and time. These five independent control variables are called state factors and were explained in depth by Hans Jenny [*Jenny*, 1980]. Together, these five state factors set the bounds for the characteristics of a particular ecosystem. Ecosystem characteristics such as air temperature, canopy cover, and soil temperature are important controls in a variety of ecological processes and are also good indicators of climate change and the magnitude of changes within an ecosystem as they are a direct measure of the overall climate encompassing a particular ecosystem [*Chapin*, 2002; *Jenny*, 1980]. Processes such as plant growth and nutrient cycling are crucial components to the overall health of an ecosystem and are highly dependent on environmental controls such as the ones mentioned above [*Vitousek*, 1994]. Therefore, quantifying and continually monitoring these parameters is increasingly important in light of global climate and land

use changes. Monitoring these parameters will enable us to identify and further quantify changes within natural environments.

In addition to present day applications these environmental characterizations, when combined with paleothermometry and carbonate isotopic analysis of paleosols to determine woody vegetation cover, can provide significant insight into the environmental conditions existing in specific areas over the past several million years. Furthermore, this information should be applicable to questions pertaining to the environmental context of human evolution.

There has been a long-standing debate about environmental conditions that existed during critical periods of human evolution. It is widely accepted, however, that the last common ancestor (LCA) between humans and chimpanzees lived in a wooded forest environment. Since the LCA 5 to 8 million years ago (mya), as the two species diverged, it is thought that habitats became less wooded and more seasonally arid [*Cerling et al.*, 2010; *Potts*, 1998; *White et al.*, 2009; *Wood and Harrison*, 2011]. Increased aridity and grassland expansion is thought to have driven the further development of bipedalism and the reduction of body hair in hominins [*Wheeler*, 1984, 1991, 1992, 1993]. The environment(s) in which the genus *Homo* evolved undoubtedly provided shade, shelter, and food. Just as importantly, this environment, or the environmental mosaic of the landscape, would have had a major influence on the evolutionary development and adaptations of the genus through time.

The following thesis is divided into two principal chapters. In Chapter 2, I discuss the delta 47 ($\Delta 47$) paleothermometer, and present deep (0.25 m) soil temperature data from modern grassland, bushland and forest environments to show that the

seemingly high paleotemperatures calculated using this method are still observed within today's soil environments. Chapter 3 presents a composite day of soil temperatures from grassland, bushland, and forested environments throughout Kenya. The aim of this chapter is to quantify the average daily soil temperature cycles observed throughout Kenya's environmental mosaic. Results from this chapter can be applied to the study of hominid energy balance and provide insight on environmental factors driving hominid evolution. Data presented in both chapters were collected in present day environments within the Kenyan Wildlife Management System. The study locations were chosen within and near the Kenyan National Wildlife Reserves because of the relatively undisturbed nature and limited anthropogenic influences. Areas on the peripheries of the reserves have been influenced heavily by people and their animals and provide valuable insight into the effects of land use change.

Because of the loose usage of the terms grassland, woodland, bushland, forest, etc. there is a need for these terms to be strictly defined early in this paper. For these definitions I adopt the definitions of such landscape types defined by the United Nations Educational, Science, and Cultural Organization [*White*, 1983] as follows.

- "Forest. A continuous stand of trees at least 10-m tall, their crowns interlocking."
- "Woodland / Bushland / Shrubland. Woodland: An open-stand of trees at least 8-m tall with a canopy cover of 40 % or more, and a field layer dominated by grasses."
- "Bushland: An open-stand of bushes usually between 3- and 8-m tall with a canopy cover of 40 % or more."

- "Grassland. Land covered with grasses and other herbs, either without woody plants or the latter not covering more than 10 % of the ground."
- "Desert. Arid landscapes with a sparse plant cover. The sandy, stony or rocky substrate contributes more to the appearance of the landscape than does the vegetation."

Kenya Meteorology

Kenya is located in equatorial Africa. This area spans more than 1.5 million km and is considered to be one of the more meteorologically complex parts of Africa [*Griffiths*, 1972; *Nicholson*, 1996]. Climates within this zone are extremely variable from hot humid coasts with over 2000 mm precipitation per year to hot dry scrubland with as little as 200 mm of precipitation per year to dense tropical forests in cool, wet highlands. Topography in Kenya is just about as diverse as climate. Kenya lies atop a geologically active zone (the Kenya Dome) that is bisected by a central rift valley. On the eastern and western margins of this rift lie the Kenyan highlands with elevations between 1700 and 2100 m on broad flat plains interrupted by mountains of still higher elevation. Southeastern Kenya is mainly flat and is < 300 m above sea level. Most of northern Kenya lies below 1000 m elevation, but small highland area also exist. Elevations range from sea level to glaciated mountain peaks above 5100 m.

There are six main meteorological features that have a large influence on Kenyan meteorology throughout the year. These include three air streams and three convergence zones. The northwest and southeast monsoon are the result of the migration of the Inter-Tropical Convergence Zone (ITCZ). Both the northeast and southeast monsoons are dry

and affect the Kenyan region during the Northern Hemisphere winter and summer, respectively. The Kenyan "long rains" and the "short rains" occur during the migration periods of the ITCZ, which occur during the Northern Hemisphere spring and fall, respectively. The third air stream that influences the Kenyan region is the Congo airstream with its westerlie and southwesterlie components. The boundary between the westerly and southwesterly components of the Congo air mass, the Congo Air Boundary, is situated perpendicular to and south of the ITCZ.

The monsoons, unlike the Asian monsoon, are convectively stable and therefore, are associated with dry conditions. Humid air flowing out of the Congo Basin is convectively unstable and therefore, associated with rain during the transition seasons [*Nicholson*, 1996]. These atmospheric features along with widely variable topography lead to an extremely complex distribution in precipitation and temperature both temporally and geographically [*Griffiths*, 1972; *Levin*, 2008 *Nicholson*, 1996]. Climatological season is defined by the Kenya Meteorology Department: December, January, and February (DJF) are the "warm and dry season," March, April, and May (MAM) are the "long rains," June, July, and August (JJA) are the "cool and dry season," and September, October, and November (SON) are the "short rains."

Geographically, the distribution of rainfall is more straightforward. Rainfall over Kenya is driest in the north and northeastern lowlands and wettest in the southwest and costal southeast. In the driest parts of Kenya, the Turkana basin, mean annual precipitation (MAP) values are less than 200 mm per year and in the wettest parts of Kenya, in the Kenyan Highlands and around Mt. Kenya, MAP values are greater than 2500 mm.

The seasonal distribution of temperature over Kenya is such that, typically, the coldest month recorded is in July or August and the warmest month is November or December [*Griffiths*, 1972]. Seasonal temperature fluctuations through the region are small if existent at all because of the close proximity to the equator, however, there are observable differences in temperature due to the rainy seasons, but these have very little to do with the small variability in solar insolation.

Temperature in Kenya is not only dependent on solar insolation, but also on the elevation of a given location. The dependence of temperature with elevation is known as the environmental lapse rate and is typically measured in units of C° of temperature drop per km of elevation gain. Therefore, it can be expected that the hottest regions of Kenya will be those that are low in elevation and the coolest will be those that are highest in elevation.

References

Cerling, T. E., N. E. Levin, J. Quade, J. G. Wynn, D. L. Fox, J. D. Kingston, R. G. Klein, and F. H. Brown (2010), Comment on the paleoenvironment of Ardipithecus ramidus, *Science 328*(5982): 1105.

Chapin, F. S., P. A. Matson, and H. A. Mooney (2002), *Principles of Terrestrial Ecosystem Ecology*, Springer, New York.

Griffiths, J. F. (1972), *Climates of Africa*, Elsevier Publishing Co., Amsterdam, New York.

IPCC, 2007: Climate Change 2007: *The Physical Science Basis*. Contribution of working group I to the fourth assessment report of the intergovernmental panel on climate change [Solomon, S., D. Qin, M. Manning, Z. Chen, M. Marquis, K.B. Averyt, M. Tignor and H.L. Miller (eds.)], Cambridge University Press, Cambridge, United Kingdom and New York, NY, USA.

Jenny, H. (1980), *The Soil Resource*, Springer, Heidelberg, Berlin.

Levin, N. E. (2008), Isotopic Records of the Plio-Pleistocene Climate and Environments in Eastern Africa. PhD dissertation, Dept. of Geol. and Geophys., Univ. of Utah Salt Lake City, Utah.

Nicholson, S. E. (1996), *A review of Climate Dynamics and Climate Variability in Eastern Africa, The Limnology, Climatology and Paleoclimatology of the East African Lakes*, pp. 25-56, edited by T. Johnson, E.B Odada, K. T. Whittaker, Gordon and Breach Science Publishers, Amsterdam, The Netherlands.

Potts, R. (1998), Environmental hypotheses of hominin evolution, *Yearbook of Physical Anthropology 41*: 93-136.

Robert, B. J., and T. R. James, et al. (2008). Protecting climate with forests, *Environmental Research Letters 3*(4): 044006.

Vitousek, P. M. (1994), Beyond global warming: Ecology and global change, *Ecology 75*(7): 1861-1876.

Wallace, J. M. and P. V. Hobbs (2006), *Atmospheric Science: An Introductory Survey*, Elsevier Academic Press, New York.

Wheeler, P. E. (1984), The evolution of bipedality and loss of functional body hair in hominids, *Journal of Human Evolution,* 13: 91-98.

Wheeler, P. E. (1991a), The thermoregulatory advantages of hominid bipedalism in open equatorial environments: The contribution of increased convective heat loss and cutaneous evaporative cooling, *Journal of Human Evolution*, 21: 107-115.

Wheeler, P. E. (1991b), The influence of bipedalism on the energy and water budgets of early hominids, *Journal of Human Evolution*, 21: 117-136.

Wheeler, P. E. (1992a), The thermoregulatory advantages of large body size for hominids foraging in savannah environments, *Journal of Human Evolution*, 23: 351-362.

Wheeler, P. E. (1992b), The influence of the loss of functional body hair on the water budgets of early hominids, *Journal of Human Evolution*, 23: 379-388.

Wheeler, P. E. (1993), The influence of stature and body form on hominid energy and water budgets; a comparison of Australopithecus and early Homo physiques, *Journal of Human Evolution*, 24: 13-28.

White, F. (1983), The vegetation of Africa, *Natural Resources Research*, 20, 1-356

White, T. D., B. Asfaw, et al. (2009), Ardipithecus ramidus and the paleobiology of early hominids, *Science*, *326*(5949): 64, 75-86.

Wood, B. and T. Harrison (2011), The evolutionary context of the first hominins, *Nature 470*(7334): 347-352.

CHAPTER 2

SPATIAL AND TEMPORAL TROPICAL SOIL TEMPERATURES

Abstract

Temperatures within the Turkana Basin are hot. Preliminary soil carbonate formation temperatures, ($\Delta 47$) paleothermometry data, from hominid sites within the Turkana Basin suggest that the absolute temperature of the soil during carbonate formation has been in excess of 30°C during much of the past 4–6 million years. In the following chapter we present soil temperature data from modern soils at 28 different sites located in national parks and wildlife refuges throughout Kenya at depths consistent with soil carbonate formation. The data presented show that soil temperatures within the Turkana Basin and at the Tana River Primate Reserve are hotter than any other area within Kenya on both seasonal and annual timescales. Average temperatures on both time scales exceed 30°C. We also present climate data collected from nearby weather stations to associate the local climate and vegetation conditions and the effects these variables have on deep soil temperatures.

Introduction

Within the paleoclimate community and the archeological community there is a need to understand the evolution of the landscape over time, particularly temperatures that may have been experienced by the present and past residents of these landscapes such as hominids [*Cerling*, 2011; *Cerling et al.*, 2010; *White et al.*, 2010]. Over the past few decades, different methods have been developed as proxy thermometers to calculate the absolute soil temperatures that were present during pedogenic carbonate formation using stable isotopes [*Eiler,* 2007]. One method, the Δ47 paleothermometer [*Ghosh et al.*, 2006] uses the rare ^{13}C-^{18}O bond in carbonate minerals for such paleothermometry. Carbonate minerals are preserved within paleosols and, when extracted and isotopically analyzed, provide a measure of the temperature of the soil environment during the formation of the carbonate. When this method of paleothermometry is applied to the hominid sites in the Turkana Basin in northern Kenya, preliminary data reveal that paleosol temperatures have been in excess of 30°C during much of the past 4–6 mya [*Passey et al.*, 2009]. Furthermore, it is commonly assumed that the mean annual soil temperature (MAST) will average 1–3° warmer than the mean annual air temperature (MAT) [*Geiger*, 1965]. This means that the air temperatures that are associated with the calculated soil temperatures in the sedimentary record are higher than mean annual air temperatures observed today and leaves open a question weather modern environments exist that produce soil temperatures, at the depths of carbonate precipitation, greater than or equal to 35°C. Because of this, it is useful to provide modern day analogs to the environments and microclimates that may have produced such high soil temperatures in the past.

Because pedogenic carbonates form at depths between .30 and .50 m in the soil column [*Cerling*, 1984; *Passey et al.*, 2009] the temperature recorded during their formation represents a seasonal averaged representation of soil temperature, and most likely a warm season biased seasonal average [*Breecker et al.*, 2009; *Passey et al.*, 2009]. Processes that occur at the soil surface, such as solar heating and infrared cooling (net radiation), evaporative cooling, and sensible heat flux, which are components of the surface energy budget, that are coupled to local weather tend to control the soil temperature at depths within the soil column. Perturbations in the surface energy budget, which are not quantified here, are conducted through the soil column at a rate that is dependent on the soil type and water content. At any depth between the surface and a few meters, the daily average temperature is similar. However, the amplitude is increasingly attenuated and phase shifted with depth. At 0.25 m depth, the daily range is drastically attenuated leaving only seasonal and longer timescale transitions resolvable, thereby providing a more accurate measure of the long-term average soil temperature [*Jury and Horton* 2004; *Lal and Shukla*, 2004]. The average in soil temperature, which is representative of the carbonate formation temperature, can then be correlated with averages of the surface climate and surface characteristics, thus providing a connection between the surface characteristics and the carbonate formation temperature.

Here we address the need for these environmental analogs to correlate with paleothermometry data by looking at modern day tropical environments located throughout the Kenyan National Park System. In doing so, the deep (0.25 m) soil temperatures will be presented on both annual and seasonal timescales using soil temperature records collected during two years at different sites throughout Kenyan

National Parks. To assess the effect that microclimates have on soil temperature, temperature sensors were placed in the soils of different ecological settings (e.g., forest, grasslands, and bushland) within each regional setting and left undisturbed for approximately two years. In addition to the deep soil temperature, we will also present some environmental characteristics of the area including regional air temperature, regional precipitation, type and density of vegetation cover.

Methods and Materials

Site selection and temperature measurement

Twenty-eight sites in 11 regional localities in Kenya were studied to characterize soil temperatures relevant to soil carbonate formation (Figure 2.1). Soil temperature sites were chosen to represent a variety of climates and ecosystems in order to characterize the range of environments that may be relevant to the geological record of sedimentary environments. Most of the sites were within Kenyan National Parks or National Reserves and thus, have minimal human disturbance. In addition, a few sites on the peripheries of the parks were monitored to provide insight into the effects of land use changes by recent human activities. Within each regional locality several individual sites were chosen to assess the effect that woody cover and shade have on the soil temperature. Because of the loose usage of the term "savanna" [*Ratnam et al.*, 2011] the definitions of the United Nations Educational, Science, and Cultural Organization [*White*, 1983] are used and are described in Appendix A.

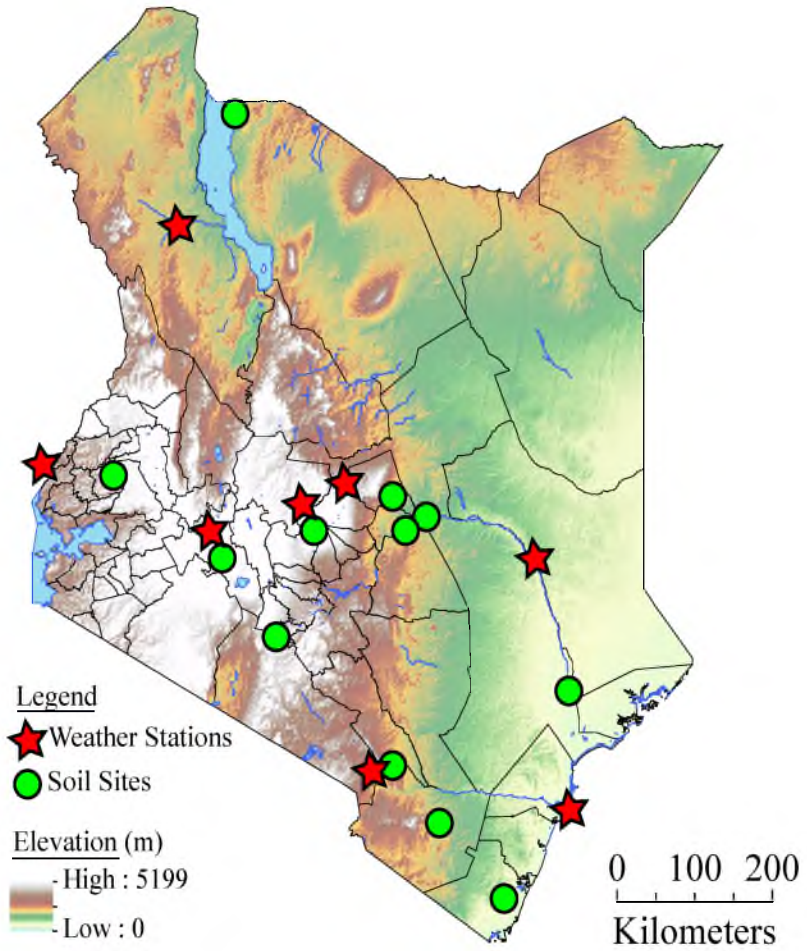

Figure 2.1 – Digital Elevation Model (DEM) of Kenya with soil temperature sites (green stars) and weather station sites (red stars).

Climate data were obtained from the Kenya Meteorological Service (KMS) using the operational weather station nearest each study site; in most cases this is within about 20 km of the field site. However, at some sites there were no nearby weather stations, so in these situations the station that was closest and judged to be most representative of the local climate was used. The elevation differences between the soil temperature sites and the climate monitoring sites were compensated for by adjusting the measured air temperatures of the climate stations based on an average environmental lapse rate (AELR) of -6.5˚C per km of elevation change [*Wallace*, 2006]. No corrections were made for precipitation because variation in precipitation cannot be directly tied to elevation; the values reported at the KMS climate sites are used without modification.

Soil temperature data collection

Soil temperature measurements were collected using HOBO Pendent® data loggers. These have a stated measurement range of -20˚C – +70˚C, with an accuracy of ±0.5˚C and a precision of 0.1˚C. At each site the temperature loggers were buried in a 0.1 m wide trench at three depths: 0.05, 0.15, and 0.25 m. After the sensors were placed, the trench was back filled with the same soil material that was removed. Where possible, three distinct environmental types, forest, grassland, and bushland environments, as described by the UNESCO classification scheme, were targeted. In two cases, at Meru National Park and Arabuko Sokoke, disturbed areas related to land use change were also monitored. The loggers were programmed to record an instantaneous temperature measurement once every 20 minutes. The soils were monitored between May 2009 and May 2011.

Quantification of site specific canopy coverage

For this study we define canopy coverage as the total area of tree crown visible directly overhead at each instrumented site. To quantify this variable we employed a 180° circular fisheye photograph. At each soil temperature site an image of the overlying tree cover was taken looking vertically upward from ~1 m above the ground using a 10.2 Mp Nikon D200 digital camera fitted with a Sigma f2.8 180° hemispherical fisheye lens.

Image J software was used to crop the images from a full 180° so that only the vertical 60° (30° off the center point) of the image was considered. Adobe Photoshop was used to define the edge of the tree crowns using its enhanced edge finding capabilities. Image pixels that were classified as tree crown were colored black and those that did not contain tree crown, tree crown gap, were colored white. Software was written in the Interactive Data Language (IDL) programming language to import the classified images and count the number of pixels classified as tree crown. The percentage of canopy cover is defined as the percentage of pixels within the image that are classified as tree crowns.

Soil data analysis

The first step in the data analysis procedure was to trim the dataset so that only full days were considered. The first three days in the time series were removed to allow for the soil column to re-equilibrate after the installation of the temperature sensors, and the day that the instrument was retrieved was also removed from the time series. To remove outliers, the trimmed, raw data were then filtered by removing data points more

than three standard deviations from the mean. Since the loggers were undisturbed during the measurement period filtering yielded no change to the time series.

The data sets were run through a series of codes written in the IDL to extract the daily high, daily low, and the daily average temperature at each depth. The daily average temperature was obtained using the average of the daily high and the daily low temperatures, which is the method that is consistent with the KMO. The other alternative is to calculate a running average of each measurement over the day; however, damping of the diurnal signal by the soil column makes the difference between the two methods negligible as shown in Table 2.1.

Next, the annual and seasonal mean temperatures were calculated by computing the average of the data sets (annual average) and the three month sections (seasonal average) of the datasets. The code written for this task is presented in Appendix B.

Results

Table 2.2 shows: the mean annual soil temperature and standard deviation calculated from the daily mean at 0.25 m for June 2009 through June 2011, $\overline{T}_{MAST}$ and σ_{MAST}, respectively; the seasonal 0.25 m soil temperature average and standard deviation calculated from the daily mean, $\overline{T}_{"Season"}$ and $\sigma_{"Season"}$, respectively; percentage canopy cover directly overhead at each site; and the annual difference between mean annual soil temperature and the mean annual air temperature, $\overline{T}_{MAST} - \overline{T}_{air}$ referred to as the anomaly. Table 2.3 shows the elevation-corrected seasonal and mean annual air temperature and precipitation averages.

Table 2.1 - Daily average computed using two different methods. The data in this table are from the Tana River Primate Reserve Open site and were recorded on December 16, 2009.

Average Method	**Daily Average (˚C)**
Max+Min/2	34.55
Average of 20 Minute Samples	34.51

Tables 2.2 - Canopy coverage, mean annual, seasonal average, and soil temperature anomaly results for soil temperatures at 25 cm depth for June 2009 – June 2011.

Site	Canopy Cover (%)	$\bar{T}_{MAST}$ (°C)	σ_{MAST}	$\bar{T}_{JJA}$ (°C)	σ_{JJA}	$\bar{T}_{SON}$ (°C)	σ_{SON}	$\bar{T}_{DJF}$ (°C)	σ_{DJF}	$\bar{T}_{MAM}$ (°C)	σ_{MAM}	$\bar{T}_{MAST} - \bar{T}_{air}$
Arabuko Brachystegia Forest	92	28.3	1.6	26.3	0.8	27.9	1.1	28.3	0.9	30.1	0.8	**1.4**
Arabuko Cynometra Forest	99	26.0	1.1	24.6	0.7	25.5	0.8	26.4	0.4	27.1	0.6	**-0.7**
Arabuko Human Disturbed		30.5	2.4	27.1	1.0	29.5	1.1	31.4	1.2	32.1	2.3	**3.5**
Arabuko Mixed Forest	99	26.4	1.2	24.9	0.7	25.7	0.9	26.9	0.3	27.6	0.7	**-0.5**
Ilcret Bush	--	35.0	2.3	35.1	1.0	33.3	1.5	31.4	1.8	31.0	1.9	**4.8**
Ilcret Grassland		34.4	2.2	35.1	0.5	34.7	1.9	33.8	2.1	33.9	1.7	**4.1**
Kakamega Forest	94	18.7	0.5	18.2	0.3	18.3	0.4	18.8	0.5	19.2	0.4	**0.2**
Kakamega Grassland	3	19.7	0.7	18.9	0.5	19.1	0.6	18.8	0.5	19.3	0.6	**0.6**
Meru Bush	54	32.9	2.1	32.4	0.6	32.5	1.7	32.2	1.7	31.9	1.6	**5.0**
Meru Human Disturbed	5	31.8	1.4	31.5	0.9	32.5	1.4	31.4	2.0	30.3	0.9	**6.1**
Meru Forest	96	28.8	1.4	28.1	0.4	28.5	1.1	28.8	1.0	28.6	1.3	**2.5**
Meru Grassland	0	30.7	0.8	30.7	0.8	31.4	1.6	30.3	2.0	29.2	0.7	**2.7**
Mt Kenya High Forest		10.9	0.4	10.7	0.5	11.1	0.3	10.8	0.4	10.5	0.4	**0.3**

Table 2.2 continued.

Site	Canopy Cover (%)	$\bar{T}_{MAST}$ (°C)	σ_{MAST}
Mt Kenya Low Forest	100	12.7	0.7
Nairobi Bush	68	20.3	0.9
Nairobi Forest	86	19.5	0.9
Nairobi Grassland	0	22.6	1.6
Nakuru Forest	76.9	20.5	0.6
Nakuru Grassland	2.2	23.0	1.5
Shimba Hills Forest	94	23.5	1.0
Shimba Hills Grassland	0	28.6	2.5
Tana Forest	96	26.7	1.2
Tana Grassland	0	33.4	2.3
Tsavo East Bush	50	26.6	1.5
Tsavo East Forest	90	25.4	0.6

$\bar{T}_{JJA}$ (°C)	σ_{JJA}	$\bar{T}_{SON}$ (°C)	σ_{SON}	$\bar{T}_{DJF}$ (°C)	σ_{DJF}	$\bar{T}_{MAM}$ (°C)	σ_{MAM}	$\bar{T}_{MAST} - \bar{T}_{air}$
12.1	0.5	12.5	0.6	12.3	0.6	13.3	0.4	**-2.3**
17.9	0.7	19.4	0.9	20.2	0.8	20.5	0.6	**0.7**
17.6	0.6	18.6	1.0	19.6	0.9	19.4	0.6	**0.6**
19.8	0.7	21.3	1.2	11.3	0.9	11.3	0.9	**3.0**
20.0	0.5	20.1	0.3	20.6	0.6	20.7	0.6	**0.3**
21.9	1.0	22.0	0.9	23.0	1.3	22.9	1.3	**2.8**
22.5	0.6	23.2	0.8	24.7	0.4	24.7	0.5	**-1.0**
25.2	0.8	27.8	1.1	28.8	2.0	29.7	2.2	**4.1**
25.2	0.6	26.2	0.9	27.5	0.5	27.6	0.7	**-3.2**
30.0	1.1	31.8	1.4	34.7	1.1	33.6	1.6	**3.4**
24.5	0.5	26.4	1.5	27.4	1.0	26.8	0.7	**-0.7**
24.6	0.4	25.5	0.8	25.8	0.6	25.5	0.4	**-1.8**

Table 2.2 continued.

Site	Canopy Cover (%)	$\bar{T}_{MAST}$ (°C)	σ_{MAST}	$\bar{T}_{JJA}$ (°C)	σ_{JJA}	$\bar{T}_{SON}$ (°C)	σ_{SON}	$\bar{T}_{DJF}$ (°C)	σ_{DJF}	$\bar{T}_{MAM}$ (°C)	σ_{MAM}	$\bar{T}_{MAST} - \bar{T}_{air}$
Tsavo East Grassland	0	29.9	1.7	27.8	0.7	29.5	1.4	30.5	1.8	30.3	1.1	**2.7**
Tsavo West Bush	34	26.7	1.6	25.5	0.7	28.1	1.3	26.4	1.2	25.4	0.8	**2.3**
Tsavo West Grassland	34	29.2	1.8	27.5	0.9	30.1	1.5	27.9	1.2	-	-	**4.8**

Table 2.3 – Elevation corrected mean air temperature and precipitation measurements from nearby climate monitoring sites. Elevation was corrected using an average environmental lapse rate of 6.8°C per kilometer. There is no correction for precipitation.

		Air Temperature °C					Precipitation (mm)				
Site	**Elevation Correction**	**JJA**	**SON**	**MAM**	**DJF**	**MAT**	**JJA**	**SON**	**DJF**	**MAM**	**Total**
Arabuko Brachystegia Forest	**-0.1**	25.6	26.5	28.3	27.2	26.9	276.4	379.7	9.5	648.7	1314.3
Arabuko Cynometra Forest	**-0.3**	25.5	26.3	28.1	27.1	26.7	276.4	379.7	9.5	648.7	1314.3
Arabuko Human Disturbed	**0.0**	25.8	26.6	28.4	27.4	27.0	276.4	379.7	9.5	648.7	1314.3
Arabuko Mixed Forest	**-0.1**	25.6	26.5	28.3	27.2	26.9	276.4	379.7	9.5	648.7	1314.3
Ilcret Bush	**0.5**	30.5	31.3	30.0	29.2	30.2	0.0	21.0	112.7	134.2	267.9
Ilcret Grassland	**0.5**	30.5	31.3	30.0	29.3	30.3	0.0	21.0	112.7	134.2	267.9
Kakamega Forest	**-2.7**	17.7	18.6	19.3	19.2	18.7	404.0	430.3	410.3	698.8	1943.4
Kakamega Grassland	**-2.3**	18.2	19.0	19.8	19.6	19.1	404.0	430.3	410.3	698.8	1943.4
Meru Bush	**-1.4**	26.5	27.8	28.7	28.9	28.0	6.7	117.9	138.3	280.0	542.9
Meru Human Disturbed	**-3.5**	24.4	25.7	26.6	26.7	25.8	6.7	117.9	138.3	280.0	542.9
Meru Grassland	**-3.0**	24.9	26.2	27.1	27.2	26.4	6.7	117.9	138.3	280.0	542.9
Meru Forest	**-1.3**	26.6	27.9	28.8	28.9	28.1	6.7	117.9	138.3	280.0	542.9
Mt. Kenya High Forest	**-7.3**	10.6	11.0	11.2	10.9	10.9	97.6	145.6	195.9	357.9	797.0

Table 2.3 continued.

Site	Elevation Correction	JJA
Nairobi Bush	**0.6**	20.1
Nairobi Forest	**-0.1**	19.5
Nairobi Grassland	**0.7**	20.2
Nakuru Forest	**0.7**	19.9
Nakuru Grassland	**0.7**	19.9
Shimba Hills Forest	**-2.4**	23.3
Shimba Hills Grassland	**-2.4**	23.4
Tana Forest	**0.6**	28.4
Tana Grassland	**0.7**	28.6
Tsavo East Bush	**3.5**	25.3
Tsavo East Forest	**3.5**	25.3
Tsavo East Grassland	**3.5**	25.3
Tsavo West Bush	**0.7**	22.6
Tsavo West Grassland	**0.7**	22.6

Air Temperature°C				Precipitation (mm)				
SON	MAM	DJF	MAT	JJA	SON	DJF	MAM	Total
20.1	17.9	20.1	19.6	303.5	724.0	118.3	186.7	1332.5
19.4	17.2	19.4	18.9	303.5	724.0	118.3	186.7	1332.5
20.1	17.9	20.2	19.6	303.5	724.0	118.3	186.7	1332.5
20.4	20.2	20.3	20.2	71.7	219.5	303.0	582.7	1176.9
20.4	20.2	20.3	20.2	71.7	219.5	303.0	582.7	1176.9
24.2	26.0	24.9	24.6	276.4	379.7	9.5	648.7	1314.3
24.2	26.0	24.9	24.6	276.4	379.7	9.5	648.7	1314.3
29.8	30.6	30.8	29.9	6.7	117.9	138.3	280.0	542.9
29.9	30.8	30.9	30.0	6.7	117.9	138.3	280.0	542.9
27.4	27.4	28.2	27.1	13.4	112.1	296.3	237.8	659.6
27.4	27.4	28.2	27.1	13.4	112.1	296.3	237.8	659.6
27.4	27.4	28.2	27.1	13.4	112.1	296.3	237.8	659.6
24.7	24.7	25.5	24.4	13.4	112.1	296.3	237.8	659.6
24.7	24.7	25.5	24.4	13.4	112.1	296.3	237.8	659.6

Because of the proximity to the equator for these sites, there is very little annual variation in mean daily soil temperature over the course of the year; the principal changes are due to the progression of the rainy seasons caused by migration of the ITCZ and the transition of the monsoons [*Nicholson*, 1996]. Throughout the soil temperature sites, the annual variance in deep soil temperature ranges from 0.5-2.5°C. The highest temperatures and variability within this data set are associated with open grassland and bushland locations where the mean annual average soil temperatures range from 20 to 35°C with an average standard deviation of 1.7° C. Conversely, the average soil temperature standard deviation in all the forest sites is 0.85° C. The hottest mean annual soil temperatures were recorded in the Turkana Basin near Ileret where daytime maximum temperatures at 0.25 m were >37 °C (Figure 2.2) during the warmest season. In the Turkana Basin mean annual soil temperatures were between 33 and 35°C (Figure 2.3). Seasonal averages of soil temperature at 25 cm depth and the associated seasonal standard deviations are presented in Figure 2.4. Seasonally there is much more variance in soil temperature, due mostly to fluctuations in soil moisture content caused by the wet and dry seasons and this varies greatly depending on the strength of the given season.

Seasonally, the two hottest locations observed are within the Turkana Basin at Ileret and at the Tana River Primate Reserve. In the Turkana Basin, the hottest season averaged over the two years of data collection is during the months of June, July, and August. At the Tana River Primate Reserve the season with the hottest deep soil temperatures is observed during the months of December, January and February and the seasonal average during this time period is 33±1.2°C.

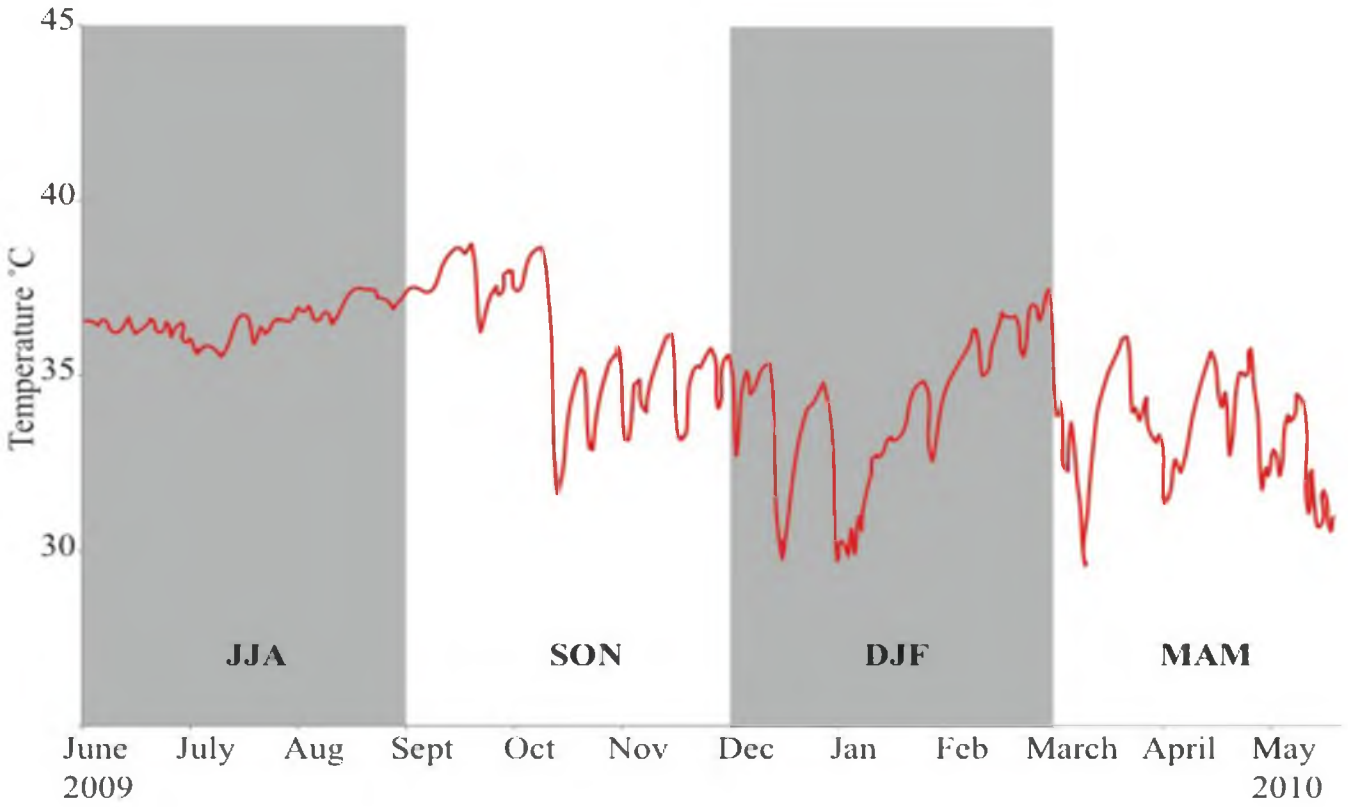

Figure 2.2 – One year of data from June 1, 2009 until May 20, 2010 at the Ileret Field station of the Turkana Basin Institute measured at 0.25 m depth. This figure illustrates the hottest deep soil temperatures observed during October 2009.

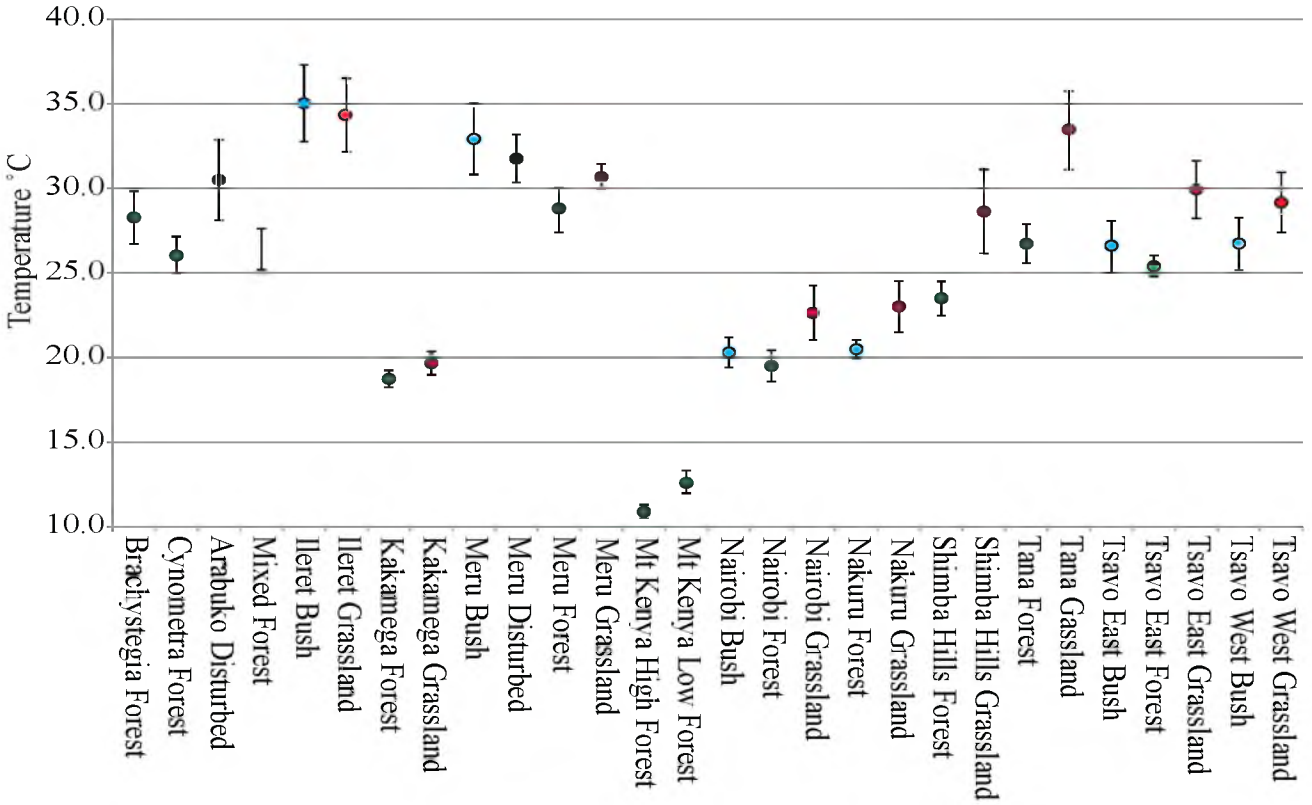

Figure 2.3 – Plotted are the mean annual soil temperatures at 0.25 m depth with standard deviation plotted on the top of each bar. Colors correspond to type of vegetation cover where red indicates grassland localities, green indicates forested localities, and blue indicates bushland localities

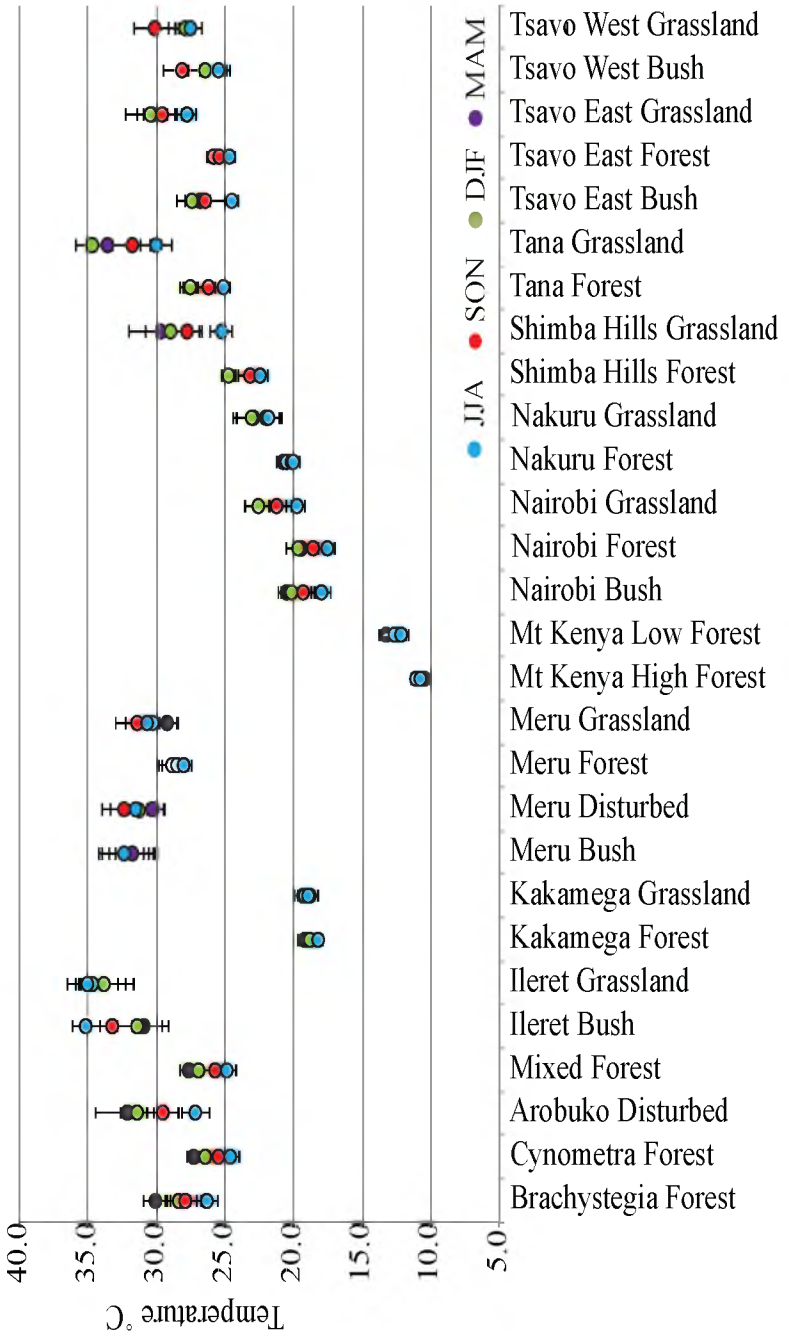

Figure 2.4 - Seasonal average soil temperatures at 0.25 m. Standard deviation over the season is plotted with the bars over each point. Colors correspond to the season where blue indicates JJA, red indicates SON, green indicates DJF, and purple defines MAM.

Temperature and precipitation from surrounding weather stations are presented in Figure 2.5 and Figure 2.6, respectively. Climate information is not directly measured at the soil temperature sites and represents regional climate conditions. The difference in observed mean annual soil temperature (MAST) and mean annual air temperature (MAT) can be described by the soil temperature difference, which is simply the difference between the observed MAT and the MAST. The soil temperature difference is presented in Figure 2.7 and is described by Equation 1

$$\Delta T_{soil-air} = \overline{T}_{MAST} - \overline{T}_{MAT} \tag{1}$$

where $\Delta T_{soil-air}$ is the temperature anomaly $\overline{T}_{soil}$ is the mean annual soil temperature and $\overline{T}_{air}$ is the mean annual air temperature that has been corrected for the elevation difference between the soil temperature sites and climate station location using the AELR. $\Delta T_{soil-air}$ is discussed further in section 2.4.1.

Discussion

Soil temperature relationship to ecology and local climate

The spatial variation in the observed soil temperature can be broken down into two parts, as both local climate and ecology have important influences on soil temperature. In the study region, temperature variations are principally a function of elevation, as shown by a regression of the mean annual soil temperatures against altitude. It is necessary to separate the sites as the thermal regimes of forest soils are much different than those in bushland and grassland locations.

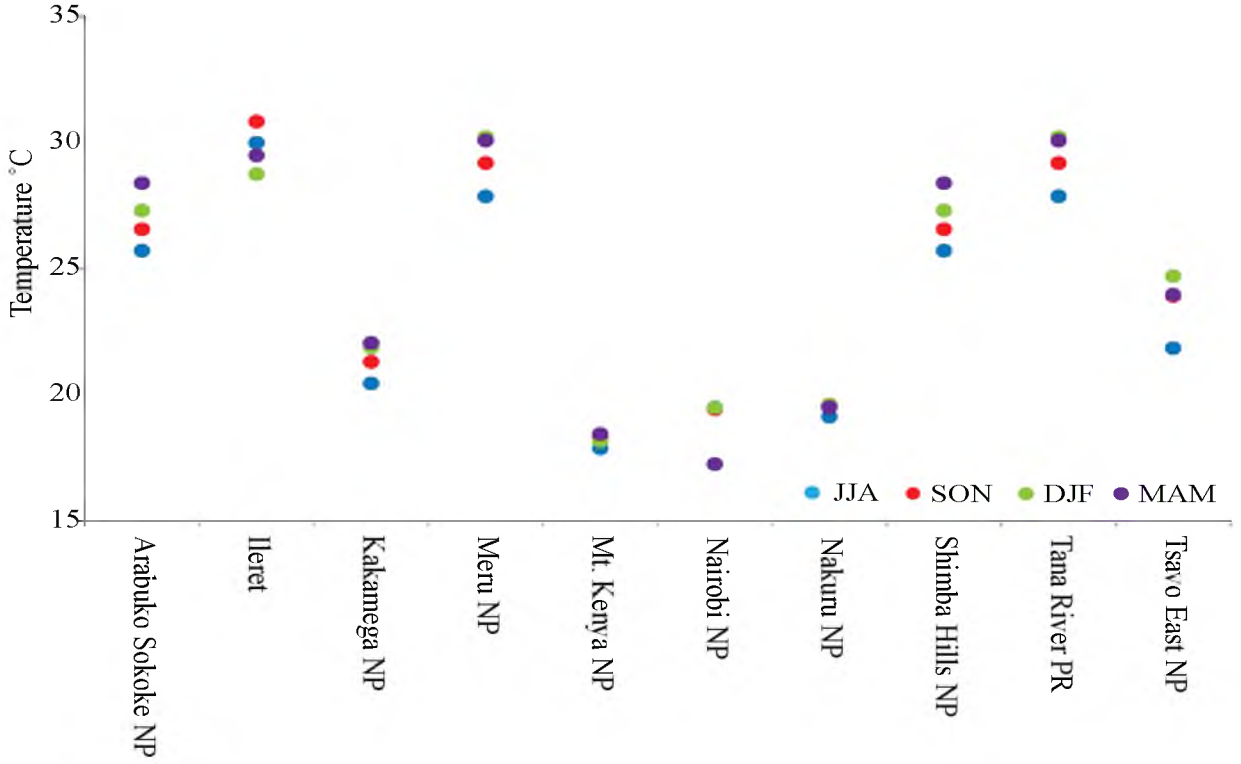

Figure 2.5 - Seasonal averaged 2 m air temperatures from nearby weather stations. The data were obtained from Kenya Meteorological Service. Colors are as in Figure 2.4.
*NP=National Park, PR= Primate Reserve

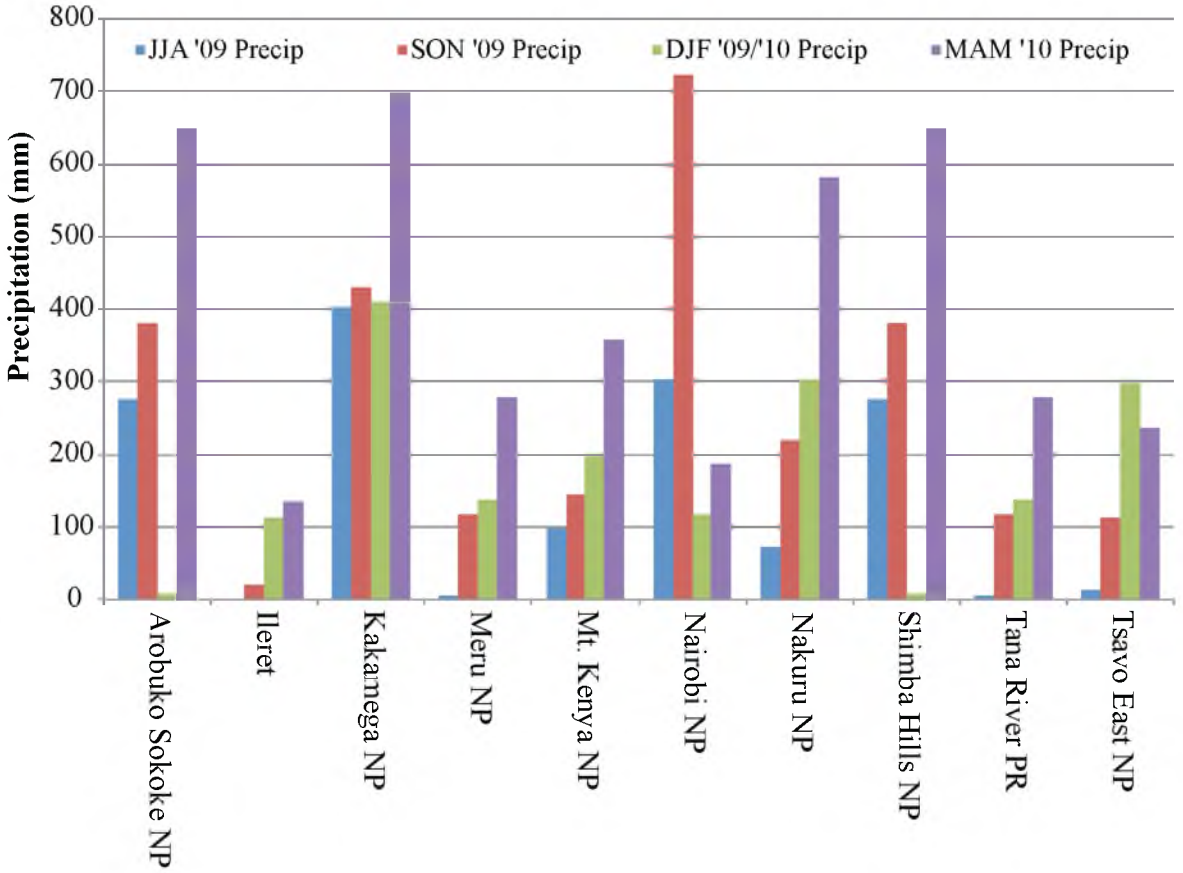

Figure 2.6 - Seasonal precipitation amounts at the weather stations near the measurement sites. Colors are as in Figure 2.4

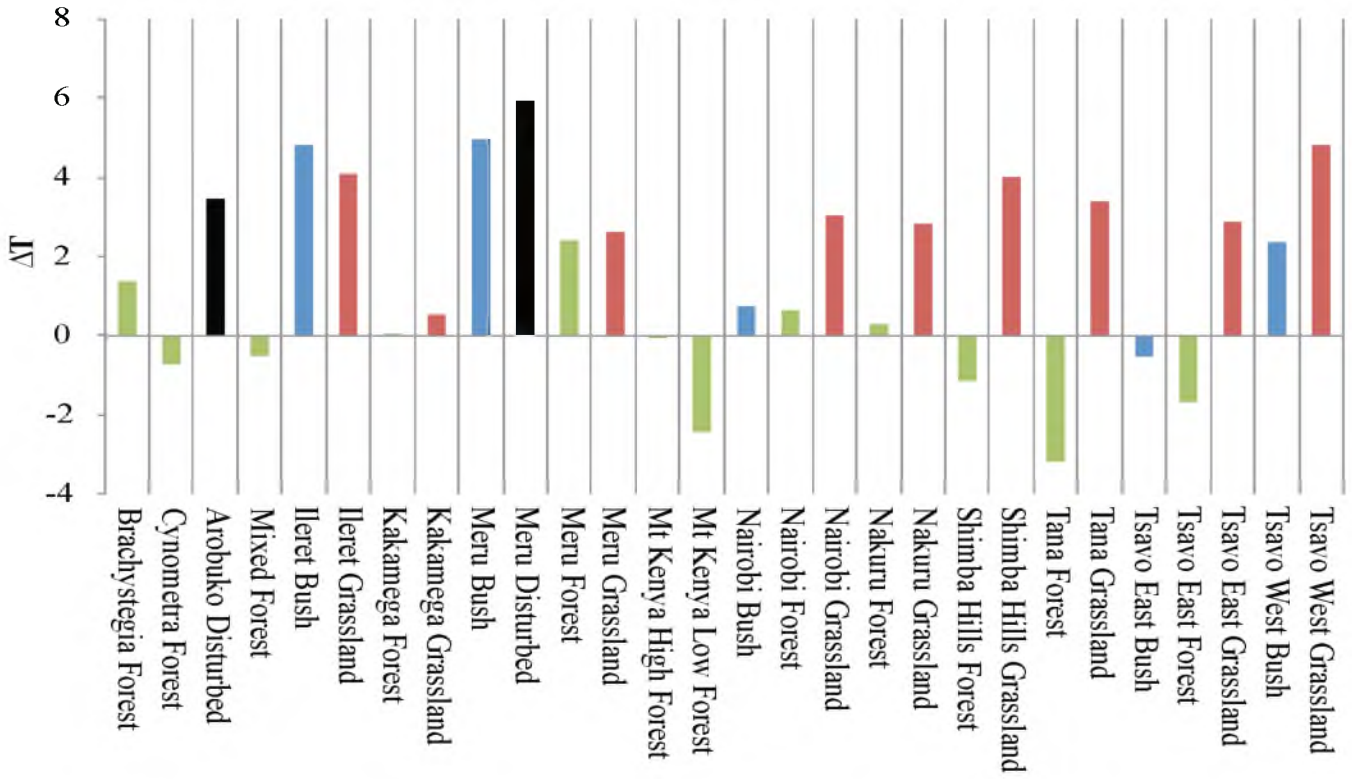

Figure 2.7 - Seasonal temperature anomalies (mean annual soil temperature difference from mean annual air temperature). Colors correspond to the type of vegetation cover: Blue, bushland; green, forest; red, open grassland. Anthropogenically disturbed areas are shown in black. For the bushland and grassland the anomaly is almost exclusively positive indicating that the ground is warmer than the air. In forested localities the ground is cooler than air because of shading from the sun.

The elevation and soil temperature relationships for Kenya are described by Equations 2 and 3 (Figure 2.8).

$$\text{Grassland/Bushland} \quad T(z) = 33.8 - 6.84z \qquad R^2 = 0.75 \tag{2}$$

$$\text{Forest} \quad T(z) = 27.6 - 5.34z \qquad R^2 = 0.94 \tag{3}$$

where z is elevation in kilometers.

We now consider the relationship between canopy cover and soil temperatures. In addition to being a strong function of elevation, soil temperature should also be a strong function of vegetation cover because of the influence of direct solar radiation on the surface energy budget and thus, the amount of available energy for heating the soil surface. In open grassland settings there is little shade so there is direct exposure of the soil surface to solar radiation. In forested settings, most of the daily solar radiation is captured in the high canopy, thus shading the understory and the soil surface. In addition, the forest soils contain more water as the root zone acts to pull deep moisture to the surface through the process of hydraulic lift [*Caldwell et al.*, 1998]. Surface shading and higher moisture content within a forest result in lower daily maximum soil and air temperatures. This effect is shown in Figure 2.9. Soil temperatures used in this figure were normalized to an elevation of zero using Equations 2 and 3 depending on the particular ecological setting. It is clear from this figure that canopy cover has a strong effect on the mean annual soil temperature, which can be described by Equation 4

$$T_{soil}(x) = 34.4 - 0.07x \tag{4}$$

where x is the percentage of forest canopy cover. As the percentage of canopy cover increases

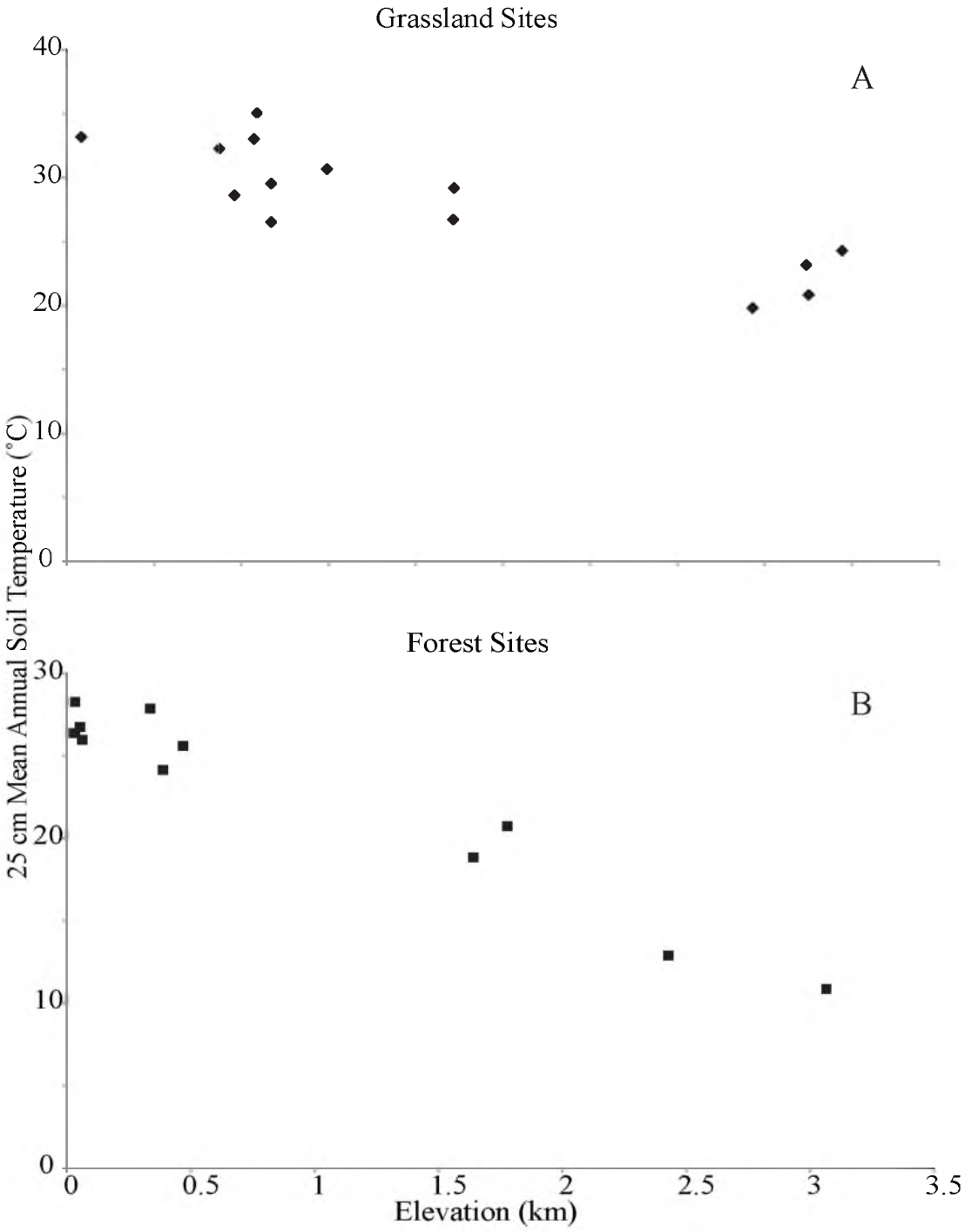

Figure 2.8 - Mean annual soil temperature and elevation. A shows this relationship for Grassland and bushland vegetation types, B shows this relationship for Forest sites.

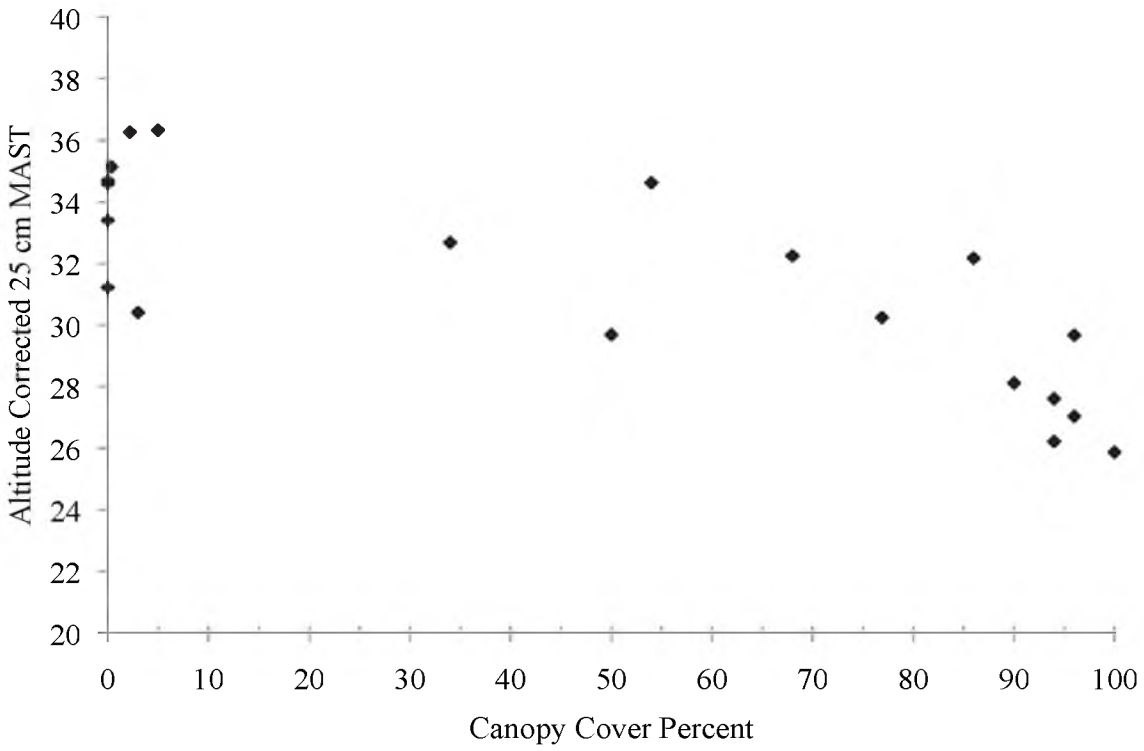

Figure 2.9 - The relationship of canopy cover to the annual mean soil temperature at 25 cm normalized to zero elevation. Temperatures were corrected using Equations 2 and 3 for the respective environments.

from opened to closed the mean annual soil temperature is greatly lowered.

The effect of vegetation cover, particularly woody forest cover, can be explored further by referring to Figure 2.7 and looking at the soil temperature anomaly. Air temperatures in this figure were corrected for the elevation difference between the place of measurement and the soil temperature site. From this figure the effect of shading by vegetation cover is that soil temperatures are similar to or slightly less than air temperatures, whereas in open and bushland sites mean annual soil temperatures are much higher and have a larger deviation from air temperature.

Soil temperature relationship to soil carbonate formation

The formation of carbonates occurs when pore water percolating within the soil column becomes supersaturated with respect to calcite. For a full review of carbonate formation and techniques for extracting the temperature of formation, refer to *Eiler* [2011] and *Cerling* [1984]. The governing equation of the reaction is demonstrated in Equation 5

$$CaCO_3 + P(CO_2) + H_2O = Ca^{2+} + 2HCO_3^- \quad K_{cal} = \frac{\left[\left(Ca^{2+}\right)\right]\left[\left(HCO_3^-\right)\right]}{\left[P\left(CO_2\right)\right]} \tag{5}$$

where $P(CO_2)$ is the partial pressure of carbon dioxide in the soil, K_{cal} is the equilibrium constant, and the brackets denote the activities of the aqueous species. It is assumed that water has an activity of 1.0. There are several ways in which carbonate formation is favored. First is a reduction in the partial pressure of carbon dioxide; this occurs during periods of high water stress on vegetation when plant growth is diminished and when root

respiration is decreased. Second is by increasing the activities of calcium or carbonate in the pore fluid; this results from chemical

discrimination as water is removed from the system due to root uptake and when calcium and bicarbonate is excluded from uptake. Third, supersaturation can result from an increase in soil temperature, thereby reducing the solubility of carbon dioxide because of its retrograde solubility. Thus, these three drivers of carbonate formation all occur during periods of elevated soil temperature and aridity and enhance each other. It is therefore likely that the carbonate precipitation may have a strong seasonal bias toward the warmest and driest seasons [*Breecker et al.* 2009].

With conditions conducive to carbonate formation in mind, along with consideration of the soil temperature and precipitation data shown in Figures 2.5 and 2.6, respectively, the seasons in which conditions most likely to be representative of periods of carbonate formation start to become clear. Because carbonates are precipitated during the "drying out" phase of the soil column we expect that the temperature preserved during carbonate formation will be representative of hotter and dryer seasons. To better elucidate the temperatures present during the hottest and driest times of the year refer to Figure 2.10 where two years of the daily average temperatures observed at 25 cm depth in each microclimatological setting at four different study areas are plotted.

In all cases the hottest temperatures are observed in the open setting. In areas such as Kakamega forest (upper right of Figure 2.10) the difference in deep soil temperature between the open and forest setting is small, ~1˚C on average. In places such as the Tana River Primate reserve (lower right of Figure 2.10), the difference between soil temperature in the forest and in the open is ~7˚C warmer than in the forest.

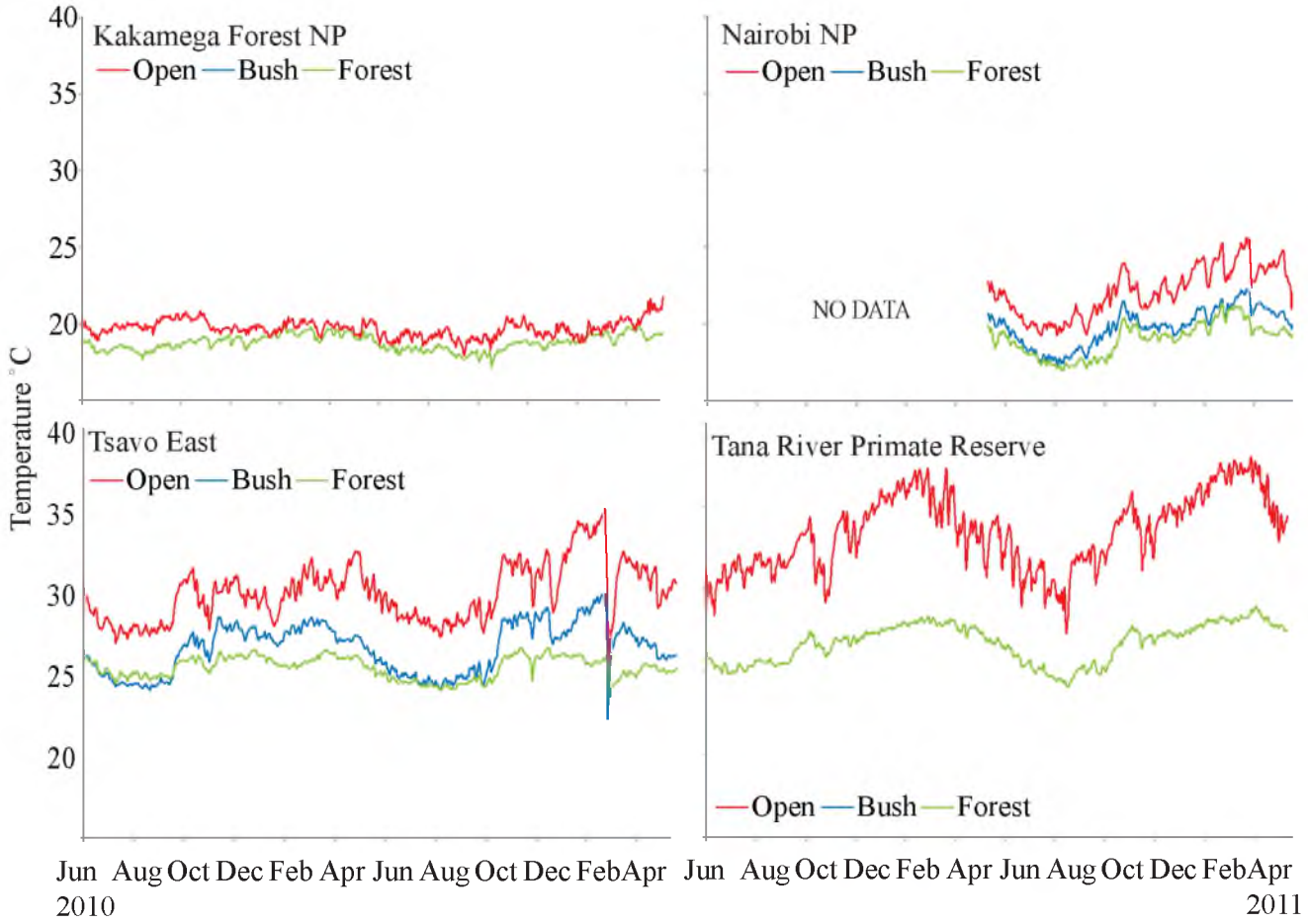

Figure 2.10 - Daily averaged temperature at a depth of 0.25 m from the different microclimatological settings from four different national parks and reserves. Colors are as in Figure 2.3.

It would be expected that soil carbonates would form, using the justification above, during the hottest parts of the year, which occur in the later part of the DJF season. Therefore, recording soil temperatures that are likely about 37-38 ˚C. However, in places such as Kakamega forest, it would be unlikely to observe much carbonate formation due to the large amounts of annual rainfall.

Land use effects on soil temperature

The areas surrounding the national parks in Kenya are prone to land use changes where pristine grassland and forests are removed for the purposes of agriculture. Over the past 50 years there has been a steady increase in the total land area used for agriculture such as cultivation and grazing, shown in Figure 2.11 [*World Bank*, 2012]. The driving factor in this increase appears to be the steady increasingly rapid rise in human population in Kenya also shown in Figure 2.11.

In this section we look at two parks that have experienced such land use changes. At Arabuko Sokoke National Forest the forest has been cleared for construction of a main road connecting Mombasa with Malindi, with small scale farming taking place between the road and the forest. At Meru National park, a small community lies along the park boundary where there has been a significant amount of cattle grazing, to the point of stripping the land to bare soil leaving only tall bushes. To assess the effects of these disturbances, soil temperatures were monitored in the disturbed areas. Referring to Figure 2.12 and comparing the community setting with the other ecological settings at Meru National Park, there are no easily discernable differences due to the effects of overgrazing. The differences observed at Meru are most likely due to the meteorological

conditions of the area during the study period. During that period there was a severe drought and limited vegetation coverage across the entire park. However, at Arabuko Sokoke National Forest (Figure 2.13) the effect of removing the forest is very clear.

Comparison of each season reveals that the cleared areas are 2–5 degrees C higher than the surrounding forested settings. In conditions of the area during the study period there was a severe drought and limited vegetation coverage across the entire park. However, at Arabuko Sokoke National Forest, in addition to the higher seasonal averages, the seasonal standard deviation of the temperature is greater than is observed in the forest indicating that the cleared areas are much more prone to daily temperature fluctuations caused by more solar insolation reaching the soil surface.

Conclusions

Soil temperatures relevant to soil carbonate formation were evaluated for tropical soils in Kenya. Seasonal variation in soil temperatures is minimized by the small seasonal temperature fluctuations near the equator. Soil carbonates generally form at depths below approximatly 25 cm, by which depth the daily temperature fluctuation is attenuated to less than 2°C. Soil temperatures are related to site air temperature, with forested sites having values similar to air temperatures within approximatly 2°C, but bush and open sites have temperatures up to 7°C higher than average meteorological air temperatures. These results confirm that high soil temperatures (30 to 40°C) recorded by paleosol carbonates in the Turkana Basin using the Δ47 method [*Passey et al.*, 2010] are in the range of observed soil temperatures for hot, arid regions of East Africa. Land use change results in higher soil temperatures, especially where forests are cleared for

farming. Soil temperatures in disturbed, previously forested areas were approximatly 4°C hotter than the equivalent ecosystem in the Arabuko Sokoke Forest.

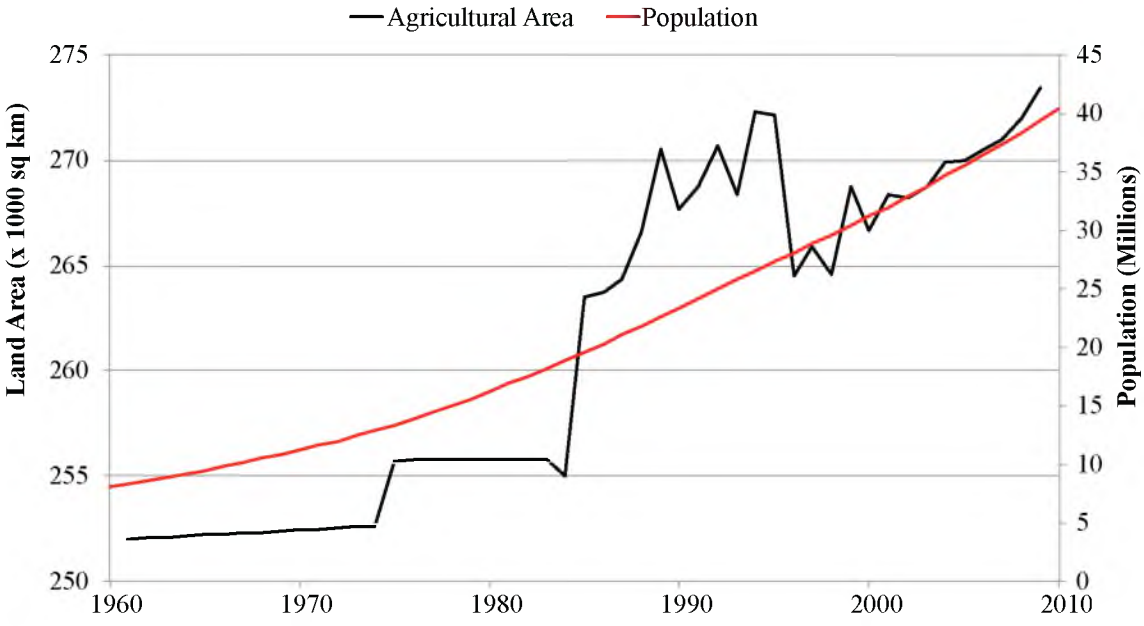

Figure 2.11 – Total land area in Kenya that has been designated for agriculture and population during the past 60 years. Data comes from the World Bank (2012).

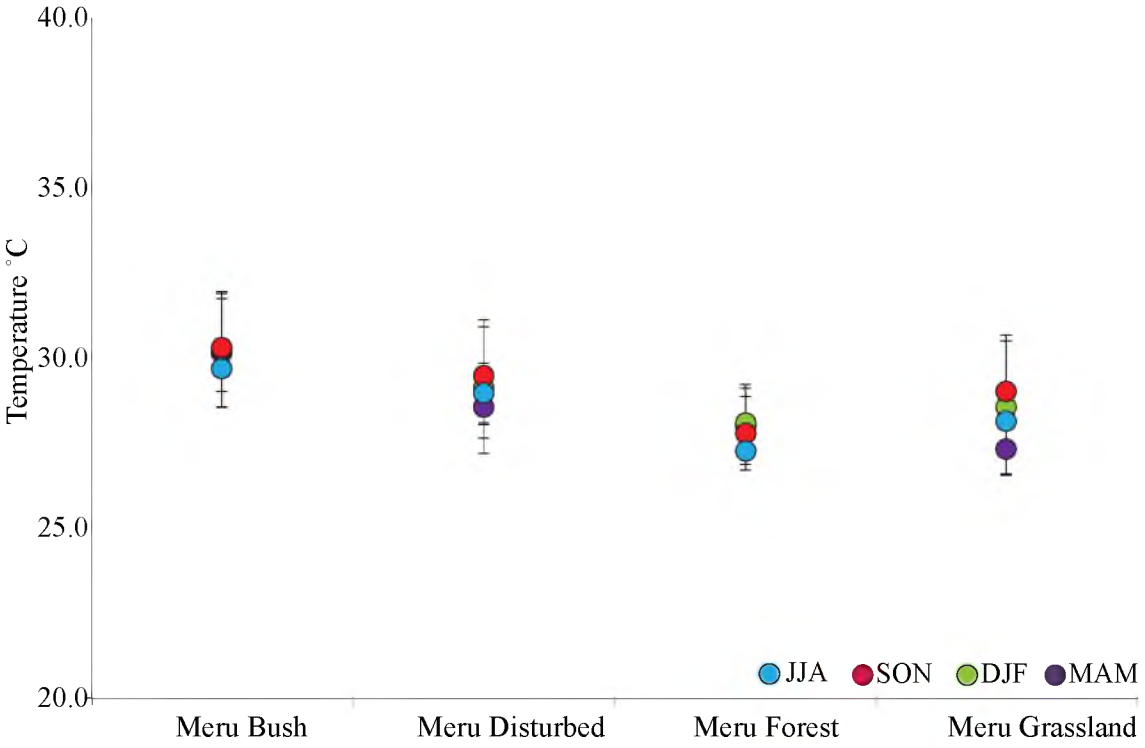

Figure 2.12 - Seasonal averaged soil temperatures at all four Meru vegetation settings. The community setting is very similar to the bush site as there is little grass and it is characterized by predominantly acacia bushes. The effects of grazing are not prevalent between the grassland and bushland sites in this plot, however, this sampling interval was skewed by a significant drought in the area.

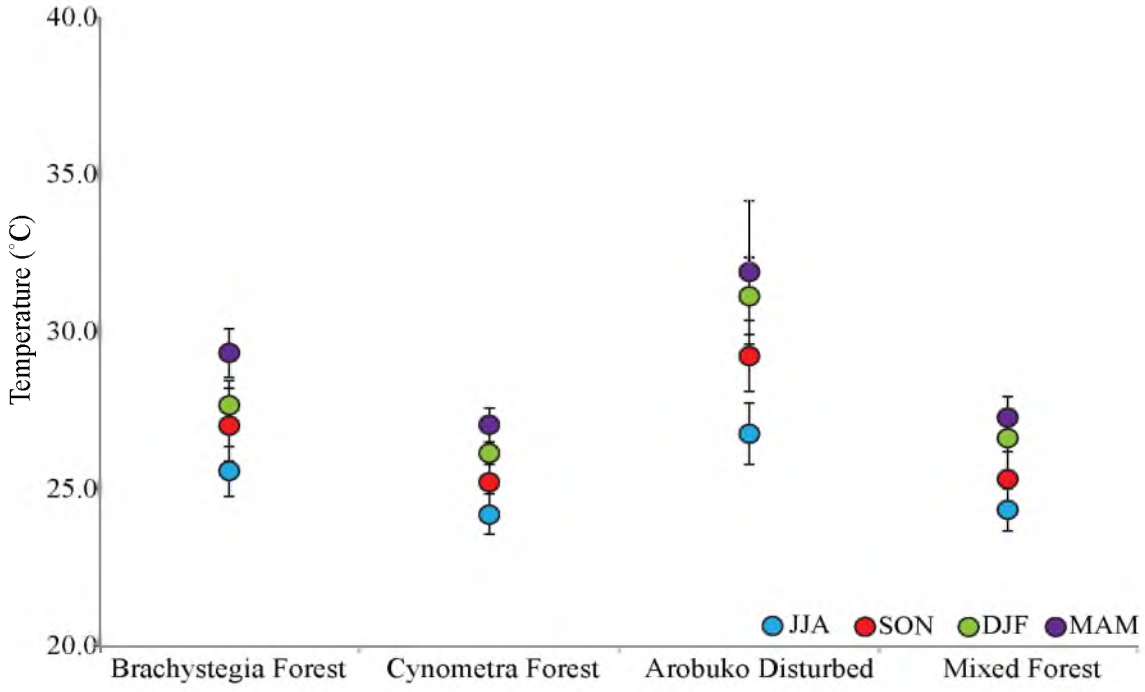

Figure 2.13 - Mean annual temperatures at Arabuko Sokoke National Forest. This figure illustrates the changes in the thermal regime of the soil because of deforestation

References

Breecker, D. O., Z. D. Sharp, and L.D. Mcfadden (2009), Seasonal bias in the formation and stable isotopic composition of pedogenic carbonate in modern soils from central New Mexico, USA, *Geological Society of America Bulletin 121*(3-4): 630–640.

Caldwell, M. M., T. E. Dawson, and J.H. Richards (1998), Hydraulic lift: Consequences of water efflux from the roots of plants, *Oecologia 113*(2): 151–161.

Cerling, T. E. (1984), The stable isotopic composition of modern soil carbonate and its relationship to climate, *Earth and Planetary Science Letters 71*(2): 229–240.

Cerling, T. E., N. E. Levin, and B.H. Passey (2011), Stable isotope ecology in the Omo-Turkana Basin, *Evolutionary Anthropology 20*(6): 228–237.

Cerling, T. E., N. E. Levin, J. Quade, J.G. Wynn, D.L. Fox, J.D. Kingston, R.G. Klein, F.H. Brown (2010), Comment on the paleoenvironment of Ardipithecus ramidus, *Science 328*(5982): 1105.

Kenya Meteorological Department (2012), Climatological Data, 2012, from http://www.meteo.go.ke/data/.

Eiler, J. M. (2007), "Clumped-isotope" geochemistry-The study of naturally-occurring, multiply-substituted isotopologues, *Earth and Planetary Science Letters 262*(3-4): 309–327.

Eiler, J. M. (2011), Paleoclimate reconstruction using carbonate clumped isotope thermometry, *Quaternary Science Reviews 30*(25-26): 3575–3588.

Geiger, R., R. H. Aron (2009), *The Climate Near the Ground*, Rowman & Littlefield, Lanham, MD.

Ghosh, P., J. Adkins, H. Affek, B. Balta, W. Guo, E.A. Schauble, D. Schrag, J.M Eiler (2006), ^{13}C-^{18}O bonds in carbonate minerals: A new kind of paleothermometer, *Geochimica et Cosmochimica Acta 70*(6): 1439–1456.

Griffiths, J. F. (1972), *Climates of Africa*, Elsevier Pub. Co., Amsterdam, New York.

Jury, W. A. and R. Horton (2004), *Soil Physics*, John Wiley, New York.

Lal, R. and M. Shukla (2004), *Principles of Soil Physics*, M. Dekker, New York.

Nicholson, S. E. (1996), A review of climate dynamics and climate variability in Eastern Africa. *The Limnology, Climatology and Paleoclimatology of the East African Lakes*, Gordon and Breach**:** 25–56, Amsterdam, The Netherlands.

Passey, B. H., N. E. Levin, T.E. Cerling, F.H. Brown, and J.M. Eiler (2009), High-temperature environments of human evolution in East Africa based on bond ordering in paleosol carbonates, *Proceedings of the National Academy of Sciences*. *107*(25):11245–11249.

Ratnam, J., W. J. Bond, R. J. Fensham, W. A. Hoffman, S. Archibald, C. E. R. Lehmann, M. T. Anderson, S. I. Higgins, and M. Sankaran (2011), When is a 'forest' a savanna, and why does it matter?, *Global Ecology and Biogeography 20*(5): 653–660.

Wallace, J. M. and P. V. Hobbs (2006), *Atmospheric Science: An Introductory Survey*, Elsevier Academic Press, New York.

White, F. (1983), The Vegetation of Africa, Natural Resources Research, Vol. 20 United Nations Scientific and Cultural Organization, Paris.

White, T. D., S. H. Ambrose, G. Suwa, and G. Woldgabriel (2010), Response to comment on the paleoenvironment of *Ardipithecus ramidus*, *Science 328*(5982): 1105.

World Bank, Agricultural Land (sq. km), Food and Agriculture Organization, electronic files and web sites, http://data.worldbank.org/, retreived from web 2012.

World Bank, Population Total, electronic files and web sites, http://data.worldbank.org/, retreived from web 2012.

CHAPTER 3

TROPICAL ENVIRONMENTAL SURFACE TEMPERATURES PRESENTED AS A COMPOSITE DAY

Abstract

The soil temperature across any landscape can vary greatly and have a large influence on the daily routines of many of the floral and faunal inhabitants. In the following study we compare soil surface temperatures from three different microclimates that are common in Kenyan landscape mosaics: grasslands, bushland, and forest. Soil surface temperatures were calculated from subsurface soil temperature profiles using an iterative inversion solution to the 1 dimentional heat diffusion equation. The results are presented as a statistical composite day, which effectively shows the average evolution of an equatorial diurnal cycle. The temperature difference observed between surface temperatures present in open grassland settings and those present in forests is often on the order of 20˚C during the hottest parts of the day. During the night the temperature difference between the different microclimates is reduced to near zero. In the open the average daily temperature range is 25–30˚C, whereas in the forest this range is 5–10˚C

Introduction

It has been proposed that hot settings, such as the Turkana Basin in Northern Kenya, the Awash Valley in Ethiopia, and Olduvai Gorge in Northern Tanzania were main stages for the development and evolution of early hominids [*Bobe*, 2009]. Preliminary paleothermometry results from East African hominid fossil sites using the Δ47 method suggest that hot environments with average soil temperatures between 30 and 40°C have existed in these areas for much of the past 1–4 million years [*Passey*, 2009] and today, environments located within the Turkana Basin are amongst the hottest 1% of places worldwide with a mean annual air temperature of 29.2˚C [*Hijmans*, 2005]. If hominids did evolve under such extreme temperature conditions, they would have had to deal with considerable thermal stress.

Thermoregulatory advantages of modern humans such as sweating, bipedalism, and reduced body hair are thought to have resulted from evolutionary adaptations to exposure in such extreme hot and dry environments [*Ruxton and Wilkinson*, 2011; *Wheeler* 1984, 1991, 1992; *Ruff*, 1991). In addition to these proposed adaptations there is evidence to suggest adaptations of the human brain [*Falk*, 1990] and skin [*Jablonski and Chaplin*, 2000, 2010] also aided in dealing with the high thermal heat load that early hominids would have been regularly exposed to in tropical midday environments. Although significant, these adaptations alone are not sufficient to have enabled hominids to survive in hyperthermic environments such as those found in sub-Saharan Africa today. It would have been likely, as it still is for modern humans today to take advantage of the spatial thermal differences and take refuge in cooler shaded areas such as a forested riparian zone or within the shade of local flora.

Across landscapes temperatures within different microclimates can be very different and are a function of the amount of shade provided by the surrounding flora [*Geiger*, 1965]. Although the differences between the different microclimates are not documented well, human and animal behaviors suggest that they can be quite large, as many seek shade during the peak of the diurnal temperature cycle. The landscape in which hominids resided is debated, and ranges from closed forests to open savannas [*Cerling et al.*, 2010; *Potts*, 1998; *White et al.* 2009; *White et al*, 2010]. Most evidence in the sedimentary record in these areas suggests that the predominant settings would have been riparian zones, deltaic environments, floodplains, and lake margins [*Feibel*, 2012; *Feibel et al*, 1991].

In the following chapter we describe continuous subsurface soil temperature profiles collected over a two year period from June 2009 until May 2011 from which we estimate the soil surface temperature and illustrate the strong environmental differences present. The areas selected for this study were chosen because they are thought to be close representatives of the types of environmental composites present in the Turkana Basin, Awash Valley, and Olduvai Gorge 1–4 million years ago during the time when humans evolved.

We use soil temperature profiles from open, bush covered, and forested sites in two lowland sites, Meru National Park and Tana River Primate Reserve, and one highland site, Nairobi National Park. Using soil diffusivity models, we invert the soil temperature time series to derive the soil surface temperature time series. We use the acquired surface temperature time series to produce a "statistical composite day" whereby, seasonal hourly averages of the ground surface temperature represent a seasonally

averaged day within different microclimates. We then discuss these results in the context of environmental differences at the landscape scale.

Methods and Materials

Soil temperature data collection

Soil temperature measurements were collected using HOBO Pendent® data loggers; these have a stated measurement range of -20°C – +70°C, with an accuracy of ±0.5°C and a precision of 0.1°C. At each site the temperature loggers were buried in a 0.1 m wide trench at three depths: 0.05, 0.15, and 0.25 m. After the sensors were placed the trench was then back filled with the same soil material that was removed. Where possible, three distinct environmental types, forest, grassland, and bushland environments, as described by the UNESCO classification scheme [*White*, 1973], were targeted. In some cases, disturbed areas related to land use change were also monitored. The loggers were programmed to record an instantaneous temperature measurement once every 20 min. The soils were monitored between May 2009 and May 2011.

Site selection and description

Latitude, longitude, and elevations for the study sites are given in Table 3.1 and a DEM with the study sites is presented in Figure 3.1.

Meru National Park (MNP) is located on the equator in Central Kenya on the eastern flank of the East African Highlands. The average elevation of the park is about 400 m and covers an area of ~900 km^2 that is composed of mostly open grassland and bushland. The Tana River runs along the southern edge of Meru Park along the boundary

with Mwingi National Reserve and Kora National Park to the south. Along the river there is a dense riparian forest that varies in width from a few meters to tens of meters. Within this riparian forest the average canopy coverage is about 70% as calculated from circular fisheye photography. Soil temperatures were logged at three locations within this park, one in grassland, one in bushland, and one in a riparian forest zone.

Nairobi National Park (NNP) is located at approximately 1.3° S latitude. It is situated south of the city of Nairobi at an average elevation of 1650 m. The park covers an area of about 117 km^2 and is composed of mostly grassland to the southeast and forest to the northwest with a transition from grassland to bushland to forest over several 100 m. A dry deciduous forest is situated in the extreme northwestern part of the park with average canopy coverage of 86%. As at Meru, instruments were placed in open grassland, under heavy bush cover, and in a forested site.

The Tana River Primate Reserve (TRPR) is located at approximately 1.8° S latitude in Eastern Kenya along the Tana River. The reserve includes a dense, closed-canopy riparian forest along the Tana River with marginal grasslands and bushland. The riparian zone in this area ranges in width from a few tens of meters to several 100 m. Canopy coverage throughout the forest zone is ca 90%. This riparian forest is home to two endangered endemic species of monkey, the Tana River Mangabey (*Cercobus galeritus*) and the Tana River Red Colobus Monkey (*Procolobus rufomitratus*). At this location, records were taken at two sites, one in open grassland/bushland and the other within the dense riparian forest.

Table 3.1 – Latitude, longitude, and elevation of the selected soil temperature sites.

Site	Latitude	Longitude	Elevation (m)
Meru Bush	-0.07013	38.41288	349
Meru Open	0.18012	38.22673	596
Meru Forest	-0.07175	38.42017	336
Nairobi Bush	-1.35137	36.79636	1701
Nairobi Forest	-1.34836	36.76731	1807
Nairobi Open	-1.35143	36.79628	1695
Tana Forest	-1.87652	40.13994	42
Tana Open	-1.87615	40.13791	37

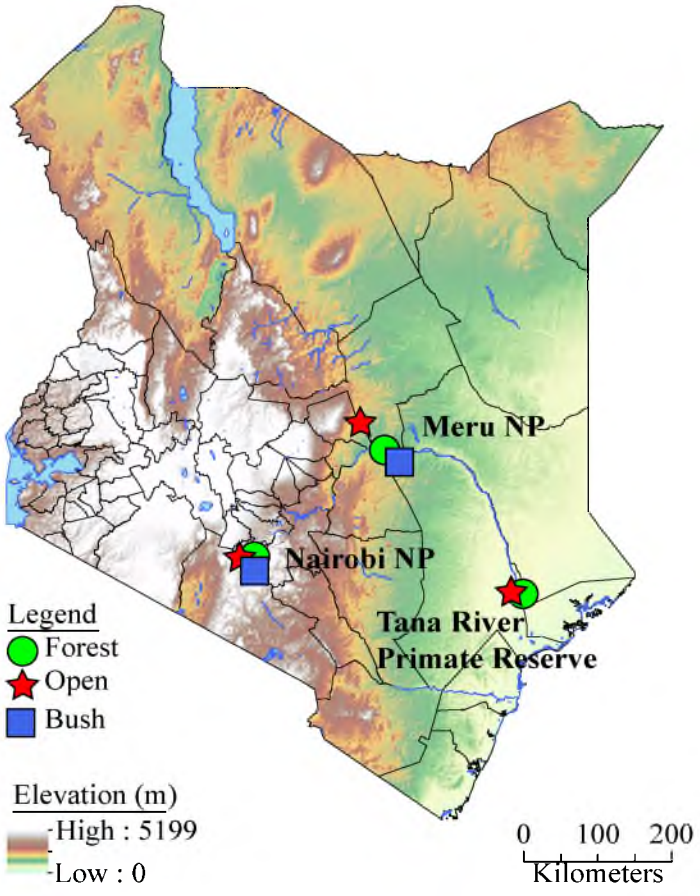

Figure 3.1 – Digital elevation model showing the locations of the study sites.

Description of the seasons

The data from Meru National Park and TRPR were collected for one year from May 2009 until May 2010; those from Nairobi National Park were collected the next year, from May 2010 until May 2011. From these data we present calculated land surface temperatures for different environments within these Kenyan national parks. The data are presented as yearly and seasonal averages of each hour of the day creating what we refer to as a statistical composite day. Seasons are defined by the Kenya Meteorological Service as: 1) a "Warm Dry Season" (December, January and February; (DJF)) where very little rainfall is observed; 2) the "Long Rains" (March, April, and May (MAM)) during which a majority of Kenya's annual rainfall occurs; 3) a Cool, Dry Season (June July and August (JJA)); and 4) the "Short Rains" (September, October and November (SON) which is a secondary rainy season associated with the migration of the Inter-Tropical Convergence Zone (ITCZ) over the area [*Griffiths*, 1972; *Nicholson*, 1996]. Further details of the meteorology of Kenya are given in Chapter 1.

Data Analysis Procedure

Here we employ a mathematical inversion method in order to obtain an accurate estimation of the soil surface temperature from continuous subsurface measurements. In summary, we use the theory of soil heat flow to calculate the thermal diffusivity of the soil [*Jury*, 2004] then we follow the methods described by [*Barttlet et al.*, 2006] to iteratively solve for the surface temperature input function from a fixed depth of 5 cm.

Temperature propagation into the soil column is described by the 1 dimensional heat diffusion equation,

$$\frac{\partial}{\partial t}T(z,t) = \alpha_{eff}\frac{\partial^2}{\partial z^2}T(z,t) \tag{1}$$

where T is the temperature, t is the time, z is depth, α_{eff} is the effective thermal diffusivity [*Carslaw and Jaeger*, 1986]. Since a temperature time series can be represented as a series of step changes we can employ the error function solution shown of Equation 1 described by *Carslaw and Jaeger* [1986]

$$T(z,t) = \sum_{n=t_0}^{i}(T_n - T_{n-1}) * erfc\left[\frac{z_{obs} - z}{\sqrt{4 * \alpha_{eff}(t_n - t_0)}}\right] \tag{2}$$

where Z_{obs} is the depth of observation and *erfc* is the complementary error function. The value of α_{eff} was not directly measured, therefore it was necessary to calculate α_{eff} using a regression of the average daily amplitude against depth.

The daily amplitude of soil temperature decreases exponentially with depth [*Jury*, 2004] following Equation 3.

$$A(z) = A_0 e^{-kz} \tag{3}$$

where *A(z)* is the amplitude of the daily temperature signal as a function of depth, z is depth; A_o is the amplitude of the daily temperature signal at the surface. α_{eff} is a material property of the soil and describes how well a heat pulse can propagate through it. The value for k in Equation 3 is the wave number of the thermal wave and is a function of α_{eff} and the period of the wave Equation 4.

$$k = \sqrt{\frac{\pi}{\alpha * \tau}} \tag{4}$$

Equation 4 can be transformed into slope intercept form by taking the natural logarithm of the right and left and sides of Equation 4, yielding Equation 5,

$$\ln(A(z)) = -kz + \ln(A_0) \quad (5).$$

Equation 5 suggests that we can take the amplitudes at three different depths and perform a linear regression on the natural logarithms of those amplitudes as a function of depth. The resulting slope of this regression line is a function of α_{eff}, which can be obtained through Equation 4. The diffusivity values used in the calculations of surface temperature are listed in Table 3.2.

Now that the value of the soil thermal diffusivity is known, we use Equation 2 to calculate the surface temperature input function following the methods described in [*Bartlett et al.*, 2006]. The drawback in using Equation 2 for such modeling is that it is exclusively a forward solution; that is, it only works to diffuse temperature down into the soil column and forward in time. In order to solve for the surface temperature we need to calculate a higher, shallower level in the soil column and, because of the phase lag, backwards in time. To address this problem it is possible to use an iterative method with Equation 2 using an initial guess for the surface input then diffusing it into the ground, using Equation 2 and comparing the fit with the observed time series. The initial guess for the surface temperature was obtained by diffusing the 0.05 m observed temperature down to 0.1 m using Equation 2. The difference in the amplitude decay and time shift of the thermal wave between the observed temperature and the diffused temperature were used as scaling factors to scale the observed 0.05 m soil temperature time series to the surface as the initial guess. The initial guess is then diffused into the soil column, using Equation 2, to the observation depth of 0.05 m. The misfit between the two time series is then used to adjust the input function for the next iteration and the process is repeated. Typically the convergence on a local minimum in the residuals was observed within 5–10

iterations of the soil temperature model (Figure 3.2). Once the minimum in the residuals is reached the result for the surface temperature has been reached. The code for this procedure is written in Matlab.

Model output for a one-month period at the TRPR grassland/bushland site predicts surface temperatures well for most of the time series; Figure 3.3 shows that the difference between the 0.05 m time series modeled from the surface input and the actual observed 0.05-m time series is commonly less than 1°C. From the figure it is observed that the largest errors occur regularly at the daily maximum. During events that cause large deviations in soil temperature (Fgure 3.3, panel B) such as heavy rain, the model performs less well as the error during these periods is larger. During periods of rain the thermal diffusivity of the soil is temporarily disturbed because of the additional water infiltrating into the soil column and the dependence for diffusivity on soil moisture content. In addition to an alteration of the thermal diffusivity, water flux into the soil column acts to advect soil heat with it [*Jury*, 2006].

Composite Day

We define a "composite day" as the average hourly temperature over a 24-hour period for each of four 3-month seasonal blocks. In this study, these time intervals correspond to DJF, MAM, JJA, and SON . We take the individual daily surface ground temperatures, as determined using the inversion methods described above, to obtain hourly temperatures of the ground surface.

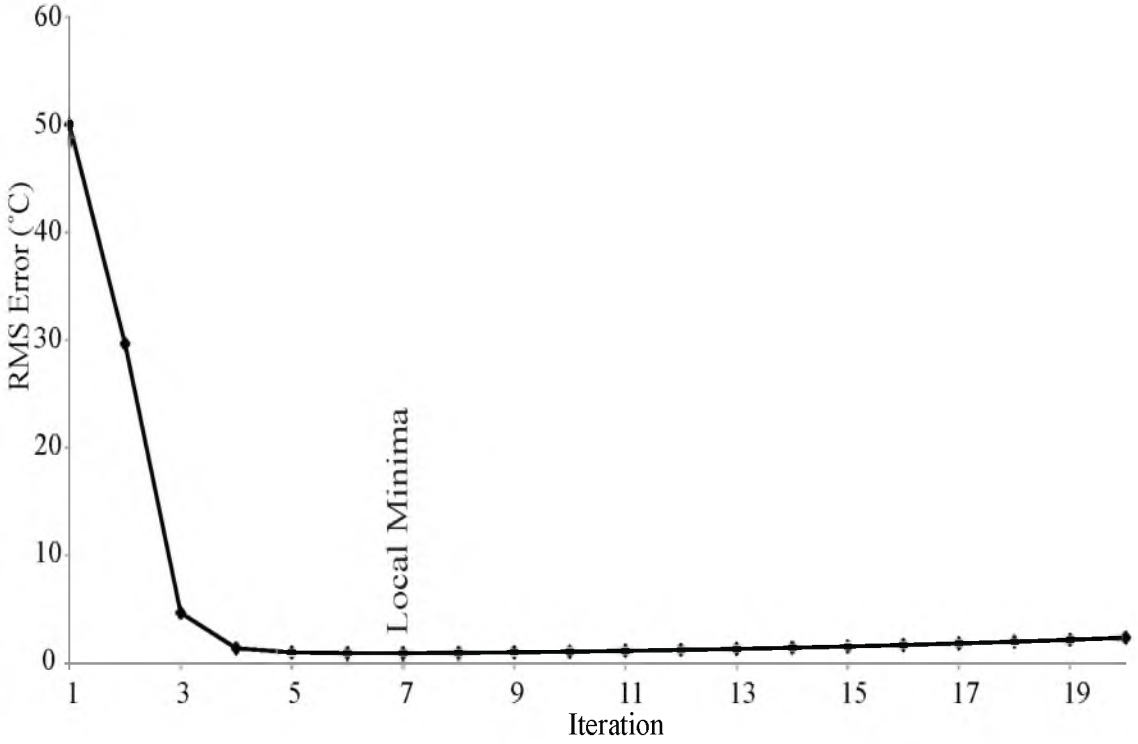

Figure 3.2 – RMS Error as a function of iteration number of the diffused soil temperature signal compared with the observed soil temperature signal at 5 cm depth. The minimum of the RMS error is at iteration number 7. The high value of 50 that is observed as the first point is an arbitrary number used to initialize the model.

Table 3.2 – Values for diffusivity (α_{eff}) for selected soil temperature sites.

Site	Diffusivity (m*m/s)	Uncertainty (±)
Nairobi Grasslan	6.4E-7	±2.0E-7
Nairobi Bush	1.8E-7	±5.4E-8
Nairobi Forest	3.8E-7	±1.1E-7
Tana River Grassland	2.6E-7	±8E-8
Tana River Forest	2.9E-7	±9E-8
Meru Grassland	1.3E-7	±4E-7
Meru Bush	4.7E-7	±1.4E-7
Meru Forest	3.7E-7	±1.1E-8

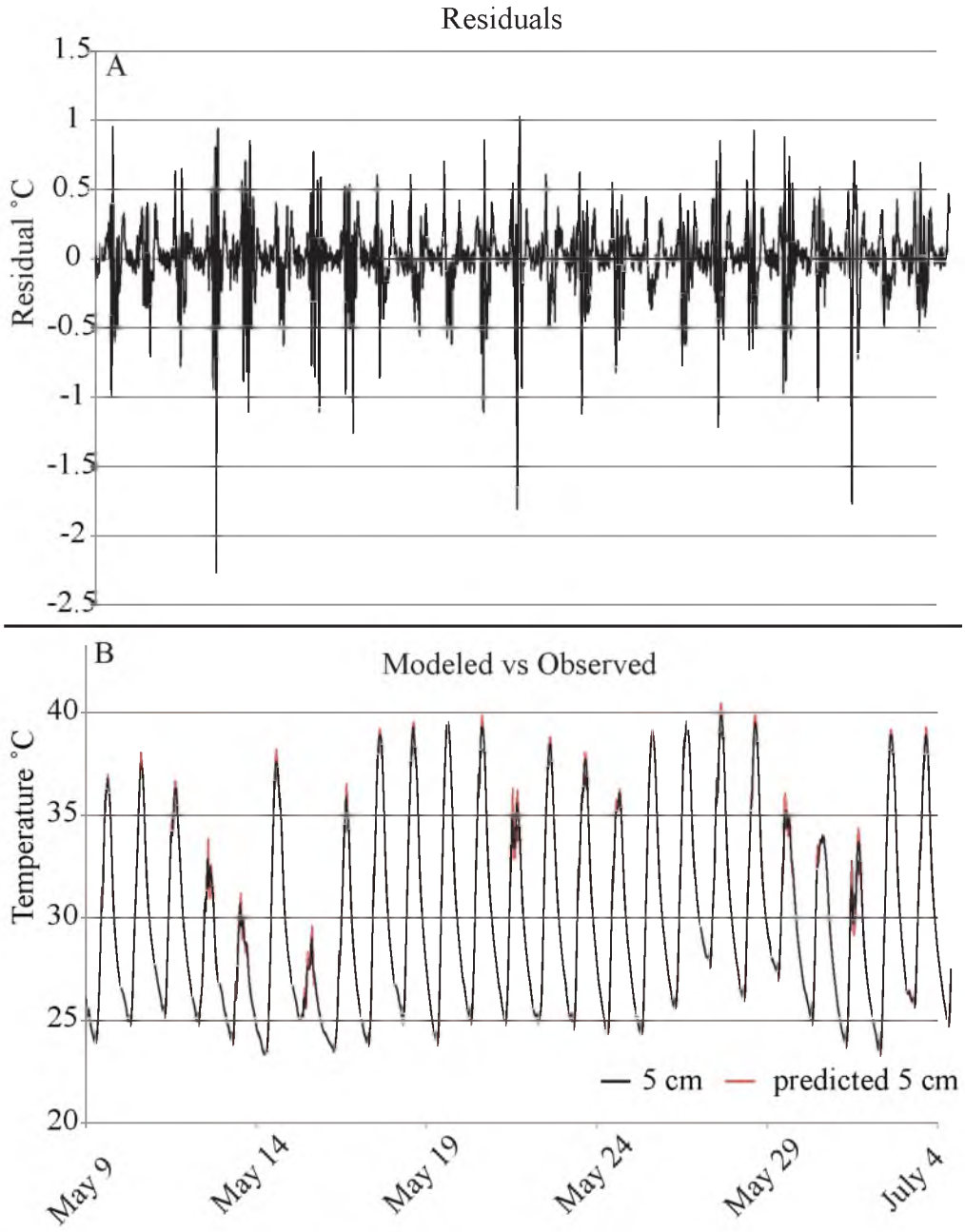

Figure 3.3 - One month of modeled data from the Tana River Primate Reserve open site during May 2009. A) Misfit between the modeled 5 cm temperature, using the calculated surface temperature as the input, and the observed temperature time series at 5 cm depth. B) Modeled and observed temperatures at 5 cm.

Results

Composite day statistics provide good descriptions of what an average day looks like throughout the course of a year at different sites, with notable variations due to local ecology. All temperatures discussed in the ensuing text in this section are soil surface temperatures. The daily minimum temperature is observed just before sunrise at about 0600 local time throughout the year. At the time of the diurnal minimum, surface temperatures in all environments (forest, bush, grassland) are close to being in radiative equilibrium with the atmosphere, so these temperatures are very similar with differences among the sites due to differences in the atmospheric water vapor burden. After sunrise, the surface warms gradually throughout the day as absorbed solar energy heats the soil surface until it reaches a peak at about 1400 local time. As the local afternoon progresses, the net radiation becomes negative and the surface begins to cool. During the night, the open environments cool slightly more than the forested sites and bush sites because the surface of the open sites is able to radiate freely to the atmosphere, whereas coverage from forests and bushes thermally insulates the soil and prevents radiative heat loss of the surface. Cooling occurs gradually at first and then rapidly as the solar angle gets smaller and the sun eventually crosses the horizon. After sunset, which occurs at about 1800 local time, the surface continues to cool and temperatures within the different environments converge as they approach radiative equilibrium with the atmosphere.

The full time series for the grassland, bush, and forest site at Meru National Park and the seasonal composite days for the four seasons allow comparisons of the composite day with the overall trend (day to day occurrences) of the season (Figure 3.4). The first few months, JJA, of the observation period were exceptionally hot and dry due to the

drought of 2009. During these months, the open and bush sites experienced large diurnal ranges and extremely high daily maximum temperatures because the soils within these areas were dry and much of the incident solar energy directly heated the soil column. The forested site during this period was much cooler throughout the day despite the drought, and it had a much lower daily maximum temperature and a smaller diurnal range. All of these features are evident in the composite day for the JJA season within the three environmental types. The remaining seasonal composites compare similarly with the first season, JJA. The exception to this, however, is the last season (MAM), where there is a distinct difference in the daily amplitude throughout all the environments as it is smaller and much more comparable than in previous seasons. This season is characterized by cooler and wetter climatic conditions in Kenya so this behavior is not a surprise. However, the temperature climatology during these cooler and wetter periods suggest that it may be possible for species that are normally confined to forest environments (because of daytime heat and nighttime predation) are able to travel across open areas for extended periods of time without the consequences that would exist during the warmer seasons.

The results from the TPRP reveal temperatures that are equally as hot as were observed at Meru and, as well, exhibit a sharp temperature contrast between forested and open environments that is obtained throughout the year (Figure 3.5). The hottest season recorded at Tana River was during December, January and February, which is consistent with the seasonal definitions discussed in the introduction to this chapter. During this season, the temperatures in the open came close to or exceeded 60°C (140°F) regularly. The composite day for this locality shows that between the hours of 1000 and 1800 temperature in the open usually exceeds 40°C (>100°F) with an average daytime

maximum during the hottest season exceeding 50°C. The average diurnal temperature range during this period is ~20–25°C in the open. Within the forest zone, despite the extreme conditions in the open areas, the average diurnal range is approximatly 5°C throughout the year and temperatures only reach daily maxima of about 30°C. This is reflected in the composite day for this environment, as the average daily high during all four seasons is less than 30°C. If the open environment is compared to the forested environment this is a 20–25°C temperature difference, on average, between open and forested environments during the hottest parts of the day.

The third park included in this discussion is Nairobi National Park. Nairobi National park is located in Central Kenya and is over 1000 m higher than the previous two sites just discussed. Therefore, it can be expected that, because of adiabatic cooling of the atmosphere, temperatures will be lower throughout the year than temperatures observed in Meru National Park or in the Tana River Primate Reserve (Figure 3.6). Despite lower average temperatures, the thermal difference between different environments is not as distinct at higher altitudes. At Meru and Tana River, where the temperature differences between the forest and the open were 20°C or more, the temperature contrast at Nairobi National Park between the environments is only about 5–10°C during the hottest season, DJF, and less than 5°C during the coolest months. Daily high temperatures in the open there rarely get above 40°C, whereas at the other locations the temperature in similar settings soared over 60°C.

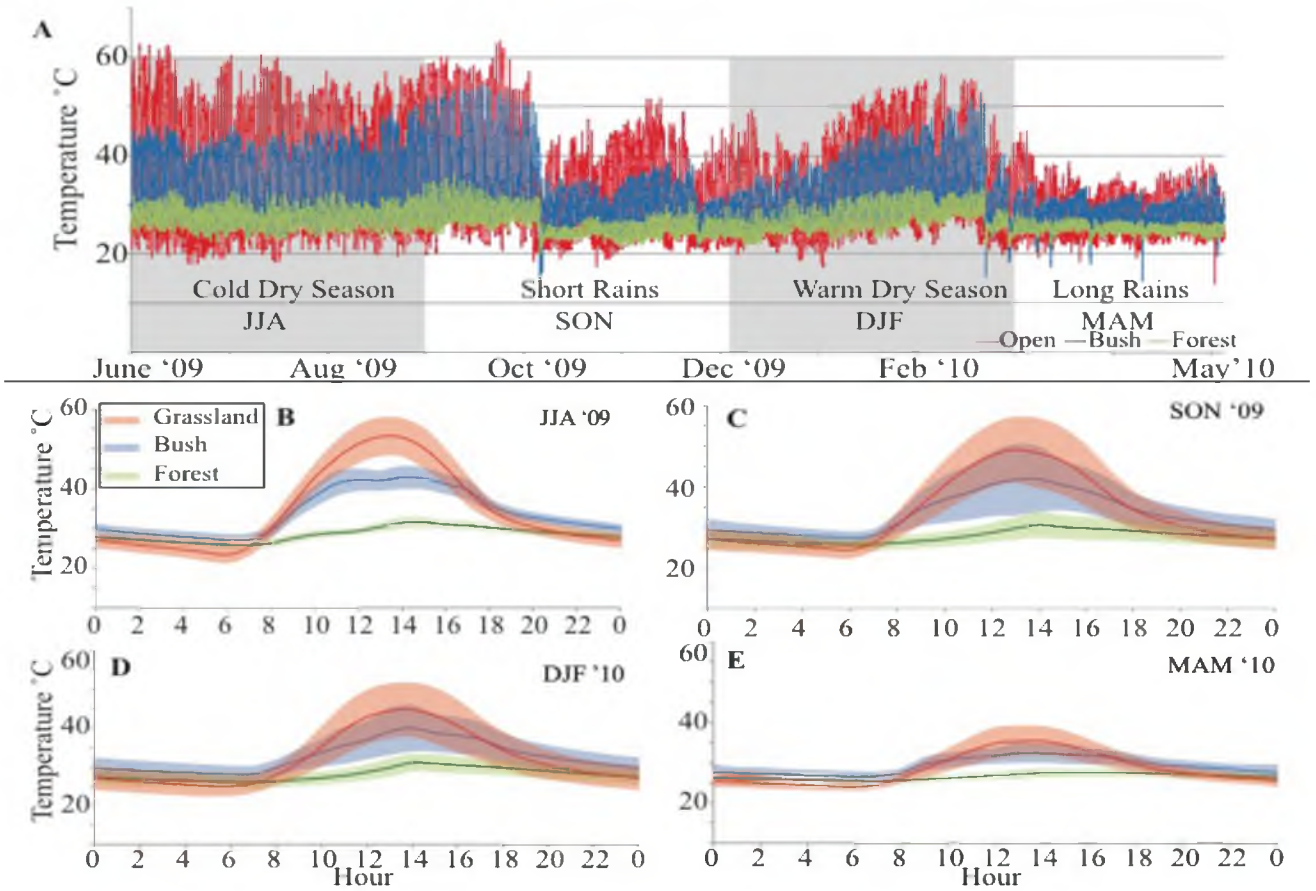

Figure 3.4 - A) One year of modeled surface temperature for the different environmental types at Meru National Park. B-E) Seasonal composite days for the different environmental types at Meru National Park. Colors correspond to type of vegetation cover where red defines grassland localities, green defines forested localities, and blue defines bushland localities.

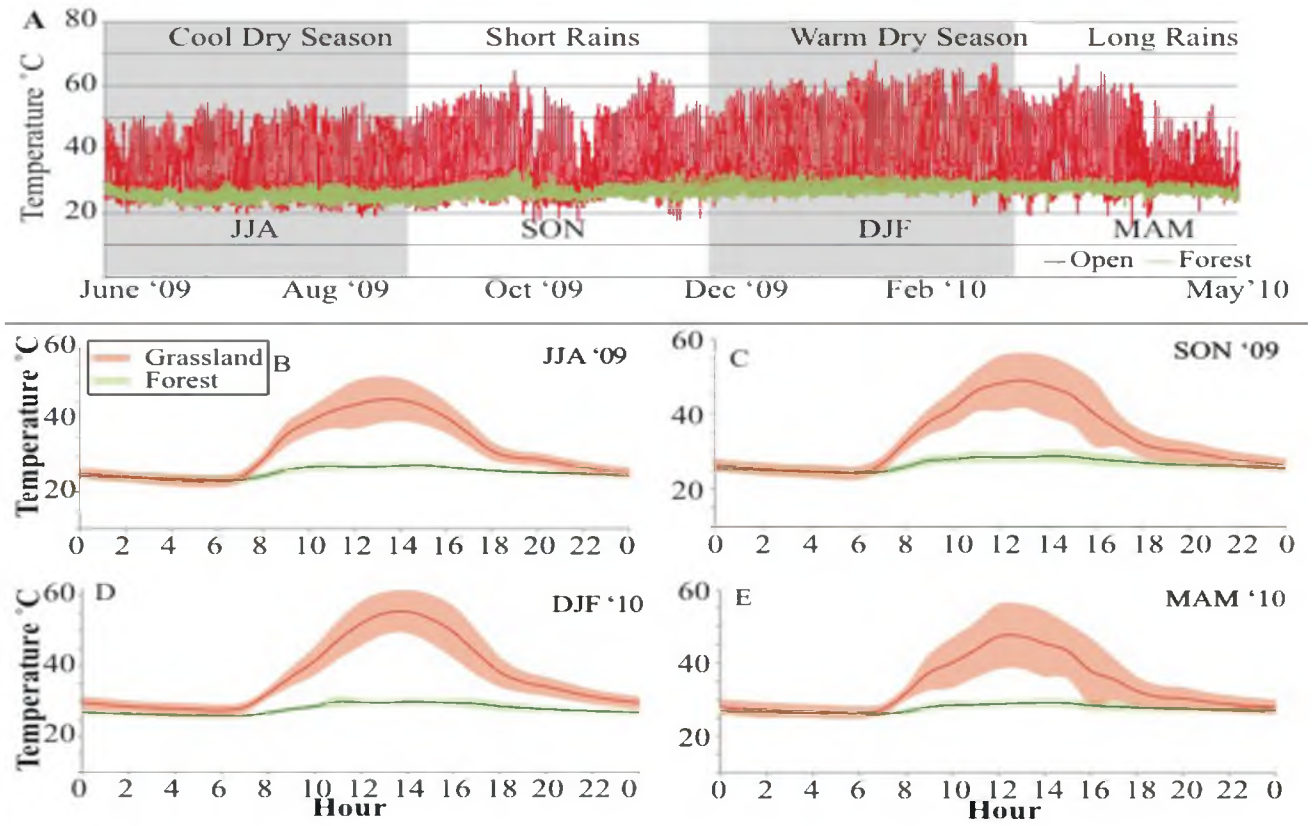

Figure 3.5 - A) One year of modeled surface temperature for the different environmental types at Tana River Primate Reserve (TRPR). B-E) Seasonal composite days for the different environmental types at TRPR. Colors correspond to type of vegetation cover where red defines grassland localities and green defines forested localities.

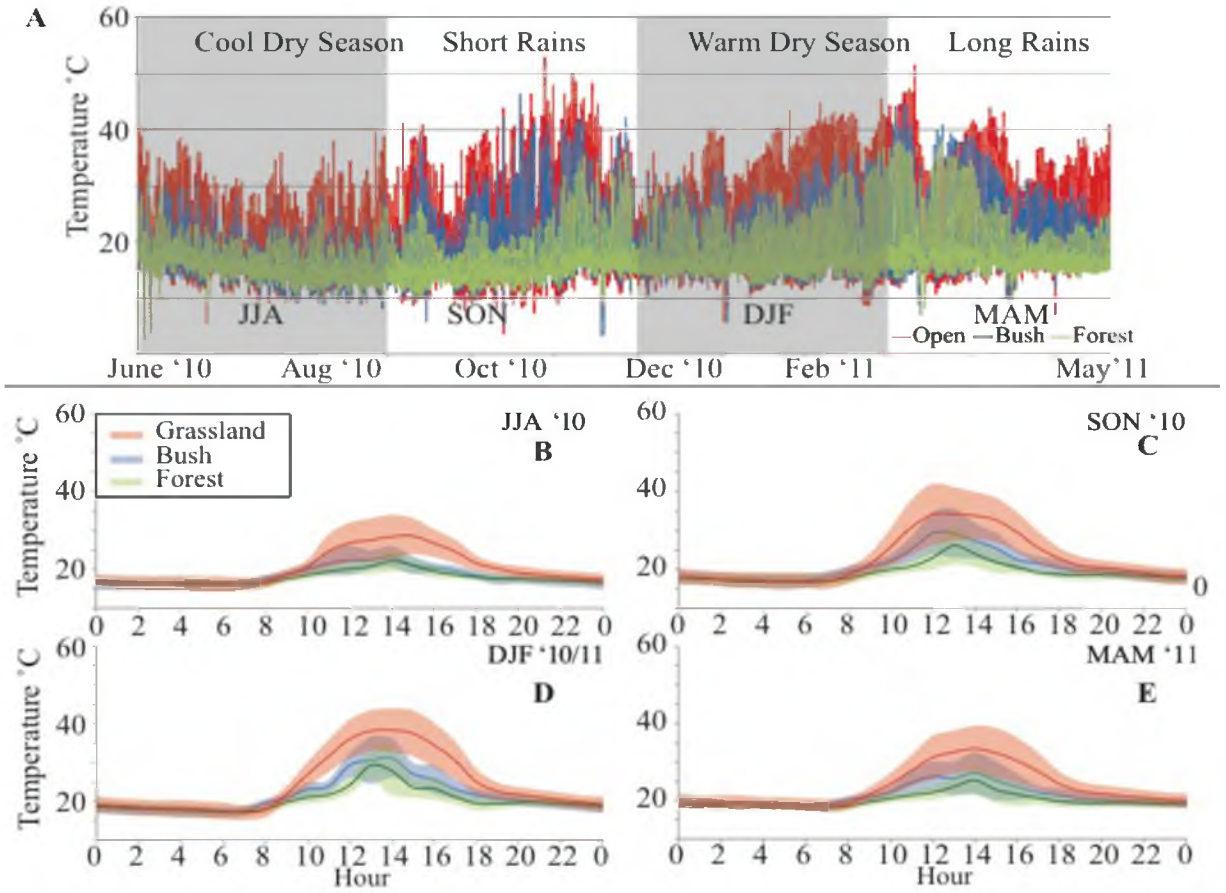

Figure 3.6 - A) One year of modeled surface temperature for the different environmental types at Nairobi National Park. B-E) Seasonal composite days for the different environmental types at Nairobi National Park. Colors correspond to type of vegetation cover where red defines grassland localities, green defines forested localities, and blue defines bushland localities.

Discussion

Validation of high soil surface temperatures

In an effort to validate the high calculated surface temperatures, a series of smaller experiments were conducted wherein a temperature sensor was placed directly on the soil surface. This method should provide a reasonable measure of the temperature at the ground surface. Because the HOBO temperature sensors are plastic and colored similarly to the surface, placing one directly on the surface should allow it to obtain the same, or at least a very similar temperature. This is shown in the following figure, where two sensors were placed close to one another for one day, one being on the surface and one being covered by 1–2 mm of soil. The temperatures of both agree well throughout the day in the sunlight and only differ during the presence of clouds, which are indicated through changes in the light intensity also plotted on Figure 3.7. Surface temperatures, based on sensors lying on the ground surface were measured for one month in the Turkana Basin; the results are shown in Figure 3.8. From this figure it can be seen that during 21 out of 23 of the days during this period, surface temperatures exceeded 50°C; furthermore, the surface temperature on 8 of those days exceeded 60°C. To further elucidate the difference that the shade provided by vegetation cover can have on the soil temperature, sensors placed under the shade of a nearby acacia tree and under a Salvadora bush during the same period of time showed a significant decrease in observed surface temperature. During the same time period, where daily maximum temperatures in the open exceeded 50°C, there were no days in the shade of either the acacia tree or the Salvadora bush where the daily maximum temperature was greater than 50°C. On most days, the surface temperatures were 15–20°C cooler in shaded areas than they were in the

open. Air temperature data from a weather station about 100 m away show that differences between the soil surfaces in different vegetative environments can be very large, especially in open exposed areas. In the open, the average temperature difference from the soil surface to 2 m above the surface is 24.3°C with a standard deviation over the period of 3.7°C. In the shade however, this difference is less by about a factor of 2, where the average difference over the observation period is ~9°C under the acacia tree and ~5.5°C under the Salvadora bush. The difference between the soil surface temperature and air temperature at the sites presented in the Results section is discussed further in the next section.

Air temperature and soil temperature comparison

Although the results presented above deal exclusively with soil temperatures, soil temperature and air temperature differ from each other quite significantly during the daylight hours and are comparable during the night. In addition, soil temperature data are difficult to obtain unless a study is conducted that deals specifically with soil temperatures to some extent. It is rare to find climate monitoring stations that operate soil temperature probes. What is more widely available are climate data such as air temperature from surface weather stations. The following discussion assesses how well these two values, soil and air temperature compare. Daily maximum and minimum air temperatures were collected from climate monitoring stations near Nairobi National Park and TRPR. The mean annual and seasonal averaged daily maximum and minimum temperatures for the soil surface and air are presented in Table 3.3.

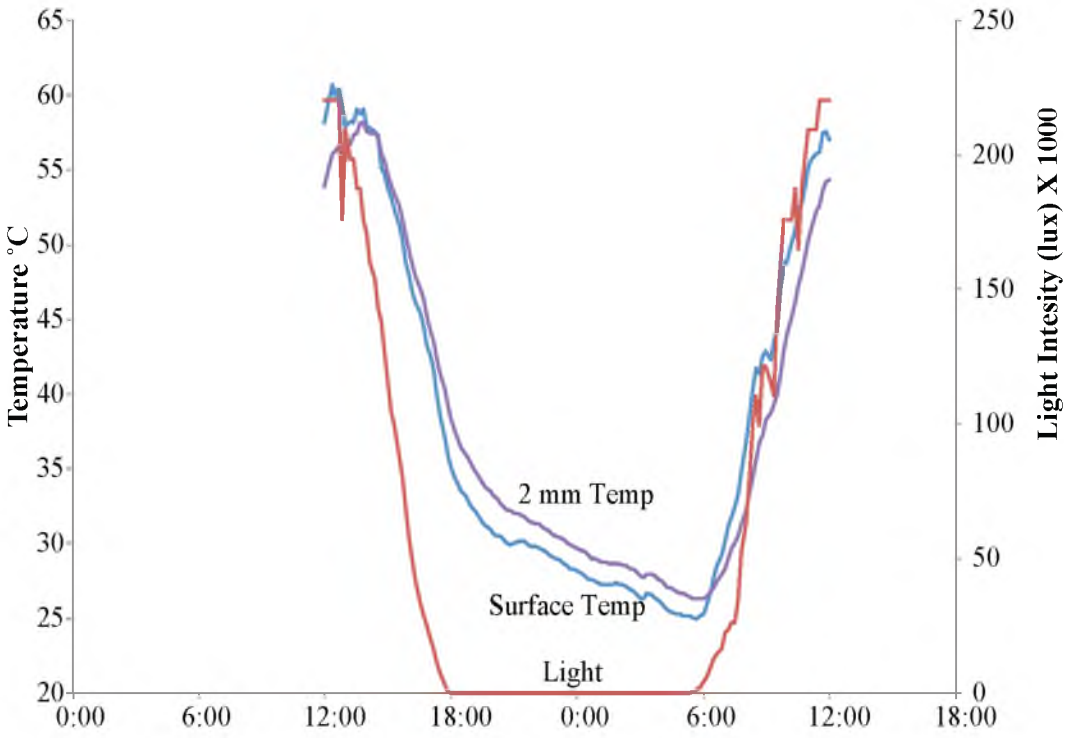

Figure 3.7 - One day of data comparing the accuracy of a soil temperature sensor that is exposed directly to the sun versus a sensor that is covered by 1–2 mm of soil. Light intensity is also plotted to show the presence of clouds.

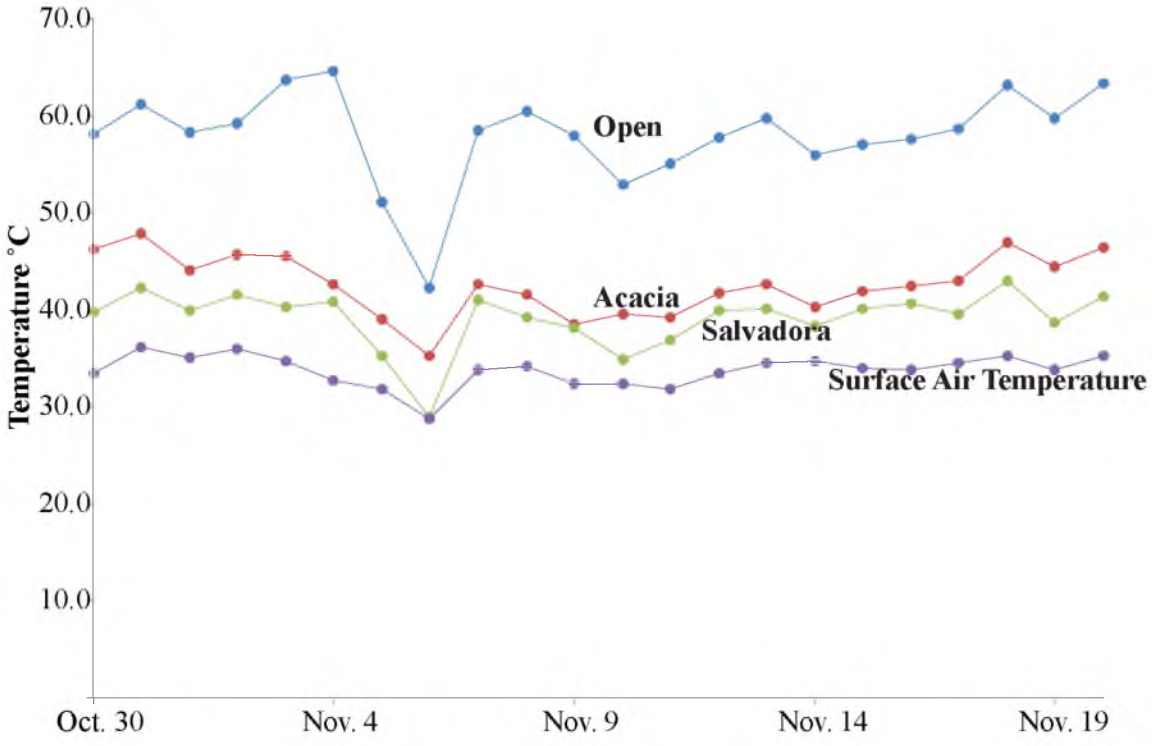

Figure 3.8 - Measured daily maximum surface temperatures at TBI Turkwel station from October 31 until November 21 2011. Data is shown for an open site, a site in the shade of an acacia tree, and a site in the shade of a Salvadora bush. Also plotted in this figure are the daily maximum air temperatures from a weather station about 100 m away.

The daily maximum soil surface temperature at Nairobi differed from the measured air temperatures to different degrees depending on the type of vegetation cover. In the open, the ground surface generally reaches maxima 10–15˚C hotter than are measured in the air. In the forest, the temperature differences between the soil surface and air temperature are smaller (~2–5˚C) as the forest surface is shaded from the sun and stays cooler. As expected, the daily minimum temperatures are quite comparable between all of the measured values. The bush site and the forested site stay warmer than the observed air temperature. This is most likely due to the vegetation cover in both of these settings acting to thermally insulate the ground surface. In the open, the effect is opposite as the lack of vegetation cover allows for rapid radiant heat loss to the atmosphere.

At Tana River, the difference in the observed air temperatures and the ground surface temperatures follow the same pattern as at Nairobi; the maximum daily temperatures are quite different and the minimum daily temperatures are similar. At Tana River however, the closest climate station was 150 km away and about 100 m lower in elevation; therefore, the air temperatures presented in Table 3.3 have been corrected for this difference in altitude using an average environmental lapse rate of -6.5˚C/km [*Wallace and Hobbs,* 2006] . In the open, the differences in the average maximum temperatures between the soil surface and the air were ~20˚C, whereas the average maximum surface temperatures of the forest floor is cooler than the maximum air temperatures by ~4-5°C.

Climate data that are available from the KMO is only daily maximum and minimum for the sites considered [Kenya Meteorological Service, 2011]. However, from the experiment that was conducted at TBI Turkwel and is discussed later, we can create

Table 3.3 - Annual and seasonal mean daily maximum, minimum, and ranges in both soil surface and air temperatures for Nairobi National Park, Tana River Primate Reserve, and Meru National Park. Air temperatures were collected from a climate monitoring station in close proximity to the soil temperature sites. The air temperatures have been corrected for the elevation difference between the climate monitoring station and the soil temperature sites using the average environmental lapse rate of 6.5°C/km. At Meru, the air temperature has been corrected to the elevation of the open soil temperature site, which is situated about 300 m higher than the bushland and forested sites.

	Nairobi Air	Nairobi Soil Open	Nairobi Soil Bush	Nairobi Soil Forest	Tana Air	Tana Soil Open	Tana Soil Forest	Meru Air	Meru Soil Open	Meru Soil Bush	Meru Soil Forest
Annual											
Max	25.1	37.8	31.5	27.3	33.9	54.2	29.8	39.2	48.3	41.1	30.8
Min	14.4	15.3	15.8	16.2	23.1	23.6	24.5	28.5	23.4	26.6	25.4
Range	10.7	22.5	15.6	11.0	9.9	30.6	5.3	10.8	24.9	14.4	5.4
JJA											
Max	22.9	34.1	27.0	24.1	32.3	49.7	28.2	37.6	56.0	44.6	32.1
Min	13.6	14.5	14.9	15.3	21.8	22.0	23.0	27.1	22.4	26.6	25.5
Range	9.3	19.6	12.1	8.7	9.6	27.6	5.2	15.0	33.6	18.0	6.6
SON											
Max	25.3	39.6	34.6	27.5	33.9	53.9	29.7	39.2	51.3	44.1	31.2

Table 3.3 continued.

	Nairobi Air	Nairobi Soil Open	Nairobi Soil Bush	Nairobi Soil Forest	Tana Air
Min	14.3	14.6	15.5	16.0	22.8
Range	11.0	25.0	19.1	11.4	10.2
DJF					
Max	26.8	41.5	35.5	31.9	35.0
Min	14.6	15.6	16.0	16.6	23.7
Range	12.1	25.8	19.4	15.3	10.5
MAM					
Max	26.5	37.1	30.0	26.5	34.4
Min	15.7	16.8	17.3	17.1	24.1
Range	10.8	20.2	12.6	9.3	9.4

Tana Soil Open	Tana Soil Forest	Meru Air	Meru Soil Open	Meru Soil Bush	Meru Soil Forest
22.5	23.9	28.2	23.6	26.7	25.3
31.4	5.8	15.5	27.7	17.4	5.9
59.6	31.3	40.4	47.4	40.9	31.6
26.4	25.5	29.1	24.2	27.5	25.7
33.3	5.8	15.8	23.3	13.5	5.9
53.1	29.8	39.7	37.8	34.2	28.2
23.6	25.5	29.4	23.1	25.4	25.1
29.5	4.3	14.8	14.7	8.7	3.1

composite days of both soil temperatures and air temperatures over the same period to assess the difference from the soil surface to 2 m throughout the day (Figure 3.9).

We chose 2 m for two reasons: 1) because this is the height of the air temperature sensors and is specified by the World Meteorological Organization; 2) because this is close to the average height of most humans and thus, their entire bodies would be exposed to this temperature difference. From the figure it can be seen that, in the open, the maximum difference between the surface and air temperature is ~20°C, whereas in the shade it is smaller with a maximum difference of ~5°. Soil temperatures deviate from the air temperature throughout the daylight hours and they reach their greatest difference when the sun is at or just beyond its' daily zenith. Air temperature lags soil temperature slightly because the air temperature is forced by the temperature of the soil. Under the dense shade of the Salvadora bush, soil surface temperature and air temperature are similar throughout the day. They do, however, deviate slightly in the afternoon and evening, which is likely due to a change in the sun angle and a change in the amount of light penetration through the bush.

Relationship to Human Heat Tolerance

Since the last common ancestor (LCA) between humans and other primates, a series of thermoregulatory adaptations have given hominids and modern humans the ability to venture into extremely hot environments without becoming dangerously overheated. Hominids and humans exhibit the continuation of an evolutionary trend toward higher heat loss capacity due to sweating and the evaporative cooling of the body provided by this mechanism [*Eichna*, 1950]. In order to maintain acceptable core body

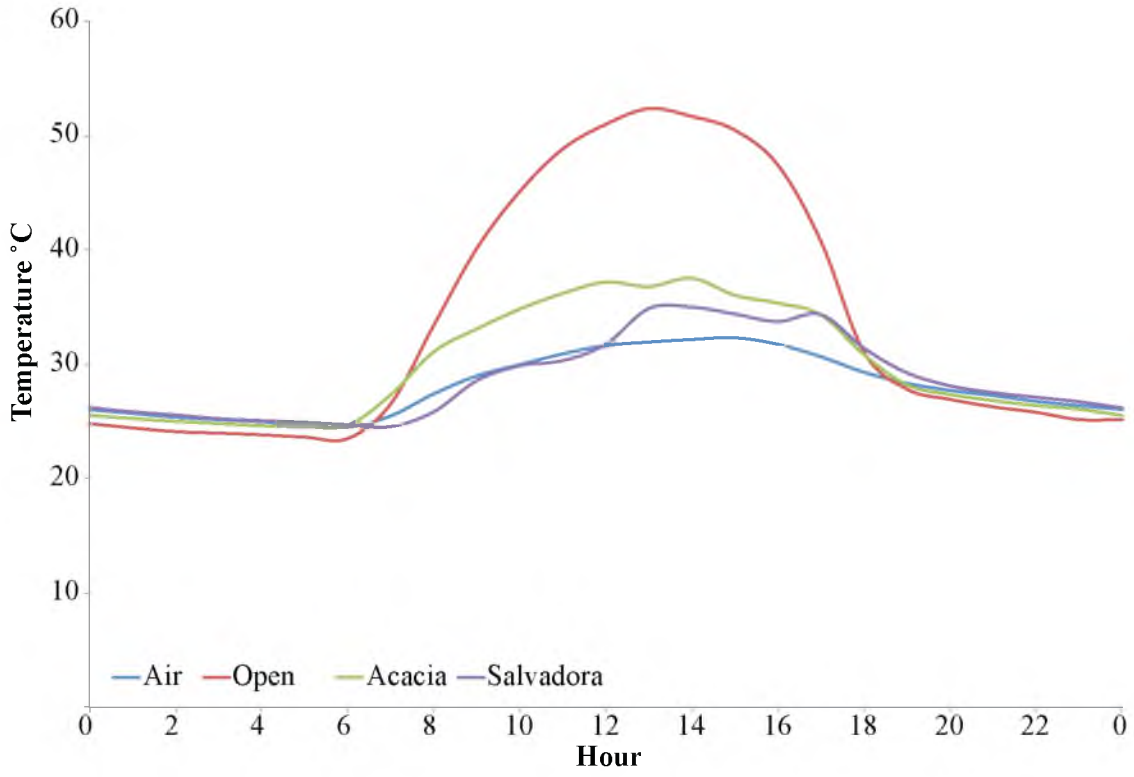

Figure 3.9 - Comparison of composite days composed from the test period October 30th through November 21st 2011 at TBI Turkwel Station. Soil surface temperatures were collected by placing a sensor directly on the surface, and air temperature was collected over the same period from a weather station about 100 m away.

temperature of 36.6-37.3˚C effectively without a thermoregulatory response, the ambient environmental temperature must be between 24–29˚C [*Kerslake*, 1972]. Within this temperature range a bare skinned individual, at rest, will be in a state of thermal equilibrium with its surroundings. Any activity or exposure to higher temperatures results in a response of the thermoregulatory system (i.e., sweating will begin). Exposure to temperatures greater than 40˚C, could begin to overload the ability for the body to cool itself, resulting in a dangerous rise in core temperature [*Kerslake*, 1972].

Analysis of the composite day for different environmental types show the temperature conditions that require only a minimal thermoregulatory response are only achievable on a regular basis during the day in forested environments; whereas in the open, under direct sun exposure, temperature conditions are much hotter warranting limited exposure during peak daytime temperatures to avoid the risk of overheating, even when considering the difference between ambient air temperature and the soil surface temperature. Therefore, it would have been critical for the survival of hominids to escape the extreme temperatures of midday open environments, or at least limit their exposure to the direct sun. From the graphs above, it can be concluded that exposure in the open from about 1000 to 1600 local time would result in a net increase in body temperature due to the heat gained from the environment and through metabolic activity.

Conclusions

We present the environmental parameter of temperature as a "statistical composite day" whereby the hourly ground surface temperature is estimated over seasonal periods; these are calculated from continuous subsurface measurements of soil temperature using

the 1-dimensional heat diffusion equation. We have shown that environmental temperature differences between different microclimatological settings are extremely high: daily maximum soil surface temperatures at low altitude open settings regularly exceed 50°C and periodically exceed 60°C in some open grassland environments. Open settings show large diurnal variation often on the order of ca. 20-30°C. Nearby forested sites have daily maximum surface temperatures in the mid 30°C. At higher elevations, steep spatial differences in ground surface temperatures exist but are much less extreme. In the open, diurnal ranges are on the order of 20°C and daily extremes in the open are regularly in the range of 40–50°C. These observations are relevant for consideration of microenvironments relevant to hominid evolution, because high soil temperatures have been measured for paleosols in the Turkana Basin.

References

Bobe, R and Leakey, MG (2009), Ecology of plio-pleistocene mammals in the Omo-Turkana Basin and the emergence of Homo. *The first humans - Origin and Early Evolution of the Genus Homo*, eds Grine FE, Fleagle JG, & Leakey RG (Springer).

Bartlett, M. G., D. S. Chapman and R.N. Harris (2006), A decade of ground-air temperature tracking at Emigrant Pass Observatory, Utah, *Journal of Climate 19*(15): 3722–3731.

Carslaw, H. S. and J. C. Jaeger (1986), *Conduction of Heat in Solids*, Oxford: Clarendon Press.

Cerling, T. E., N. E. Levin, J. Quade, J.G. Wynn, D.L. Fox, J.D. Kingston, R.G. Klein and F.H. Brown (2010), Comment on the paleoenvironment of Ardipithecus ramidus, *Science 328*(5982): 1105.

Eichna, L. W., C. R. Park, N. Nelson, S. M. Horvath and E. D. Palmes (1950), Thermal regulation during acclimatization in a hot, dry (desert type) environment, *The American Journal of Physiology 163*(3): 585–597.

Falk, D. (1990), Brain evolution in Homo: The "radiator" theory, *Behavioral and Brain Sciences 13*(2): 333-381.

Feibel, C. S. (2012), A geological history of the Turkana Basin, *Evolutionary Anthropology 20*(6): 206–216.

Feibel, C. S. and J. M. Harris(1991), Palaeoenvironmental context for the late neogene of the Turkana Basin, *Koobi Fora Research Project 3*: 321–370.

Geiger, R., R. H. Aron (2009), *The Climate Near the Ground*, Rowman & Littlefield, Lanham, MD.

Griffiths, J. F. (1972), *Climates of Africa*, Elsevier Pub. Co., Amsterdam, NY.

Hijmans, R. J., S. E. Cameron and J. L. Parra, (2005), Very high resolution interpolated climate surfaces for global land areas, *International Journal of Climatology 25*(15): 1965–1978.

Jablonski, N. G. and G. Chaplin (2000), The evolution of human skin coloration, *Journal of Human Evolution 39*(1): 57–106.

Jablonski, N. G. and G. Chaplin (2010), Human skin pigmentation as an adaptation to UV radiation, *Proceedings of the National Academy of Sciences of the United States of America 107*(SUPPL. 2): 8962–8968.

Jury, W. A. and R. Horton (2004), *Soil Physics*, John Wiley & Sons, Hoboken, NJ.

Kerslake, D. M. (1972), *The Stress of Hot Environments*. Cambridge Univ. Press, Cambridge, MA.

McFarlane, W. V. (1968), Adaptation of ruminants to tropics and deserts. *Adaptation of Domestic Animals*. E. S. E. Hafez. Philidelphia.

Nicholson, S. E. (1996), A review of climate dynamics and climate variability in Eastern Africa. *The Limnology, Climatology and Paleoclimatology of the East African Lakes*, Gordon and Breach**:** 25–56, Amsterdam, The Netherlands.

Passey, B. H., N. E. Levin, T.E. Cerling, F.H. Brown and J.M. Eiler (2009), High-temperature environments of human evolution in East Africa based on bond ordering in paleosol carbonates, *Proceedings of the National Academy of Sciences 107*(25):11245–11249

Potts, R. (1998), Environmentsal hypotheses of hominin evolution, *Yearbook of Physical Anthropology 41*: 93–136.

Ruxton, G. D. and D. M. Wilkinson (2011), Avoidance of overheating and selection for both hair loss and bipedality in hominins, *Proceedings of the National Academy of Sciences of the United States of America 108*(52): 20965–20969.

Wallace, J. M. and P. V. Hobbs (2006), *Atmospheric Science: An Introductory Survey*, Elsevier Academic Press, New York.

Wheeler, P. E. (1984) The evolution of bipedality and loss of functional body hair in hominids, *Journal of Human Evolution 13*(1): 91–98.

Wheeler, P. E. (1991), The thermoregulatory advantages of hominid bipedalism in open equatorial environments: The contribution of increased convective heat loss and cutaneous evaporative cooling, *Journal of Human Evolution 21*(2): 107–115.

Wheeler, P. E. (1992), The influence of the loss of functional body hair on the water budgets of early hominids, *Journal of Human Evolution 23*(5): 379–388.

White, F. (1983), The vegetation of Africa, *Natural Resources Research 20*.

White, T. D., S. H. Ambrose, G. Suwa and G. Woldgabriel (2010), Response to comment on the paleoenvironment of *Ardipithecus ramidus*, *Science 328*(5982): 1105.

White, T. D., B. Asfaw, Y. Beyene, Y. Haile-Selassie, C. O. Lovejoy, G. Suwa and G. WoldGabriel (2009). "*Ardipithecus ramidus* and the paleobiology of early hominids." *Science 326*(5949): 64, 75–86.

CHAPTER 4

SUMMARY AND CONCLUSIONS

In the previous two chapters we presented soil temperature data for the purpose of assessing the spatial variability of soil temperatures in Kenya over a range of elevations and vegetation types. From this work we can arrive at the following conclusions.

1. Variability of soil temperature throughout Kenya is high. The hottest soil temperatures are observed in low-lying grassland and bushland settings, whereas the coolest temperatures are observed in the higher altitude forested settings.
2. In all instances, soil temperatures within forested settings are cooler than those in direct exposure to the sun.
3. The warmest soil temperatures at 25 cm, which is consistent with depths in which soil carbonate formation is observed, are found within the Turkana Basin at Ileret and at the Tana River Primate Reserve.
4. At Ileret the mean annual average soil temperature at 25 cm is 34˚C with the hottest temperatures observed being just shy of 39˚C during the DJF season
5. At Tana River the mean annual soil temperature at 25 cm is 33˚C with the hottest temperatures observed during the DJF season also being just shy of 39˚C.
6. A statistical composite day is an effective way of distinguishing the averaged diurnal features such as the daily maximum, minimum, and range. The creation

of a composite day for each season clearly illustrates the differences caused by seasonal monsoon cycles driving the long and short rainy seasons.

7. Daily maximum temperature differences between shaded and unshaded environments at low elevations can be as great as 25°C and at higher elevations can be 10–15°C. During the night, when different environmental types come into radiative equilibrium, the temperature difference between them is very small.
8. Temperature variability on daily, seasonal, and annual scales within a forest is much smaller than it is in the open as the forests limit the amount of solar insolation during the day and IR radiation at night. Therefore, diurnal ranges in soil temperature in the forest are ~5°C, whereas they can be as high as 30°C in the open.
9. The temperature difference from the soil surface to the air temperature measured at 2 m above the ground can be quite significant during the day and are quite similar at night. This difference is also dependent upon the type of vegetation cover at the site. At higher elevations, in Nairobi, the difference between soil surface and air temperatures in the open is 10–15°C, whereas it is only 2–5°C in the forest. At lower elevations the difference from the soil surface to 2 m are on the order of 20°C in the open, whereas average maximum temperature of the soil surface in the forest is cooler than the elevation corrected air temperature by ~4–5°C.

APPENDIX A

SITE LOCATION AND DESCRIPTION

In this appendix we lay out the various site descriptions. The exact location of each site can be found in Table A.1.

Meru National Park

Meru National Reserve is located on the equator in Central Kenya. The park covers and area of around 900 km^2. At Meru, the closest permanent weather station is located at Isiolo, which is 34 mi northwest of Meru National Park. At Isiolo, the mean annual precipitation is 650 mm. The mean annual air temperatures for this location are 23.5˚C. Temperatures are highest in February and March and lowest in July and August, however, the deviation is small with a standard deviation of only 1˚C through the year.

Within this park there were three locations selected including grassland, bushland, and riparian forest zones. In addition, there was one location selected in a bushland community area immediately adjacent to the park. Both of the bush sites at Meru have about 50% canopy cover. The open site at Meru has no notable canopy cover but has dense grass coverage about 1 m high. The forested site at Meru is a dense tropical riparian forest with approximately 96% canopy cover.

Kakamega Forest National Reserve

Kakamega Forest National Reserve is located in the western highlands of Kenya. Annually the area receives 2000 mm of rain. The closest weather station is located at Busia, which is approximately 85 km east of the park. Mean annual air temperature at the park is 22˚C.

At this location there were two measurement sites. One site was located in a dense tropical forest and the other was located in open grassland. The open site at Kakamega forest has approximately 3% canopy cover, and acacia trees mainly provide this cover. The forested site at this location is a dense highland forest system; the canopy cover within this forest is 99%.

Lake Nakuru National Park

Lake Nakuru National Park is located between Mt. Kenya and Kakamega forest. Annually the area receives 1000 mm of rain. Mean annual air temperature at the park is 17.5˚. Daily air temperature highs are in the rage of 25˚C with the hottest temperatures observed in February and March. At this location two sites were instrumented in 2009 and three additional sites emplaced in 2010. In 2009 we selected one site located in a stand of *Acacia xanthophloea* with approximately 39% canopy cover and the other from this period was in an open grassland site with no canopy only grass coverage. During May of 2010 we chose to add three more locations, one located in a bushland area, an additional open grassland site located approximately 30 m from the lake margin, and a second forested site within an Olea forest.

Table A.1 – Latitude, Longitude, and Elevation of Soil Temperature Sites.

Site	Latitude	Longitude	Elevation (m)
Arabuko Sokoke Brachystegia	-3.32153	39.92542	31
Arabuko Sokoke Mixed	-3.32155	39.93288	27
Arabuko Sokoke Cynometra	-3.32079	39.88726	59
Arabuko Sokoke Disturbed	-3.30236	39.9968	25
Ileret Open	4.28808	36.26057	430
Ileret Bush	4.28809	36.26057	440
Kakamega Open	0.3479	34.86915	1572
Kakamega Forest	0.35604	34.860662	1628
Meru Open	0.18012	38.22673	593
Meru Bush	-0.07013	38.41288	343
Meru Disturbed	-0.28043	38.20503	514
Meru Forest	-0.07175	38.42017	330
Mt Kenya High	-0.16975	-0.16975	3072
Mt Kenya Low	-0.1729	37.15321	240
Nairobi Open	-1.35143	36.79628	1691
Nairobi Bush	-1.351383	36.796399	1690
Nairobi Forest	-1.34836	36.767312	1792
Nakuru Open	-0.41755	36.12577	1781
Nakuru Forest	-0.417950	36.124970	1785
Shimba Hills Open	-4.23394	39.41922	380
Shimba Hills Forest	-4.23464	39.41929	390
Tana Forest	-1.87652	40.13994	43
Tana Open	-1.87615	40.13791	37
Tsavo West Open	-2.74728	38.12858	886
Tsavo West Bush	-2.74705	38.12828	884
Tsavo East Open	-3.36249	38.64526	507
Tsavo East Forest	-3.36228	38.64492	507
Tsavo East Bush	-3.3625	38.645289	507

Mt. Kenya National Park

Two locations were selected on Mt. Kenya. Both are high elevation sites and are located within dense bamboo forests with bamboo canopy coverage of 100%. Air temperatures at these locations are much cooler than the rest of Kenya and differ from each other significantly. Rainfall is also variable because of the high elevations. The closest weather station to Mt. Kenya is Nanyuki, which is unrepresentative of what actual conditions would be on site.

Tana River Primate Reserve

Tana River Primate Reserve is located in Eastern Kenya along the Tana River. This riparian forest is home to two endangered endemic species of monkey, the Tana River Mangabey and the Tana River Red Colobus Monkey. At Garissa, 170 km north of Tana River Primate Reserve, annual precipitation is 300 mm and the mean annual temperature is 29˚C.

At this location there were two sites selected, one in an open setting with no canopy or bush cover. The other site was located within the dense tropical riparian forest consisting of approximately 96% canopy coverage.

Tsavo National Park

Tsavo National Park is located between Nairobi and Mombasa. The park is split into Tsavo East and Tsavo West. At Tsavo West there were two measurement locations: one in open grassland, and the other under the shade of a bush. At Tsavo West the grassland location has no notable tree canopy coverage but has approximately 38% of decent short (0.5 m) shrub coverage and medium (0.5 m) height grass coverage. The bushland site at Tsavo West was located underneath a bush that stands approximately 3 m high that provided about 50% canopy coverage to the site.

At Tsavo East there were three sites: open grassland, bushland, and a small isolated forest. The open site had no canopy cover and only short grass; the bush site was located under a dense bush that provides about 40% canopy cover. The forest location was located under a mixture of a large tree and bush coverage that provide a significant amount of cover, approximately 70%.

Arabuko Sokoke Forest Reserve

Arabuko Sokoke National Reserve is located in Southeastern Kenya. The park lies about 10 km inland from the Indian Ocean and about 20 km southwest of Malindi, Kenya. Arabuko Sokoke Reserve is the largest stretch of costal dry forest remaining in East Africa and is entirely a forested ecosystem. The reserve is comprised of three forest types: mixed forest, brachystegia woodland, and cynometra woodland. All three forest types are dense forests with greater than 70% canopy coverage. MAP in this region is about 1000 mm annually. At the closest meteorology station, Malindi, the mean annual air temperature is 26˚C. The warmest daily maximum temperatures, around 30˚C, are recorded in December, January and February and the coolest daily maximum temperatures, around 27˚C, are recorded in June, July and August. Lows throughout the year are about 22˚C.

Shimba Hills National Reserve

Shimba Hills is located approximately 30 km south of Mombasa. The park is comprised of costal forest ecosystems, open bushlands, and open grassland rages. Next to Arabuko Sokoke, Shimba Hills holds one of the largest costal forests in East Africa. MAP in this region is about 1000 mm annually. At the closest meteorology station (Malindi), the MAAT is 26˚C. The warmest daily maximum temperatures, around 30˚C, are recorded in December, January, and February and the coolest daily maximum temperatures, around 27˚C, are recorded in June, July, and August. Lows throughout the year are about 22˚C. At this location, temperature pendent strings were located in a

dense costal forest and also in an adjacent open field. The two monitoring locations were at approximately the same elevation of 300 m.

APPENDIX B

ILERET AND TURKWEL WEATHER STATIONS: THE FIRST YEAR OF DATA

In May of 2010 two permanent weather stations were installed at the Ileret and Turkwel field camp locations. These weather stations were installed in conjunction with the Turkana Basin Institute (TBI) because of the lack of climate monitoring coverage in the area. Previously, the only station that was recording any climate data within and surrounding the Turkana Basin was located at the Lodwar airport and was operated by the Kenya Meteorological Service (KMS). In addition to the limited data coverage, the ability to obtain the data from KMS is somewhat of a challenge and quite expensive. The weather stations installed at both locations are identical weather stations made by Onset Computer Corporation. A list of components and part numbers can be found in Table B.1.

As stated before, the weather stations are located at the Turkwel and Ileret field stations and are situated on either side of Lake Turkana, and separated by approximately 135 km. The coordinates for the stations and elevations are given in Table B.2. The TBI staff maintains the weather stations and the data are downloaded on a weekly basis (typically Sunday) and the files are transferred via email in a proprietary format (.HOBO).

Sensor Descriptions

Each weather station was comprised of 12 sensors. Below is a brief description of the sensors and their locations. An annotated picture of the weather station is presented in Figure B.1.

- **Soil Temperature** – There were three soil temperature thermistors buried adjacent to the weather station. The thermistors were buried at 0.05 m, 0.15 m, and 0.25 m to correspond with the soil temperature monitoring project. The soil in both locations was mostly sandy with very little vegetation.
- **Soil Moisture** – There were two soil moisture sensors buried at 0.05 m and 0.25 m. These sensors were buried adjacent to the soil temperature sensors.
- **Temperature/RH** – The temperature and relative humidity probe was located approximately 2 m off the ground and attached to the main mast of the tripod. It was shielded using an unaerated radiation shield.
- **Barometric Pressure** – The barometric pressure sensor was located directly outside the data logger housing and was attached directly to the main tripod mast.
- **Wind Speed** – Wind speed was measured using a cup anemometer located atop the main mast of the tripod.
- **Wind Direction** – Wind direction was measured using a wind vane located adjacent to the cup anemometer. The wind vane was oriented true north.
- **Solar Radiation** – Incident solar radiation was measured using a silicon pyrometer located atop the main tripod mast. Because of the geolocation of the weather stations this sensor was oriented so that no shadowing will occur from either the tripod mast of the wind sensors.

- **Rain** – Rain amount was measured using a tipping bucket rain gauge that is located on the main mast of the tripod opposite the temperature sensor.

Data Processing

Data Processing for the weather stations is done using two programs, the first is a proprietary software, HOBOware® Pro and the second is the Interactive Data Language (IDL) programming language. The proprietary HOBOware® software is required in order to interface with the weather station and download data. Additionally, basic plots and statistics can be obtained with this software; however, it is not very useful beyond basic functions. From HOBOware® the data must be exported as a comma separated file in order to import the data to excel or conduct further processing and quality control. Further processing and quality control is conducted using IDL. These programs output eight data sheets of varying timescales. Fifteen min, daily, monthly, and annual averages are updated with new data as it becomes available. In addition to the data tables, the programs output weekly "quick look" images for each sensor on the station; this gives the user the ability to observe any misbehaviors or faulty sensors.

First Year of Data and Results

Plotted in Figures B.2 and B.3 are the daily air temperature maximum, minimum, average, and range for Ileret and Turkwel, respectively. It is quite incredible that at both locations the average daily temperature, calculated as the average of the daily high and daily low, is frequently in excess of 30°C. Annually, the average daily temperatures for Ileret and Turkwel compare quite well at 31°C. Although daytime temperatures are

Table B.1 – Parts list for the weather stations at Ileret and Turkwel Field Stations.

Part Number	**Description**	**Price (US$)**
SOLAR-6W	6 Watt Solar Panel	149
BHW-PRO-CD	HOBOware Pro Mac/Win	99
U30-NRC-VIA-10-S045-000	USB Weather Station Data Logger	527
S-BPB-CM50	Barometric Pressure Smart Sensor	249
S-LIB-M003	Solar Radiation Sensor (Silicon Pyranometer)	210
S-RGA-M002	.01" Rain Gauge Smart Sensor (2m cable)	410
S-THB-M008	12-bit Temperature/RH Smart Sensor (8m cable)	195
S-SMC-M005	S-SMC-M005 - Soil Moisture Smart Sensor	139
S-TMB-M006	12-Bit Temp Smart Sensor (6m cable)	105
S-WSET-A	Wind Smart Sensor Set - S-WSET-A	560
RS3	Solar Radiation Shield	59
M-TPA-KIT	HOBO Weather Station 3-Meter Tripod Kit	275

Table B.2 – Latitude, longitude, and elevation of the weather stations. In November of 2011 the weather station at Turkwel was moved because of the construction of a new building. The data contained within this discussion is all from the old location.

Site	**Latitude**	**Longitude**	**Elevation (m)**
Ileret	4.28767	36.26105	438
Turkwel (Old Location)	3.13957	35.86455	460
Turkwel (New Location)	3.14169	35.86354	467

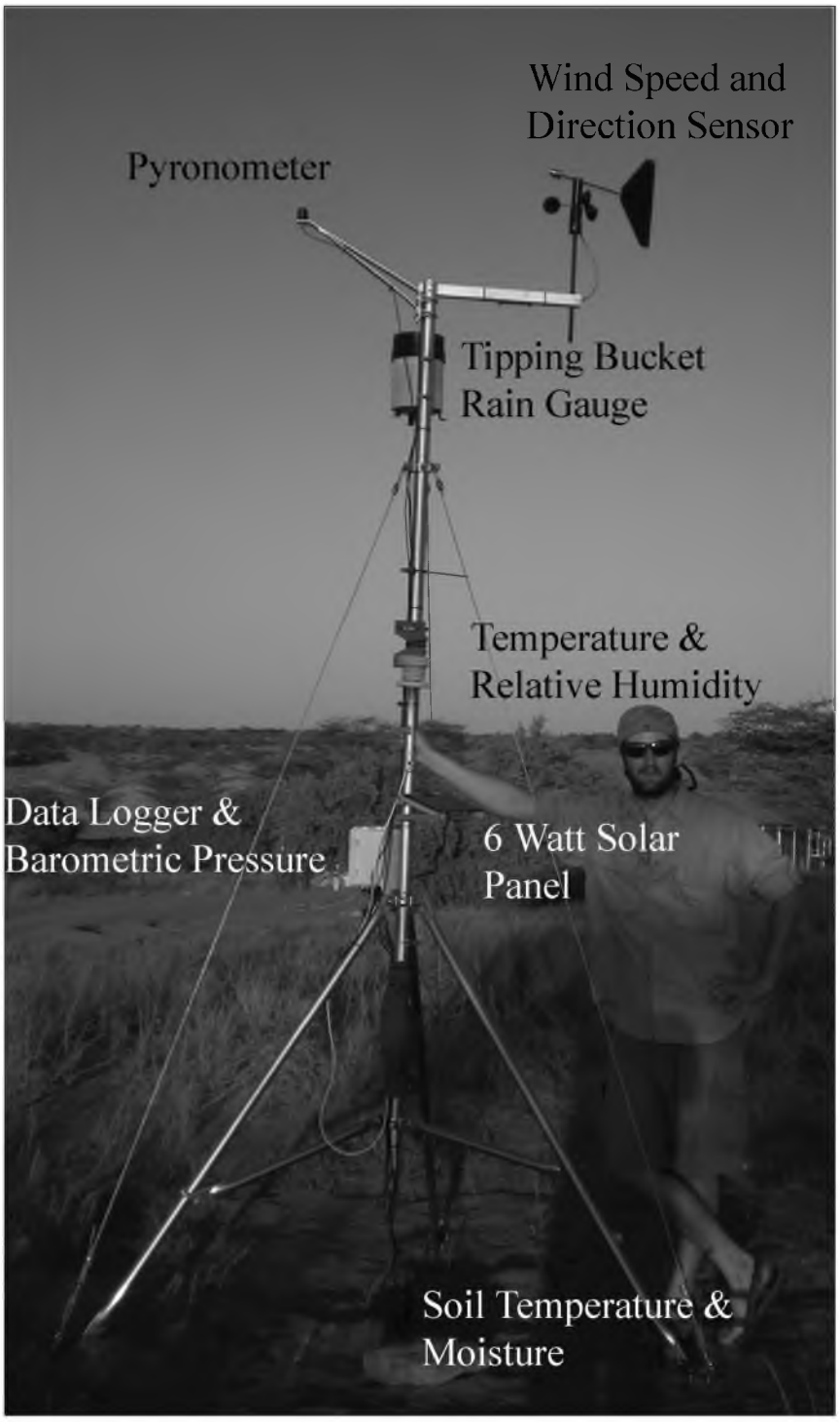

Figure B.1 – Annotated image of the weather station that is located at Turkwel Field Station. The Station located at Ileret is identical.

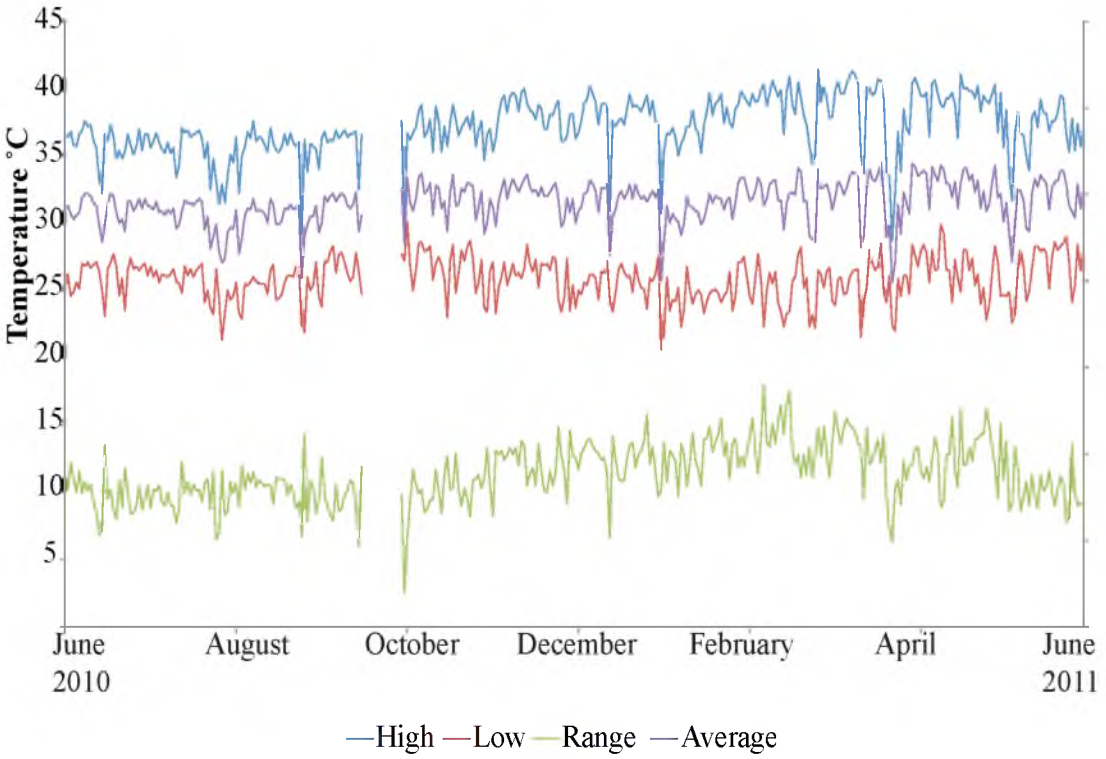

Figure B.2 – Daily air temperature high, low, range, and average at Ileret on the east side of Lake Turkana from June 2010 through May 2011.

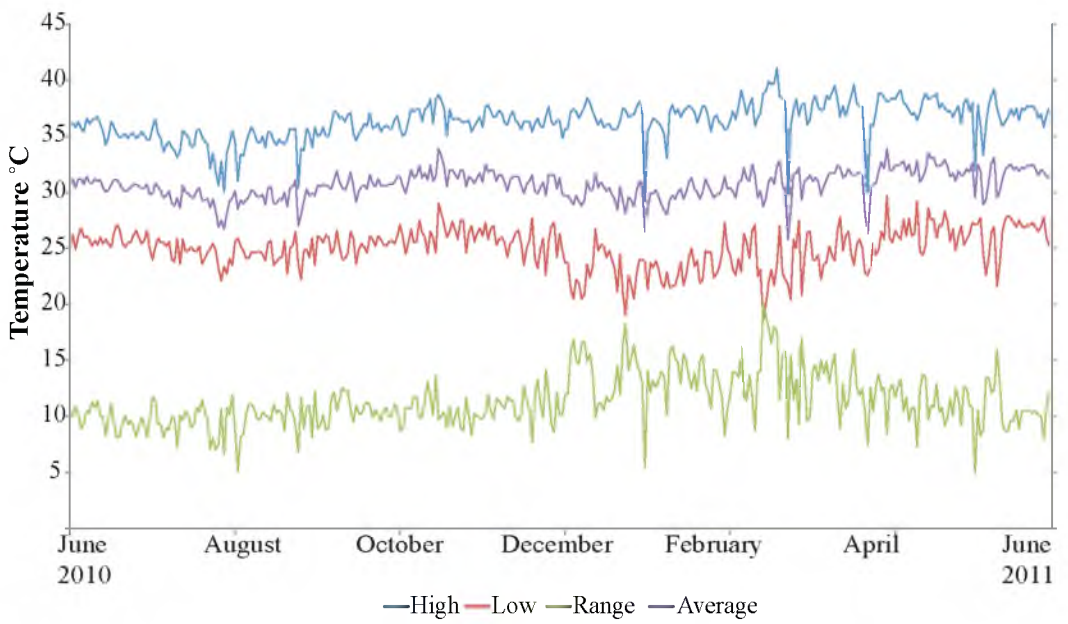

Figure B.3 - Daily air temperature high, low, range, and average observed at the Turkwel weather station on the west side of Lake Turkana from June 2010 through May 2011.

consistently quite warm, it is the nighttime lows that keep the daily average so high as they rarely fall below 25˚C. It is easily seen from these figures why the Turkana Basin is amongst the hottest 1% of places on earth [*Hijmans*, 2000].

In addition to being one of the hottest places on earth, the Turkana Basin, in contrast to many other tropical environments, is very dry [*Griffiths*, 1972]. During the first year of these stations being operational there was a mere 130 mm of rain that fell at Ileret. It was much drier at Turkwel with a pitiful 22 mm of rain that fell over that year. Contrast this with other areas within Kenya that receive over 2000 mm of rain each year. The dryness of the basin can also be seen in the soil moisture and temperature measurements. The daily averaged soil moisture measurements are presented in Figure B.4 and B.5, for Ileret and Turkwel, respectively. During all periods, except during and immediately following rain events, the soil moisture is close to the detection limit of the sensor, and therefore, just noise. As dry soil surface absorbs solar radiation, all of the energy that is not reflected is transformed into sensible heat and thus, results in very hot soil temperatures. Soil temperatures for Ileret and Turkwel are presented in Figures B.6 and B.7, respectively. Also plotted on these figures is the total daily rainfall measured by the tipping bucket rain gauge. It is interesting the large effect the rainfall has on the soil temperature. This drop in soil temperature results from the advection of soil heat as the meteoric water infiltrates the soil column and also the partitioning of surface energy into evaporation of soil moisture [*Kiehl*, 1997].

Solar insolation in this region is very intense, shown in Figures B.8 and B.9 for Ileret and Turkwel, respectively. Plotted in this figure is the daily averaged solar radiation. For midlatitude locations this value would change significantly throughout the

year as the sun angle changes with seasons. For the Turkana basin, which lies 3°N of the equator, solar intensity is consistent throughout the year with an average of 250 w/m^2. Deviations are only observed as storm systems and cloud cover changes.

Winds within the Turkana Basin are driven by the Turkana Jet, and at times can be very strong [*Kinuthia*, 1992]. The Turkana Jet is the result of wind channeling between the Ethiopian Highlands and the East African Highlands. Winds enter the channel from the southeast and continue on this trajectory throughout, becoming strongest where the channel narrows and significantly weaker where the channel is widest. This is consistent with the winds observed at Ileret, as they are predominantly from the southeast. However, at Turkwel the Turkwel River channel drives the winds so they are predominantly from the west.

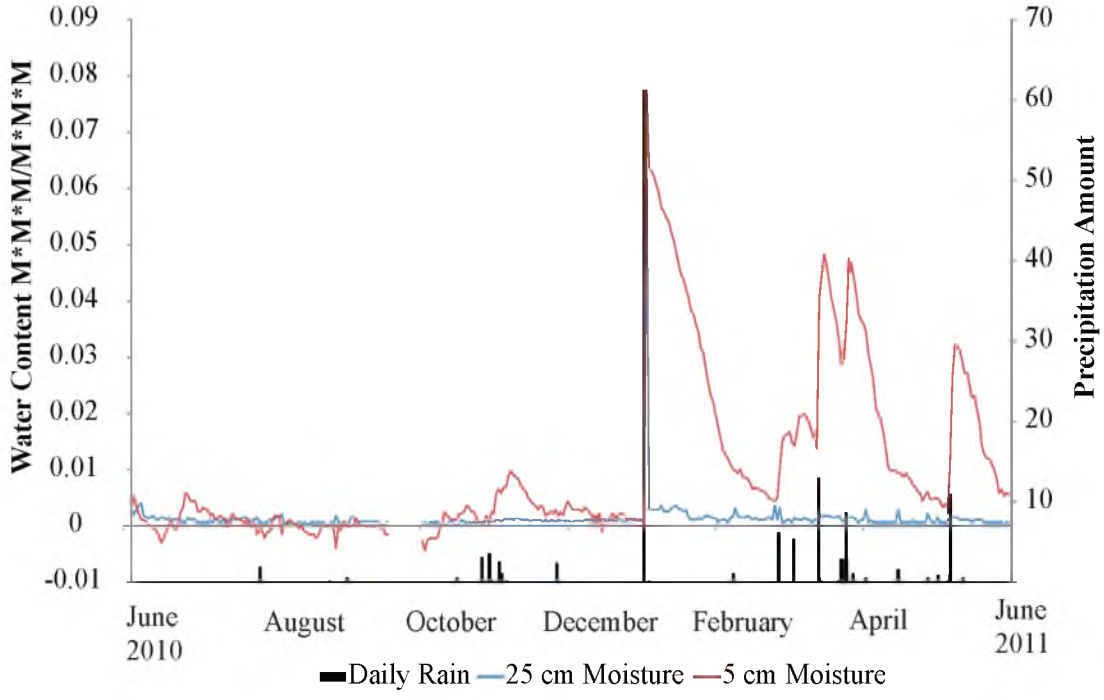

Figure B.4 – Soil moisture and precipitation measured at the Ileret weather station from June 2010 through May 2011. Soil moisture measurement depths are 0.05 and 0.25 m.

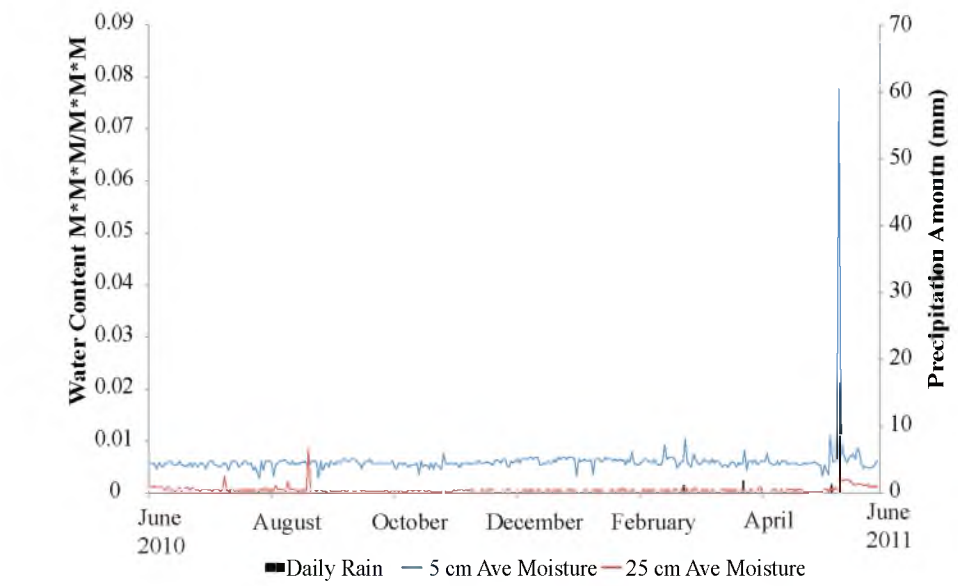

Figure B.5 – Soil moisture and precipitation measured at the Turkwel weather station during June 2010 through May 2011. Soil moisture measurement depths are 0.05 and 0.25 m.

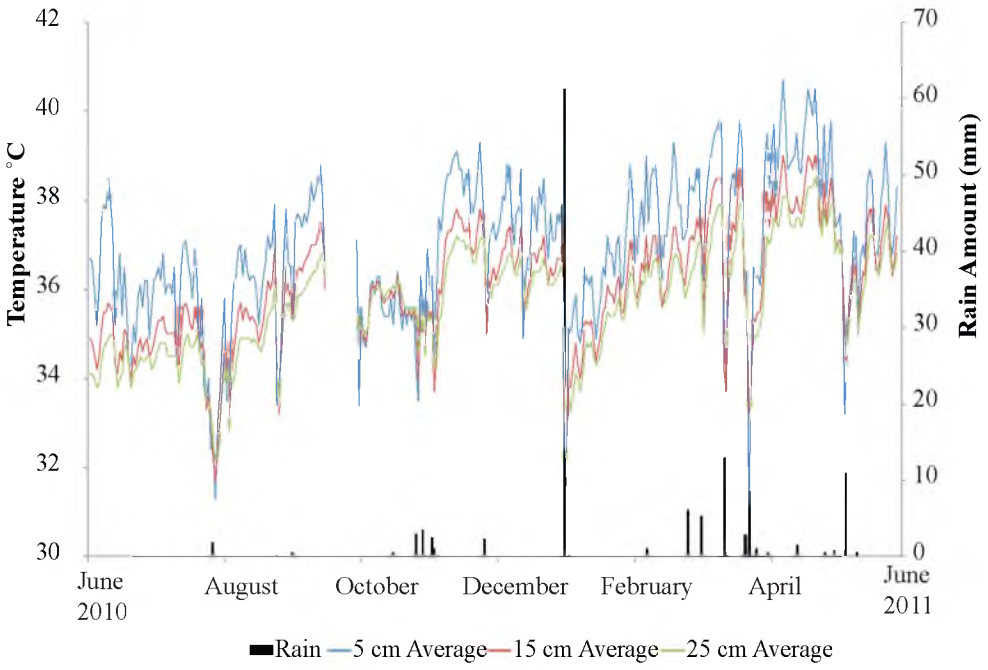

Figure B.6 – Soil temperature and precipitation at the Ileret weather station measured June 2010 through May 2011. Soil Temperature depths are: 0.05, 0.15 and 0.25 m.

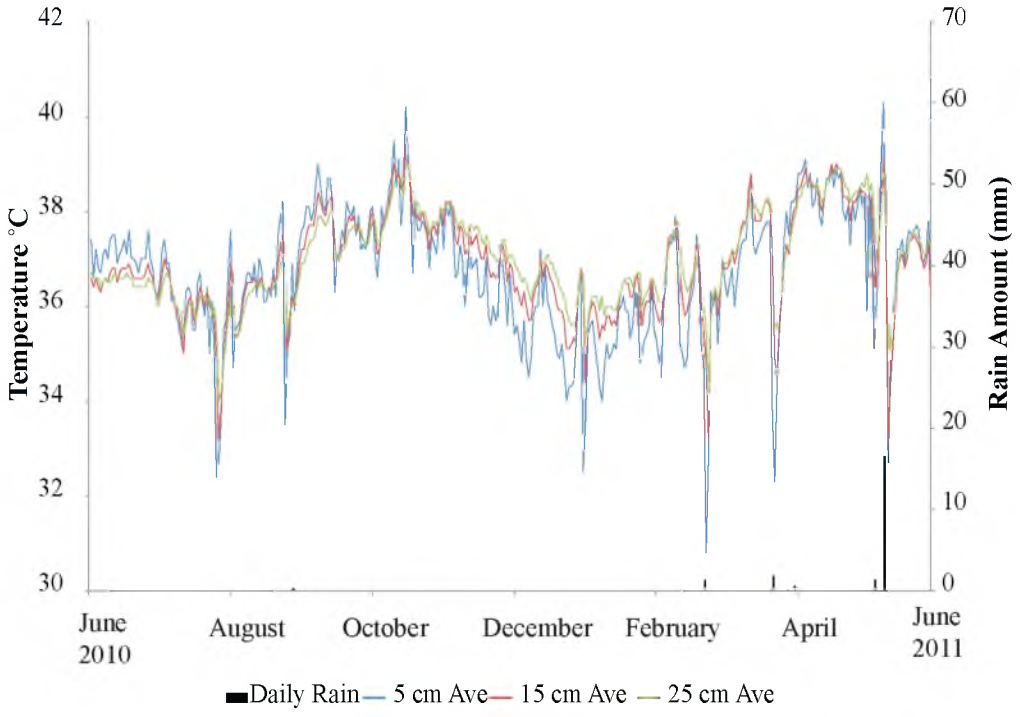

Figure B.7 - Soil temperature and precipitation at the Turkwel weather station measured June 2010 through May 2011. Soil Temperature depths are: 0.05, 0.15 and 0.25 m.

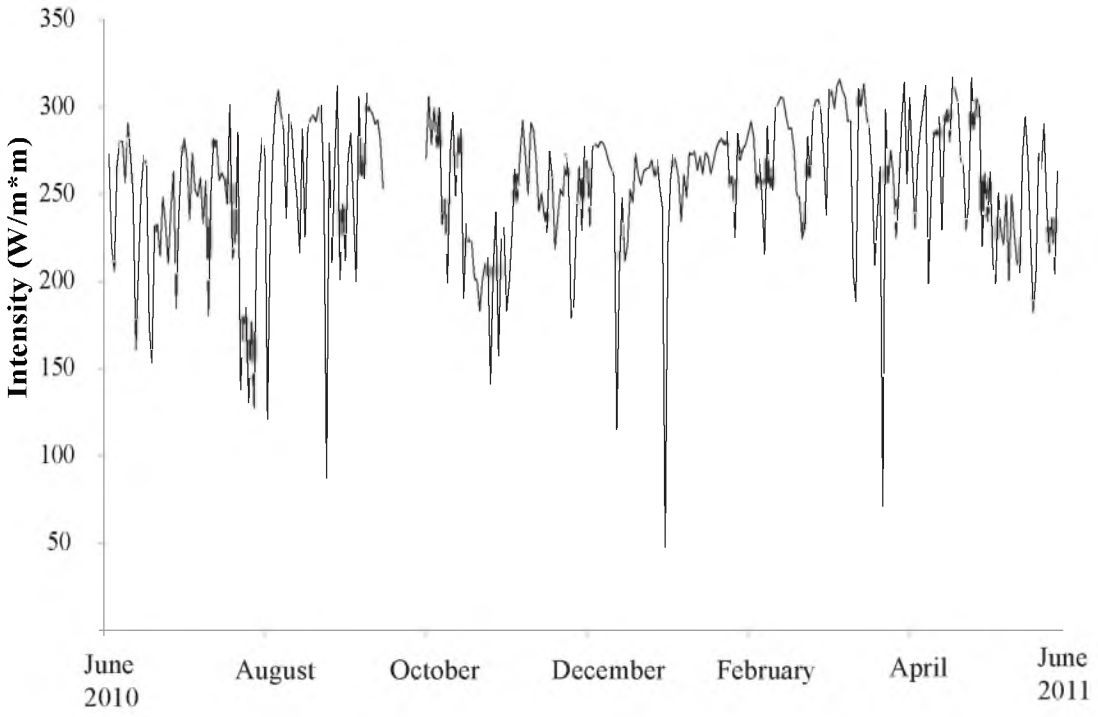

Figure B.8 – Daily averaged solar insolation measured at the Ileret weather station during June 2010 through May 2011.

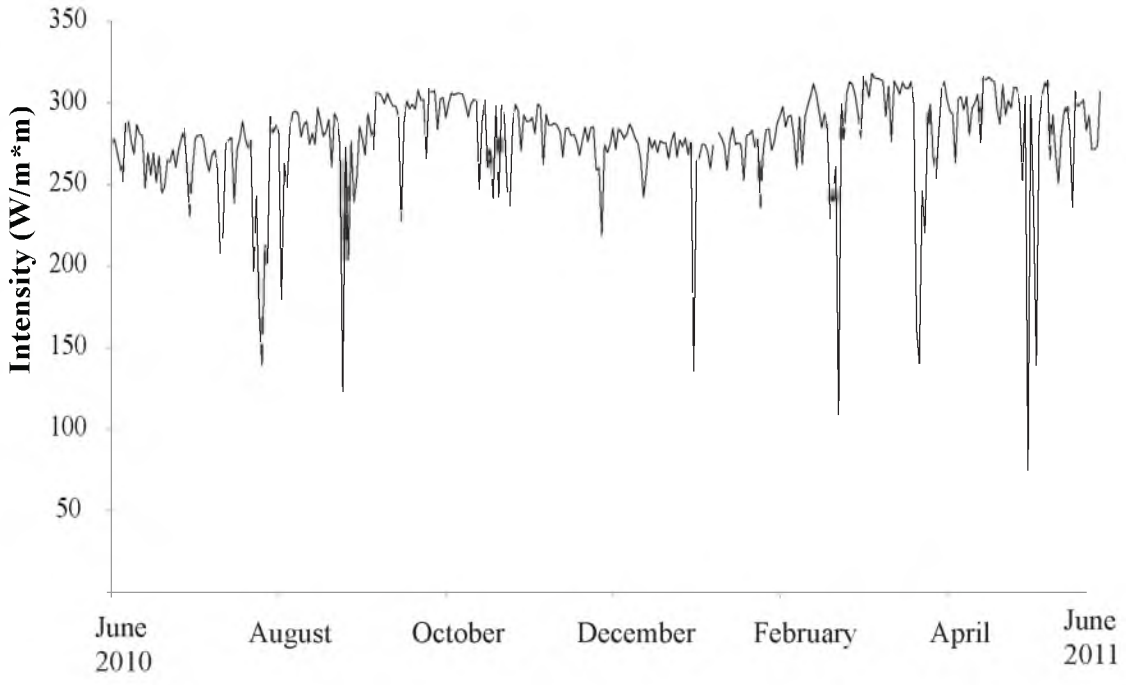

Figure B.9 - Daily averaged solar insolation measured at the Turkwel weather station during June 2010 through May 2011.

References

Griffiths, J. F. (1972), *Climates of Africa*, Elsevier Pub. Co., Amsterdam, NY.

Hijmans, R. J., S. E. Cameron, et al. (2005), Very high resolution interpolated climate surfaces for global land areas, *International Journal of Climatology 25*(15): 1965–1978.

Kiehl, J. T. and K. E. Trenberth (1997), Earth's annual global mean energy budget. *Bulletin of the American Meteorological Society 78*(2): 197–208.

Kinuthia, J. H. (1992), Horizontal and vertical structure of the Lake Turkana jet, *Journal of Applied Meteorology 31*(11): 1248–1274.

APPENDIX C

ADDITIONAL TWO YEAR DATASETS

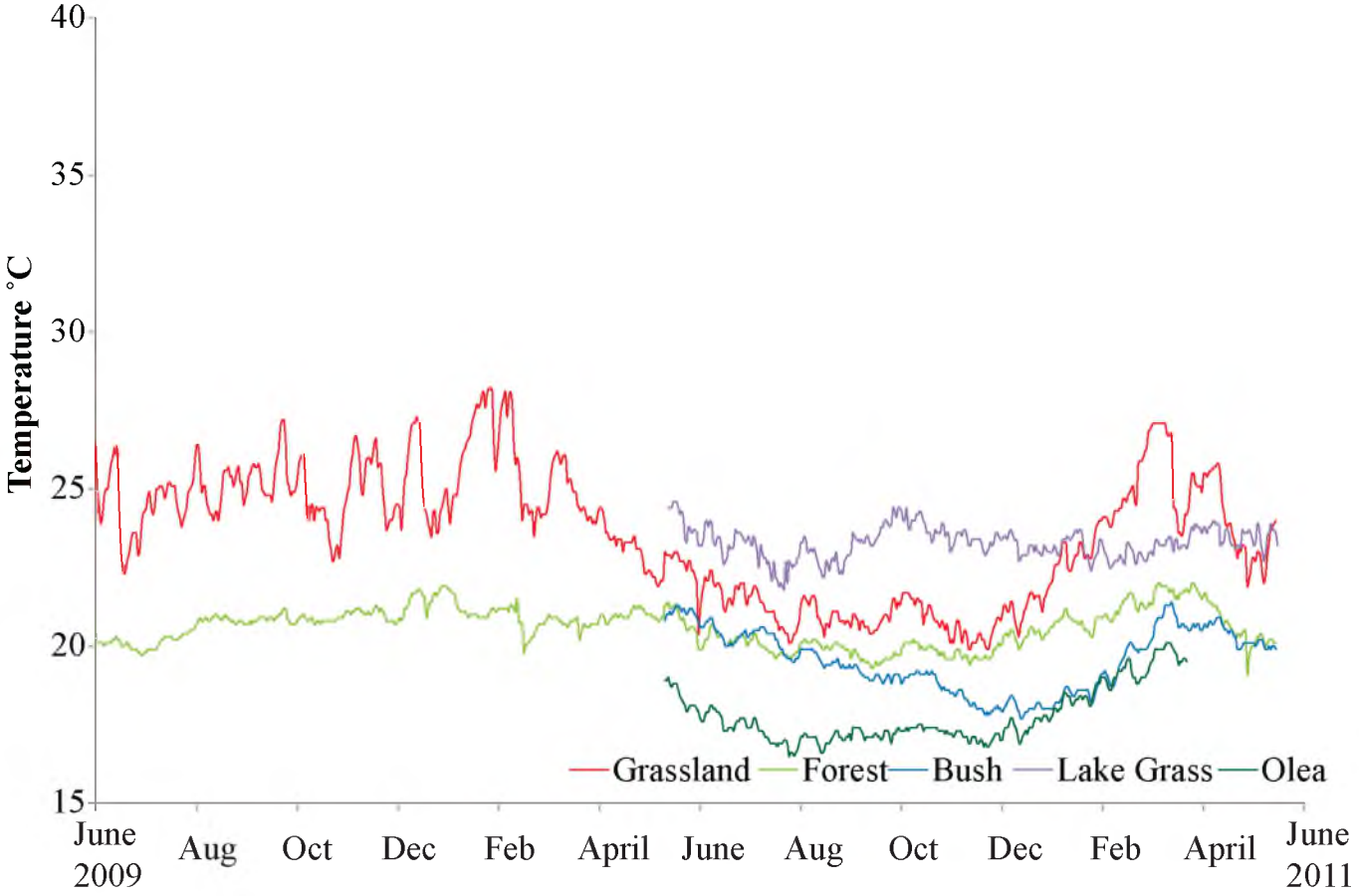

Figure C.1 – Daily average temperature for Nakuru National Park for two years, from June 2009 until May 2011.

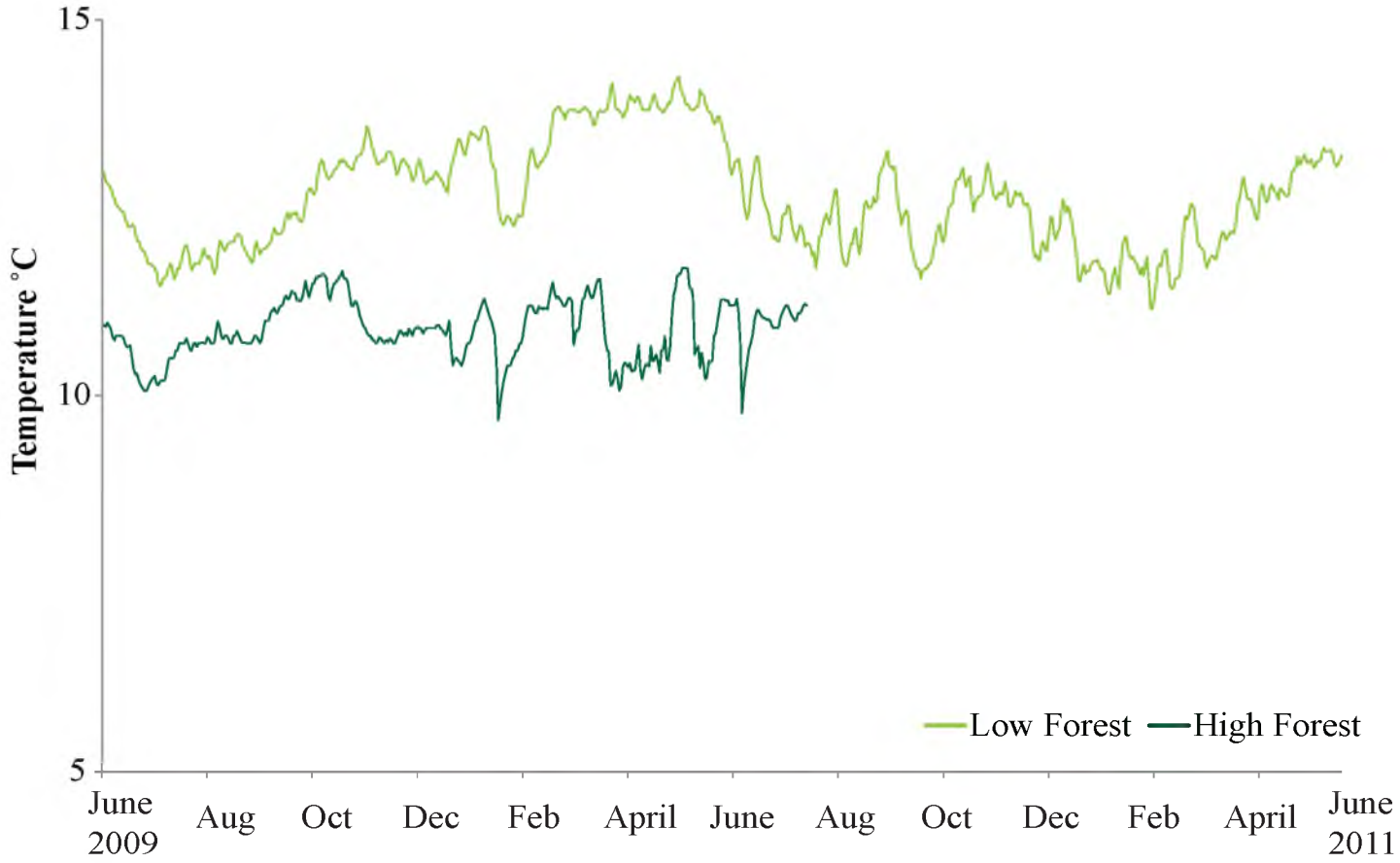

Figure C.2 – Daily average temperature for Mt. Kenya National Park for two years, from June 2009 until May 2011.

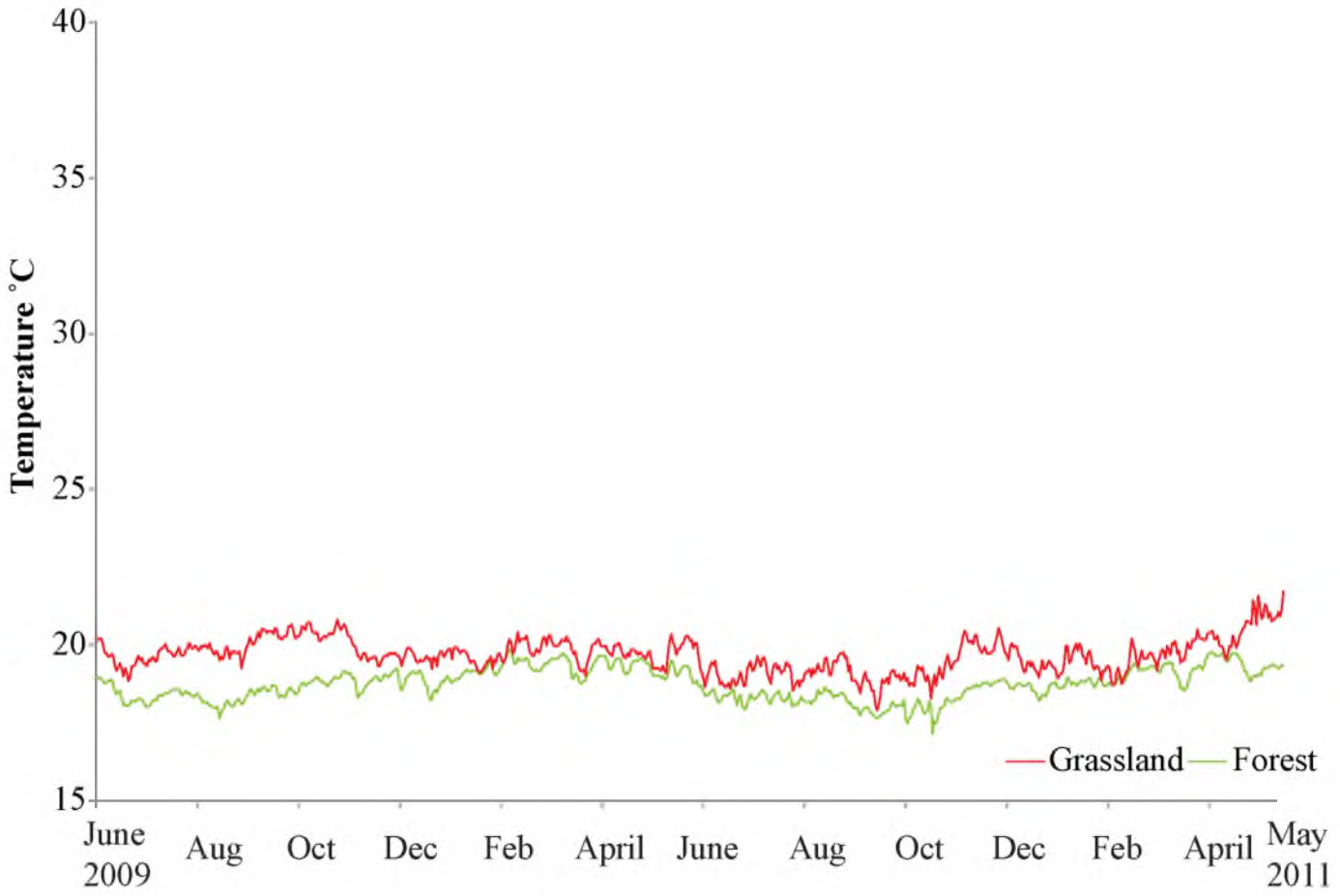

Figure C.3 – Daily average temperature for Kakamega Forest National Park for two years, from June 2009 until May 2011.

Figure C.4 – Daily average temperature for Shimba Hills National Park for two years, from June 2009 until May 2011.

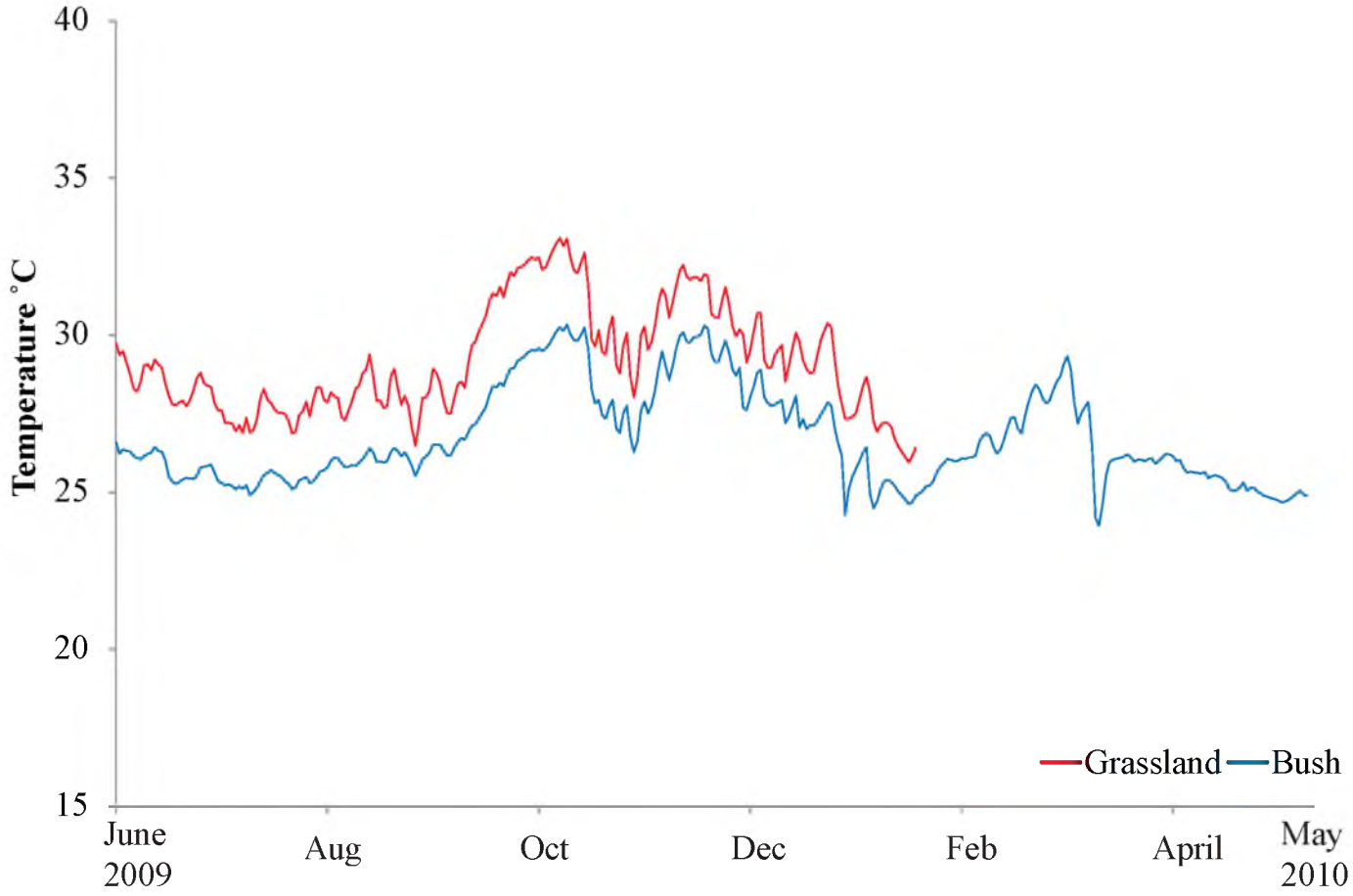

Figure C.5 – Daily average temperature for Tsavo West National Park for one year, from June 2009 until May 2010.

APPENDIX D

ADDITIONAL COMPOSITE DAY FIGURES

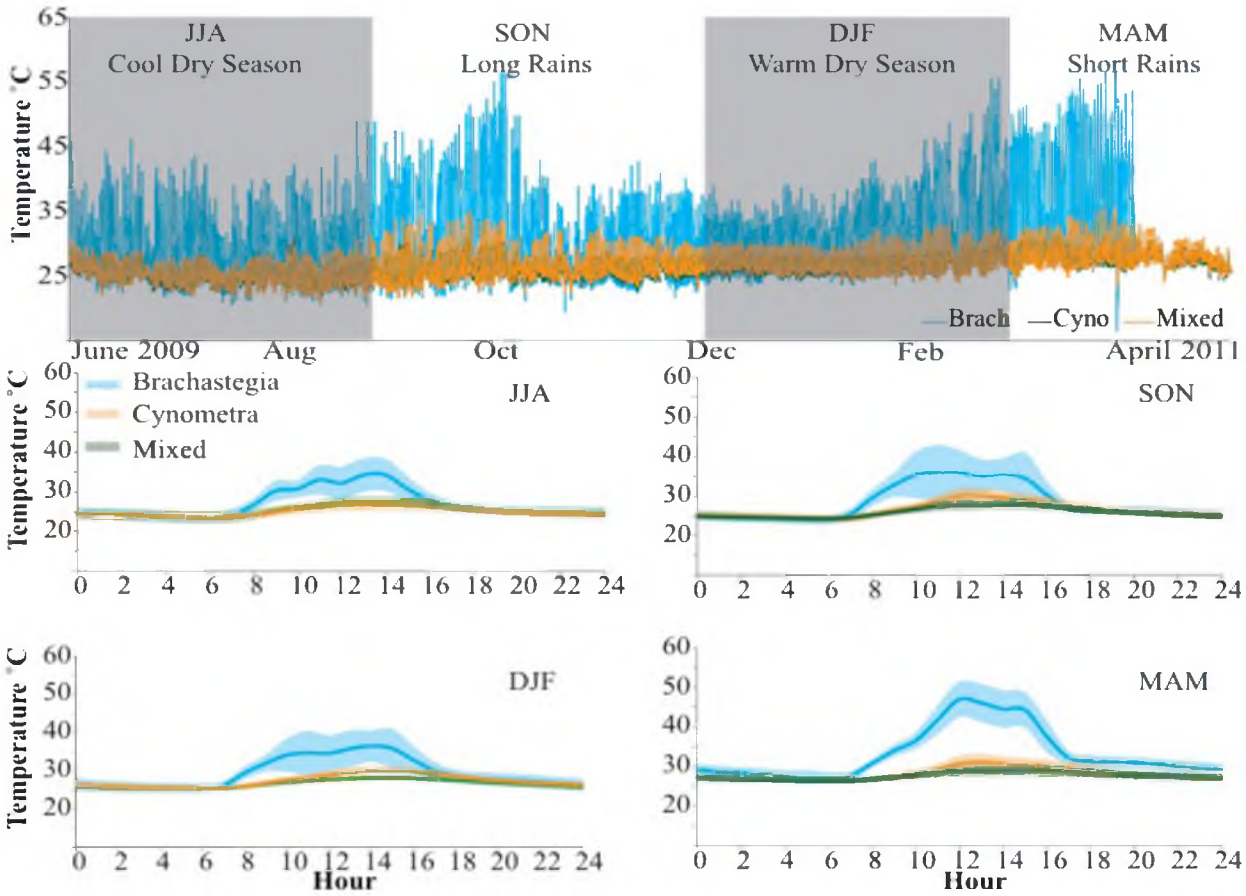

Figure D.1 – Composite day for Arobuko Sokoke National Park from June 2009 to May 2010. The top panel is the full year of surface temperatures and the lower panel is the composite day for the individual seasons.

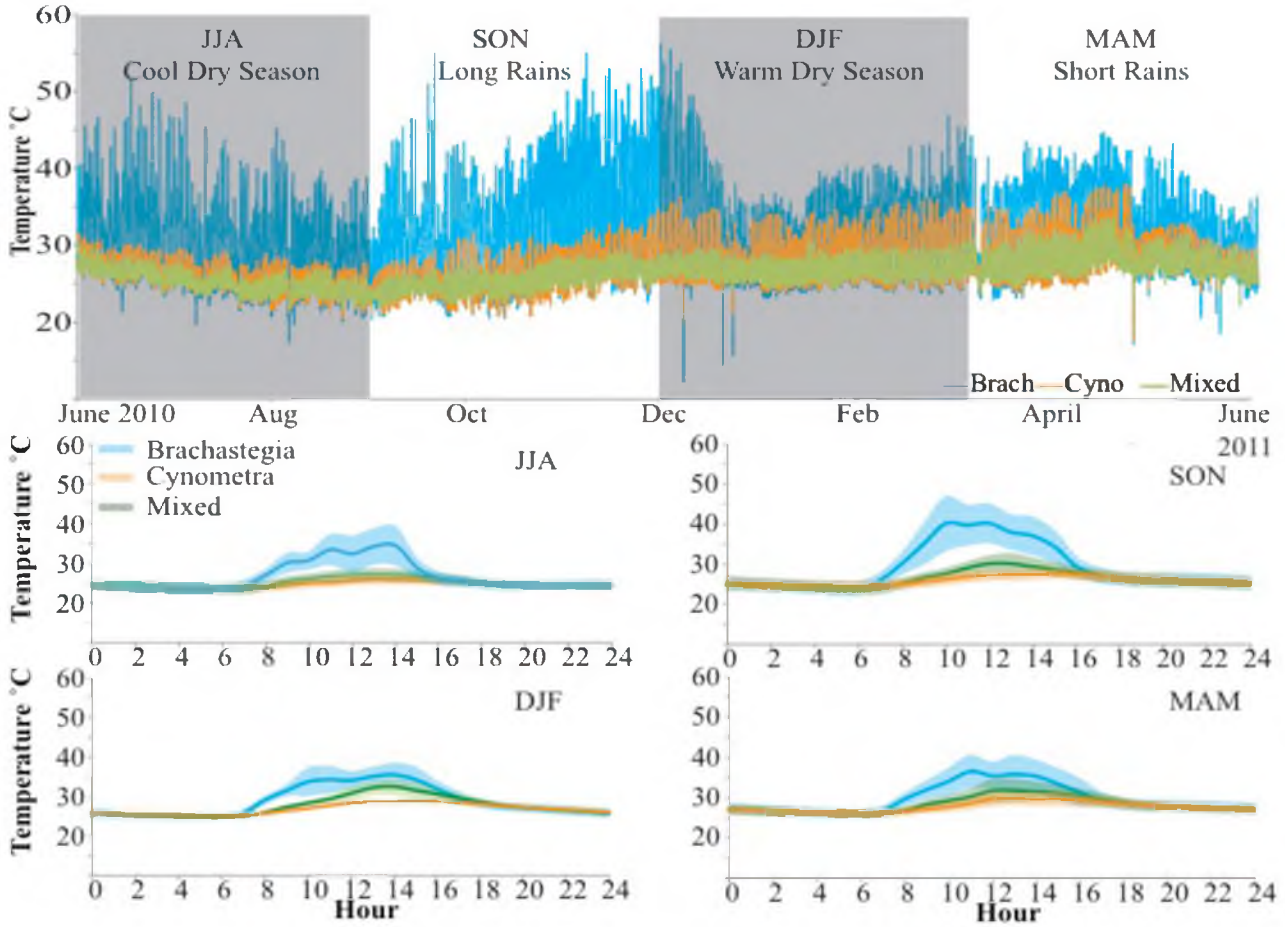

Figure D.2 – Composite day for Arobuko Sokoke National Park from June 2010 to May 2011. The top panel is the full year of surface temperatures and the lower panel is the composite day for the individual seasons.

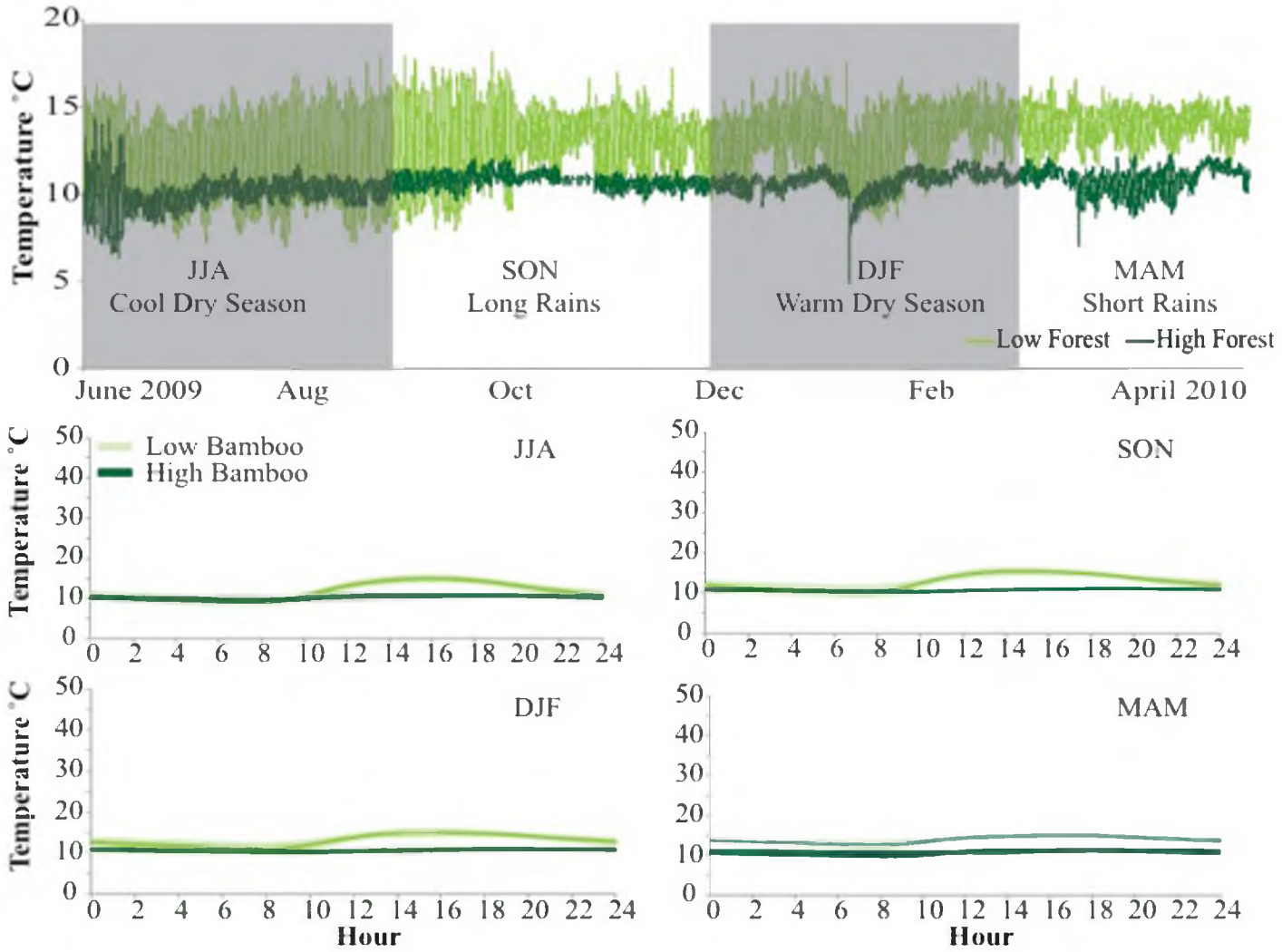

Figure D.3 – Composite day for Mt. Kenya National Park from June 2009 to May 2010. The top panel is the full year of surface temperatures and the lower panel is the composite day for the individual seasons.

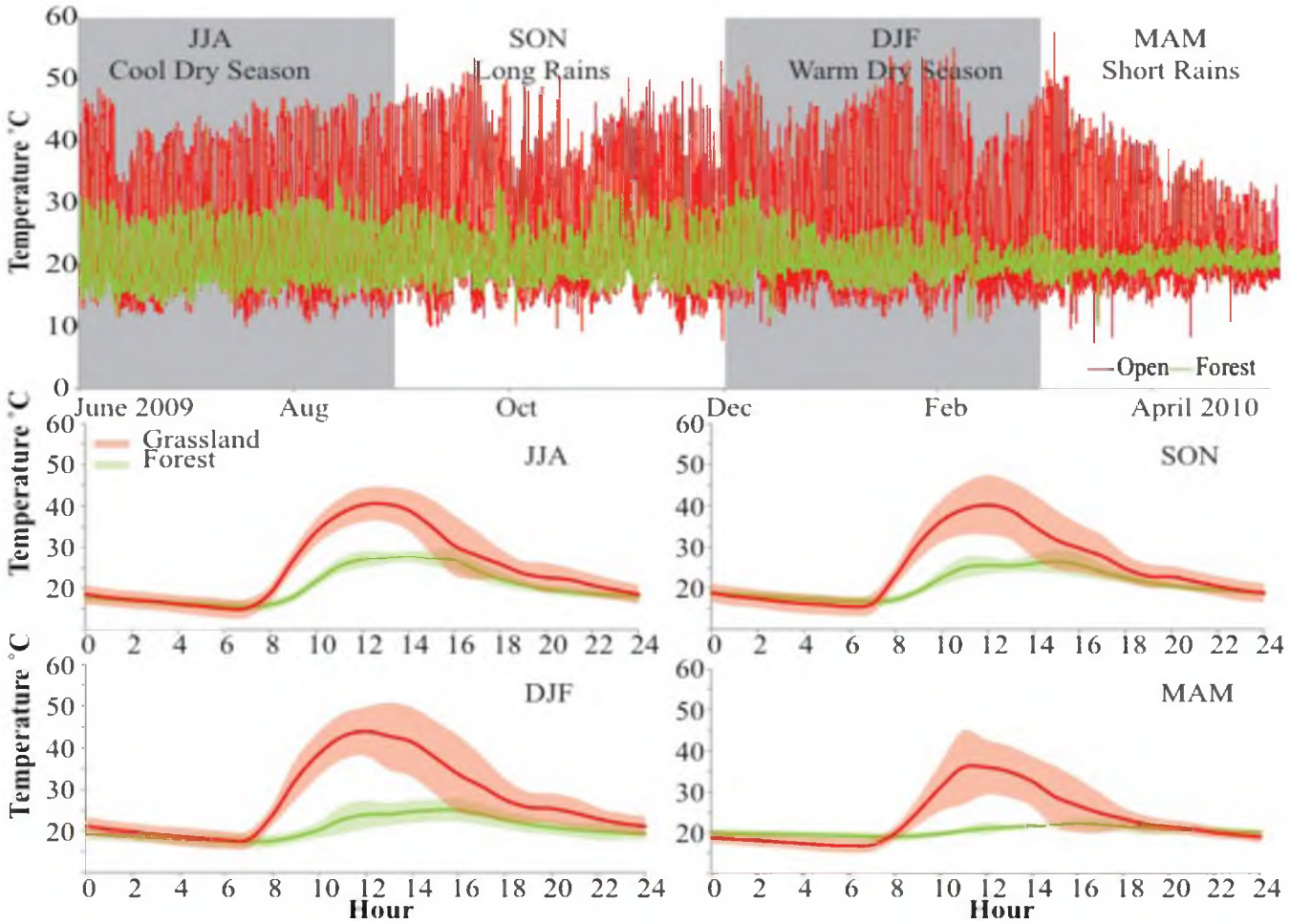

Figure D.4 – Composite day for Nakuru National Park from June 2009 to May 2010. The top panel is the full year of surface temperatures and the lower panel is the composite day for the individual seasons.

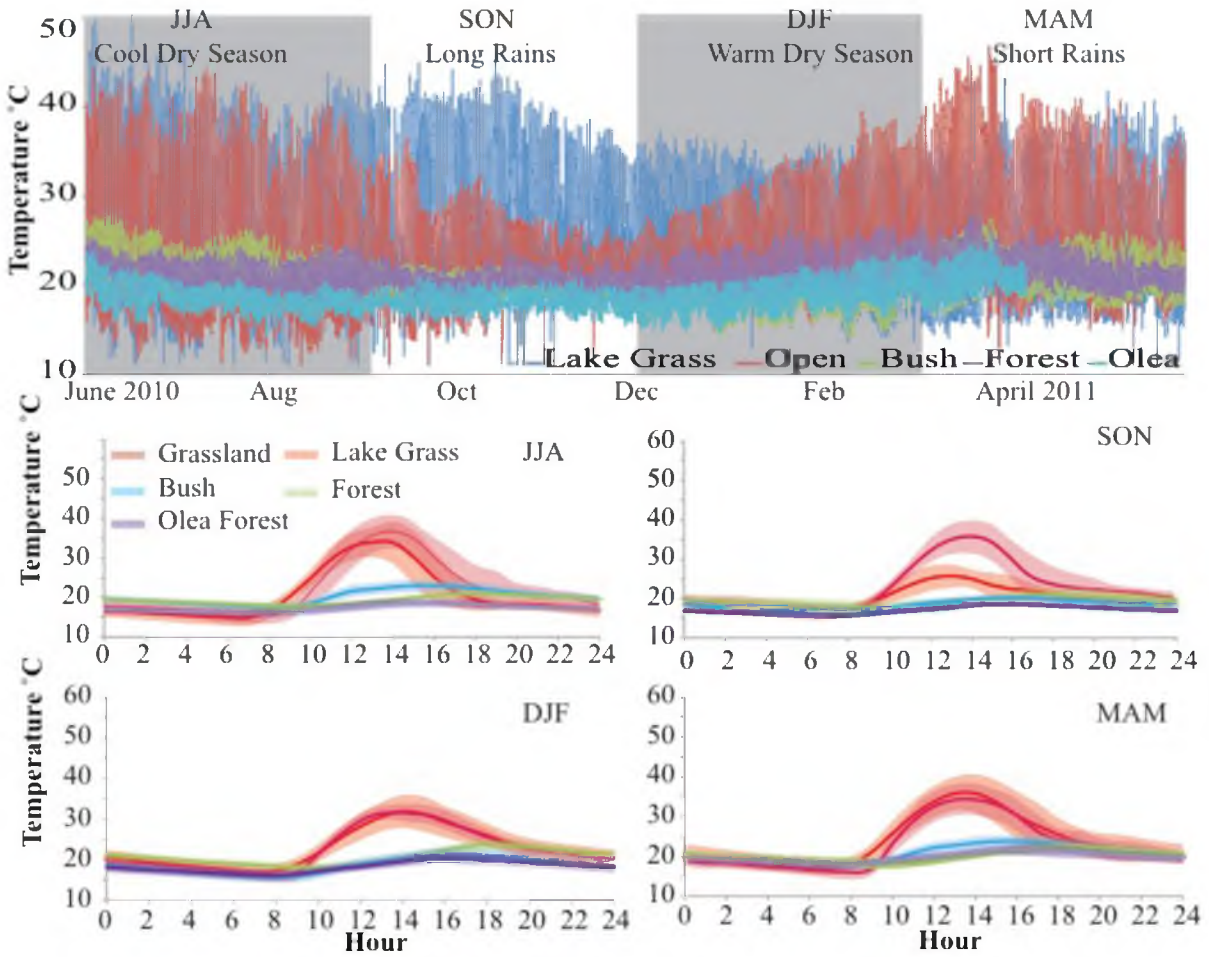

Figure D.5 – Composite day for Nakuru National Park from June 2010 to May 2011. The top panel is the full year of surface temperatures and the lower panel is the

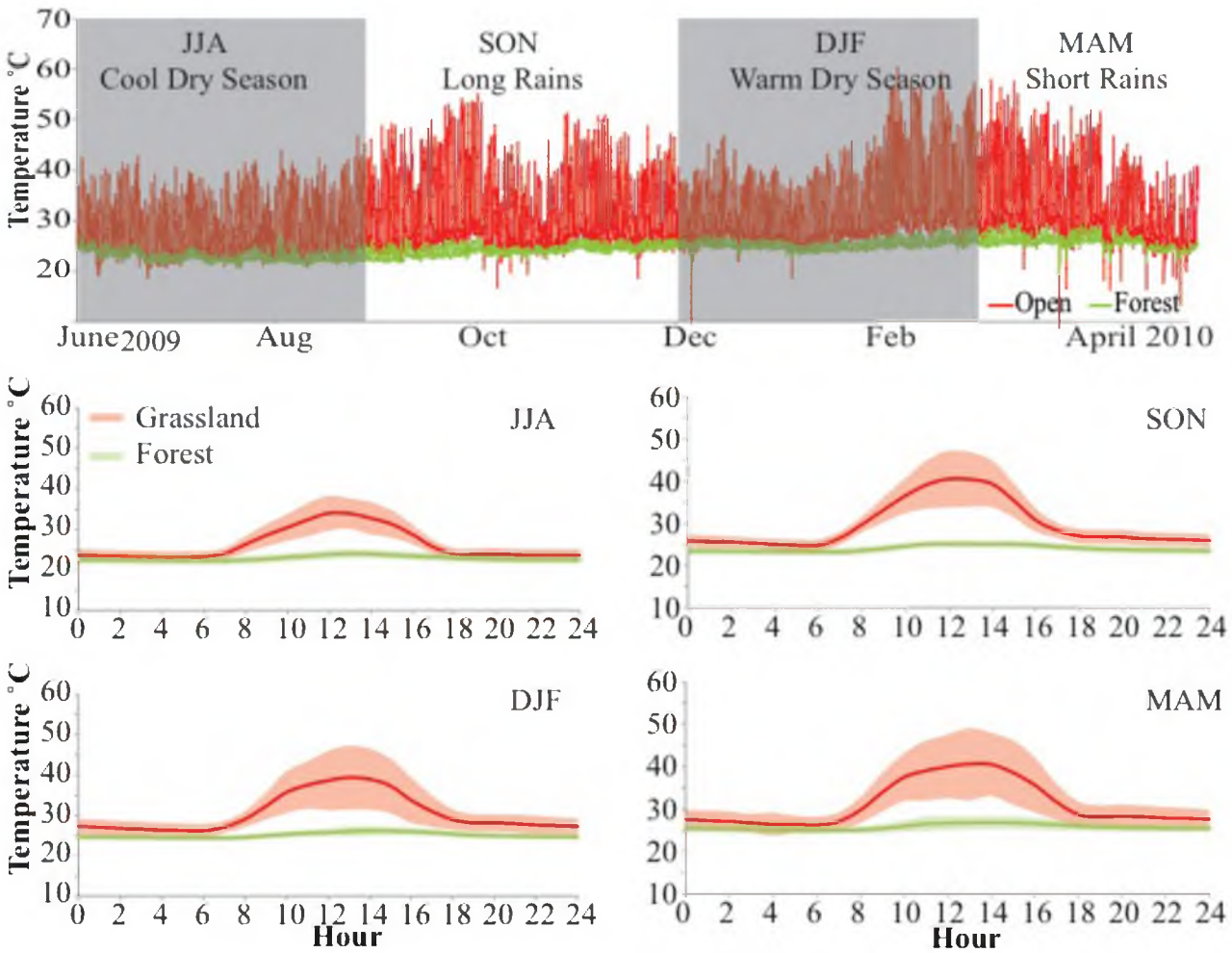

Figure D.6 – Composite day for Shimba Hills National Park from June 2009 to May 2010. The top panel is the full year of surface temperatures and the lower panel is the composite day for the individual seasons.